Asociación de pranoprofeno a sistemas nanoestructurados para administración tópica

Guadalupe Abrego Escobar

UNIVERSIDAD DE BARCELONA

FACULTAD DE FARMACIA

DEPARTAMENTO DE FISICOQUÍMICA

ASOCIACIÓN DE PRANOPROFENO A SISTEMAS NANOESTRUCTURADOS PARA ADMINISTRACIÓN TÓPICA

GUADALUPE ABREGO ESCOBAR, 2015

UNIVERSIDAD DE BARCELONA

FACULTAD DE FARMACIA

DEPARTAMENTO DE FISICOQUÍMICA

PROGRAMA DE DOCTORADO: INVESTIGACIÓN, DESARROLLO Y CONTROL DE MEDICAMENTOS

ASOCIACIÓN DE PRANOPROFENO A SISTEMAS NANOESTRUCTURADOS PARA ADMINISTRACIÓN TÓPICA

Memoria presentada por Guadalupe Abrego Escobar para optar al título de doctor por la Universidad de Barcelona.

Directoras

Dra. María Luisa García López. Dra. Ana Calpena Campmany.

Doctoranda

Guadalupe Abrego Escobar.

Tutora

Dra. María Luisa García López.

GUADALUPE ABREGO ESCOBAR, 2015

AGRADECIMIENTOS

Deseo expresar mi más sincero agradecimiento a las Dras. **Ana Cristina Calpena Campmany** y **María Luisa García López**, quienes con mucha dedicación me han asesoraron para llevar a cabo esta investigación. Les agradezco por haberme facilitado el uso de las instalaciones, el equipo de investigación y todo lo necesario para llevar a cabo este trabajo. Al mismo tiempo, agradezco a la Dra. Calpena su amistad sincera, sus sabios consejos. Lejos de mi país y de mi familia en ti encontré una amiga y una hermana.

Al mismo tiempo, le doy las gracias a las Dras. **María Antonia Egea**, **Lyda Halbaut Bellowa, Elisabet Gonzalez**, **Marta Espina y al Dr. Saša Nikolić**, por toda la inestimable ayuda, orientación y apoyo técnico que me han brindado.

A la profesora **Amélia María da Silva**, por haber aceptado mi solicitud de estancia de investigación en la Universidade de Trás-os-Montes e Alto Douro, Villa Real, Portugal, tiempo durante el cual, tuve la fortuna de contar con su inestimable ayuda en los estudios de citotoxicidad celular. Muchas gracias, por el tiempo tan valioso que me dedicaste y por tu amistad. Así mismo, agradezco a la profesora **Eliana B. Souto** de la Universidad de Coimbra, Portugal, por toda la inestimable ayuda que me proporcionó en la revisión técnica de los artículos científicos comprendidos en este trabajo.

Mi más profundo agradecimiento al **Ministerio de Asuntos Exteriores y de Cooperación – Agencia Española de Cooperación Internacional para el Desarrollo** (MAEC - AECID), por haberme concedido la beca para estudiar el Máster y el doctorado en Investigación, Desarrollo y Control de Medicamentos.

A mi mejor amiga, **Bessy Guevara Granados,** por animarme a continuar adelante, porque siempre consigues hacer que sonría aun en los momentos más dificultosos de mi vida. Me siento afortunada, porque la vida me brindó la oportunidad de conocer a una persona tan valiosa y especial como tú.

A mis **hermanas**, por animarme, apoyarme y por estar siempre pendientes de mí. Aun en la distancia he sentido su cercanía.

A mis amigos y compañeros de trabajo de la Facultad de Química y Farmacia de la Universidad de El Salvador (El salvador), por su amistad y por sus manifestaciones de apoyo. Agradezco especialmente a **Eliseo Ernesto Ayala,** por todo el tiempo y el esfuerzo que te ha causado llevar a cabo todas las gestiones administrativas relacionadas a mi estancia en España. Eres un gran amigo y un gran compañero de trabajo. Muchísimas gracias por tu amistad. Mis más sincero agradecimiento a **Ivonne Arévalo**, **Rocío Ruano, Irma de Majano y Javier Antonio Guzmán,** por confiar en mí, por su inestimable amistad y por el apoyo incondicional que me han dado.

A mis compañeros de doctorado de la universidad de Barcelona: **Paloma Flórez**, **Martha Vázquez, Alexander Parra, Mireia Mallandrich, Nora Provenza, Ana Flo, Cristina Cañada**, **Francisco Fernández, Gladys Ramos** y **Elena Sánchez**, por todos los momentos tan agradables que viví a su lado. También, me gustaría agradecer a otras personas que realizaron una estancia en la Universidad de Barcelona y a quienes tuve el placer de conocer: **Joana Fangueiro**, **Berenice Andrade**, **María Luisa Garduño** y **Valeri Domínguez**. Además, me gustaría agradecer especialmente a **Helen Alvarado Bonilla**, por su sincera y valiosa amistad. Eres una gran amiga y compañera de lucha. Las eternas horas de trabajo durante la semana y/o fin de semana en la universidad, se hicieron más llevaderas en tu compañía.

Agradezco a mis amigos externos a la universidad; a **Estaban Gracia**, a su esposa, **María Jesús**, a su hija **Mónica** y a sus hijos **Oscar** y **German**. Al mismo tiempo, agradezco a **Francisco Terol**, a su esposa **Montserrat**, a su hija **Alicia** y a sus hijos **Alejandro** y **Alberto**. Muchas gracias, por la amistad tan sincera y cercana que me han proporcionada, por los inolvidable momentos de convivencia, en los que me sentí como en casa.

ÍNDICE GENERAL

ABREVIATURAS

AFM: Microscopia de fuerzas atómicas

AINE: Analgésico antiinflamatorio no esteroideo

DSC: Calorimetría diferencial de barrido

EE : Eficiencia de encapsulación

FTIR: Espectroscopia infrarroja con transformada de Fourier

HG: Hidrogel

IP : Índice de polidispersión

LD: Difracción laser

NPs: Nanopartículas

PBS: Solución búfer fosfato

PCS: Espectroscopia de correlación fotónica

PF: Pranoprofeno

PLGA: Ácido poli-láctico-co-glicólico

PVA: Polivinil alcohol

SEM: Microscopia electrónica de barrido

TEM : Microscopia electrónica de transmisión

TMP: Tamaño medio de partícula

XPS: Espectroscopia de fotoelectrones generado por rayos X

ZP : Potencial zeta

1. INTRODUCCIÓN

1.1. PENETRACIÓN DE FÁRMACOS POR VÍA TÓPICA.

1.1.1. Características anantomofisiológicas de la vía ocular.

La administración ocular de fármacos se utiliza habitualmente para el tratamiento de los trastornos superficiales y/o internos del ojo. El reto principal de la terapia ocular es alcanzar una concentración óptima del fármaco en el lugar de acción. Sin embargo, la baja biodisponibilidad de los fármacos a partir de las formas de dosificación clásicas está vinculada principalmente a la estructura anatómica y fisiológica de la vía ocular.

Los **procesos fisiológicos** del ojo disminuyen significativamente la biodisponibilidad de los fármacos en la superficie ocular, limitando su absorción y favoreciendo la eliminación del mismo.

La superficie corneal y conjuntival están cubiertas por la película lagrimal, cuyo espesor oscila en el rango de 7 a 8 µm. Está película está constituida por tres capas: la capa posterior está formada por las células calciformes del epitelio conjuntival y es rica en glicoproteínas; la capa intermedia, acuosa, contiene proteínas tales como, lisozima con actividad antibacteriana; y la capa oleosa externa, producida mayoritariamente por las glándulas meibomianas, cuya función es retardar la evaporación de la lágrima. El volumen de la lágrima en un adulto es alrededor de 9 µL [1] y la secreción lagrimal basal es de 1.2 µL/ min en humanos, mientras que el saco lagrimal tiene una capacidad de almacenamiento de 30 µL. Sin embargo, el volumen de una gota de una forma de dosificación convencional oscila entre 40 y 50 µL, por lo que después de la instilación del fármaco en el ojo, el exceso de volumen es eliminado de la superficie ocular (aproximadamente 20 µL) y a continuación los nervios de la córnea inducen la formación de lágrimas reflejas, cuyo volumen varía entre 3 a 400 µL/ min. Este volumen varía de acuerdo con las propiedades irritantes del fármaco y/o de la formulación administrada. El aumento en la formación de lágrimas favorece el drenaje del fármaco de la superficie ocular y su dilución. Después de la instilación del fármaco, se activa el reflejo de parpadeo provocando un aclaramiento acelerado del fármaco a través de las lágrimas. El incremento de volumen de fluido en el saco es llevado rápidamente al sistema

de drenaje lagrimal por acción de los canalículos asociados con los movimientos palpebrales. En 90 segundos, la mayor parte del fármaco instilado es eliminado del área pre-corneal [1]. Adicionalmente, la unión del fármaco a las proteínas de la lágrima disminuye la cantidad efectiva del mismo en contacto con la córnea y además, la acción amortiguadora del ácido carbónico y los ácidos orgánicos débiles presentes en la lágrima facilitan la ionización del fármaco [2].

El fármaco instilado en la superficie ocular, que no fue eliminado por los procesos fisiológicos del ojo puede ser absorbido en el **área pre-corneal** a través de la esclera y/o conjuntiva.

La **conjuntiva** es una membrana mucosa, delgada y vascularizada que reviste la superficie interna de los parpados y la parte anterior de la esclera. El área superficial de la conjuntiva (16 -18 cm^2) es superior al área de la córnea (1 cm^2), por lo que la absorción de los fármacos a través de la conjuntiva es usualmente mayor respecto a la córnea. La conjuntiva es más permeable a macromoléculas hidrófilas por vía paracelular que la córnea [1,3].

La **esclera** es un tejido fibroso, rígido y grueso, formado por colágeno y mucopolisacaridos. La esclera ofrece una menor resistencia a la penetración de los fármacos respecto a la córnea. Sin embargo, los fármacos que son absorbidos a través del tejido conjuntival y/o esclera pueden pasar a la circulación sistémica, lo que constituye una vía importante en la eliminación del fármaco administrado tópicamente, con la posibilidad de inducir a efectos adversos.

En el **área corneal**, el fármaco administrado tópicamente que no fue absorbido por la conjuntiva y/o esclera o eliminado por la fisiología ocular, puede penetrar la córnea a través de dos mecanismos: paracelular (a través de los espacios intercelulares) y/o transcelular (a través de los espacios intracelulares) [4]**.**

La córnea actúa a modo de barrera protectora que impide la entrada de sustancias extrañas y a su vez, modifica el transporte de los iones. El diámetro y radio de curvatura de la superficie anterior de la córnea es 11. 7 mm y 7.8 mm, respectivamente; y su espesor está en el rango de 0.5 a 0.7 mm. La córnea es un tejido ópticamente transparente que consta de cinco capas, del exterior al interior son: epitelio, membrana de Bowman, estroma, membrana

Descement y endotelio (Figura 1). Sin embargo, en la penetración transcorneal de los fármacos, únicamente tres de estas capas limitan significativamente el paso del fármaco a las estructuras internas del ojo: epitelio, estroma y endotelio [5].

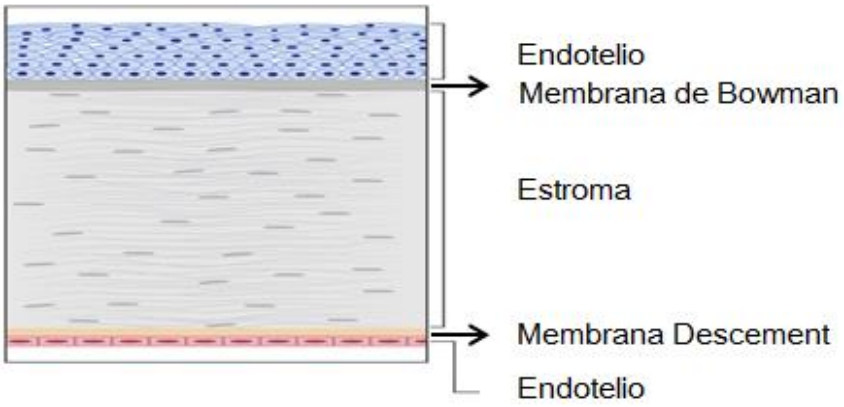

Figura 1. Estructura anatómica de la córnea.

El **epitelio** de tipo escamoso, estratificado no queratinizado, consta de una capa basal de células columnares, dos o tres capas de células y una o dos capas externas de células superficiales de forma poligonal y escamosa. El epitelio posee una abundante cantidad de lípidos en su estructura celular. Las células superficiales del epitelio presentan uniones intercelulares estrechas, lo que constituye una barrera selectiva para moléculas lipófilas pequeñas y excluye la penetración de macromoléculas ($r > 10$ Å) por la vía paracelular, en consecuencia el epitelio corneal es considerado como la principal barrera para la penetración de los fármacos en los tejidos intraoculares. Algunos investigadores han reportado que los niveles de calcio celular y los filamentos de actina probablemente desempeñan un papel importante en la integridad de las uniones estrechas [6].

El **estroma** corneal es un tejido hidrófilo, compuesto principalmente por agua, lo que favorece la penetración de moléculas hidrófilas. Este tejido está formado por fibras de colágeno, estructuradas en forma láminas paralelas entre sí, formando haces de colágeno de diferente espesor y diámetro [7]. Los fibroblastos corneales (queratocitos) son el principal componente celular del estroma y representan del 2 al 3 % del volumen total del estroma [8].

El **endotelio** corneal consta de una única capa de células hexagonales que recubre la superficie posterior de la córnea. Este tejido se encuentra en contacto directo con el humor acuoso. Las uniones intercelulares estrechas, también están presentes en este tejido, sin embargo, son menos estrechas respecto a uniones intercelulares del epitelio. El endotelio posée en su estructura celular una gran cantidad de fosfolípidos, por lo que las sustancias lipófilas pueden atravesar fácilmente esta membrana.

El endotelio mantiene la hidratación normal en la córnea y regula el paso de sustancias desde el humor acuoso al estroma [6,4]**.**

La absorción transcorneal es un proceso que ocurre más lentamente que la eliminación del fármaco de la superficie ocular. La constante de eliminación de muchos fármacos es de aproximadamente 0.5 a 0.7/min, mientras que la constante de absorción es cercana a 0.001/min [4].

El fármaco que fue absorbido a través de la córnea pasa a los tejidos internos del ojo. En el **área posterior de córnea**, la porción del fármaco instilado que ha atravesado las barreras oculares es distribuido y/o eliminado a través del humor acuoso. El humor acuoso fluye a una velocidad de 2 ó 5 µL/min para llevar nutrientes y oxígeno a los tejidos vasculares del ojo y facilita eliminación de la materia de desecho de los tejidos circundantes. Por otra parte, la unión de los fármacos a algunos componentes de los tejidos tales como, la melanina presente en el iris puede disminuir el aclaramiento ocular. Por otra parte, esta unión también es capaz de reducir la concentración de fármaco en el humor acuoso y, en consecuencia, disminuir la respuesta farmacológica.

El iris y el cuerpo ciliar poseen una capa intensamente pigmentada de células epiteliales. El tejido del iris es altamente poroso, vascular y posee una gran superficie, por lo que se produce rápidamente un equilibrio de distribución del fármaco disuelto en el humor acuoso. La unión de los fármacos a los tejidos pigmentados del iris y el cuerpo ciliar puede afectar su biodisponibilidad. Los gránulos pigmentados liberan lentamente el fármaco. Por lo que, la alta afinidad de unión de los pigmentos a los fármacos disminuye la concentración de fármaco libre en el reservorio de la cámara anterior.

El cristalino situado detrás del iris y delante del vítreo, está rodeado por una cápsula de colágeno. El núcleo está formado por materia celular rígida y densa que impide el paso de los fármacos a través de ella [1].

En suma, los fármacos son eliminados principalmente del área pre-corneal por el drenaje de la solución instilada, por efecto de la lagrimación y por la absorción no productiva llevada a cabo a través de la conjuntival y/o transescleral del ojo. Estos factores y la relativa impermeabilidad de la córnea limitan la penetración intraocular del fármaco administrado, en consecuencia un porcentaje inferior (< 5 %) de a la dosis del fármaco administrado es capaz de llegar a los tejidos internos del ojo, mientras que la mayor parte de la dosis es absorbida sistémicamente (Figura 2).

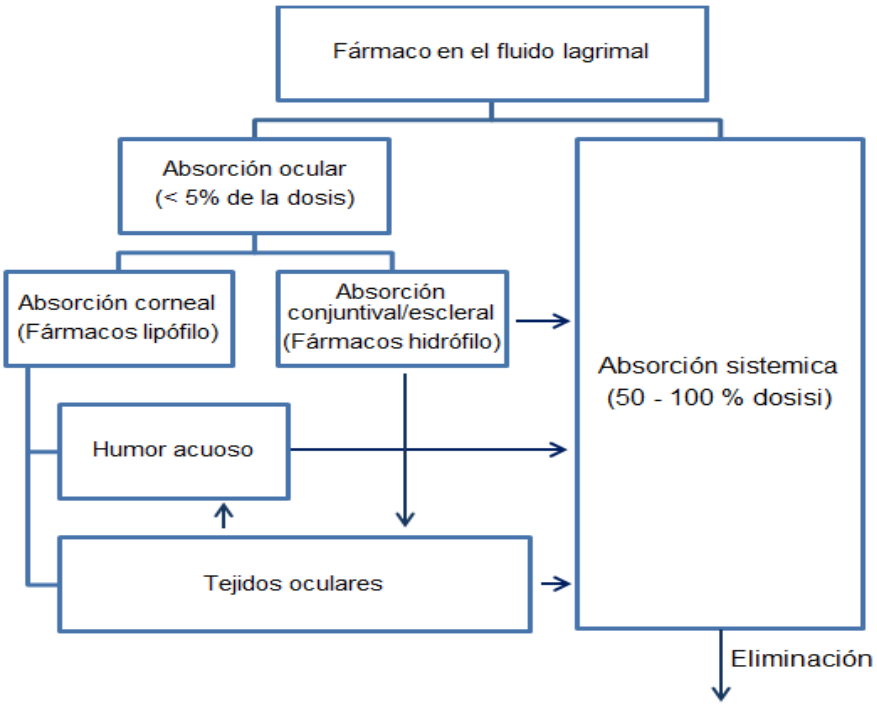

Figura 2. Absorción, distribución y eliminación de los fármacos administrados por vía ocular.

1.1.2. Características anantomofisiológicas de la vía dérmica.

La piel es el órgano más extenso del cuerpo humano, con un área superficial cercana a 2 m^2 y representa aproximadamente el 15 % de peso total del cuerpo de un adulto. Está compuesta por tres capas (Figura 3): epidermis,

dermis e hipodermis y además, posee estructuras anexas tales como, los folículos pilosos y las glándulas sudoríparas y sebáceas [9].

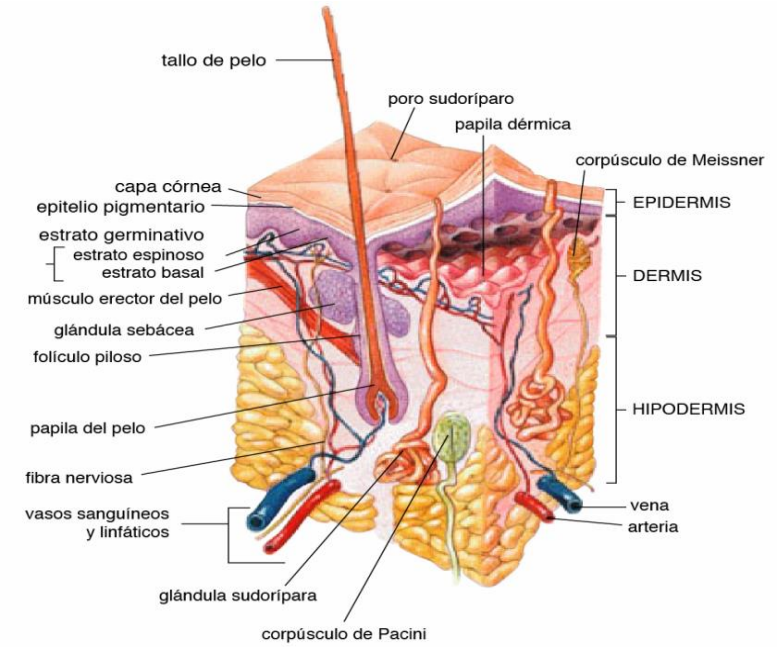

Figura 3. Estructura anatómica de la piel.

La **epidermis** es la capa más externa de la piel, relativamente impermeable, escamoso estratificado queratinizado no vascularizado. Este tejido está formado principalmente por queratinocitos (95%), los cuales sintetizan la queratina (proteína estructural de la epidermis) y producen citocinas en respuesta a una lesión [10]. Adicionalmente, en la epidermis se encuentran los melanocitos, cuya función está vinculada a la formación de melanina; células de Langerhans y células de Merkel, responsables de la respuesta inmune y transmisión de la respuesta sensorial, respectivamente [11]. En atención al estado de diferenciación de los queratocitos, la epidermis se divide en 4 estratos, del interior al exterior de la epidermis son: basal, espinoso, granuloso y córneo. El estrato basal es una capa única de células, compuesto mayormente por queratinocitos. En el estrato basal las células basales están dispuestas hacia la superficie, se pueden identificar las células de Langerhans pueden ser identificadas dentro de este estrato. El estrato granuloso es una capa de queratocitos en forma granular. Las células de este estrato liberan sus componentes lipídicos dentro de los espacios intercelulares, formando una barrera que evita la cohesión intercelular dentro del estrato córneo. La capa

más externa de la epidermis es el estrato córneo, está formado por las células que migran del estrato granuloso, denominadas corneocitos.

La **dermis** tiene un espesor que dependiendo de la región del cuerpo puede oscilar entre 0.5 y 5 mm. Se encuentra delimitada externamente por la epidermis e internamente por la hipodermis. Se sub-divide en dermis papilar o superficial y dermis reticular o profunda. La dermis papilar es una capa delgada con proyecciones cónicas que permite establecer mayor contacto entre la dermis y epidermis. Esta capa está altamente vascularizada e inervada. La dermis reticular está formada por fibras de colágeno y elásticas, ambas constituyen la mayor parte de la dermis [12].

La hipodermis es la capa más interna de la piel y está compuesta por adipocitos o células grasas que constituyen la base de la formación de folículos pilosos y glándulas sudoríparas. El pelo crece a partir de los folículos pilosos, el cual comprende un bulbo piloso, una papila asociada a glándulas sebáceas y sudoríparas y un músculo erector del pelo. Las glándulas sudoríparas, se dividen en ecrinas (localizadas en toda la superficie corporal) y apócrinas (focalizadas principalmente en axilas y genitales) [11].

Entre las **funciones de la piel** pueden destacarse las siguientes: la piel actúa como una barrera física defensiva, reduciendo la pérdida del agua debido a la impermeabilidad al agua del estrato córneo, es que evita la invasión de microorganismos debido a la producción de sustancias antimicrobianas (células de Langerhans). La piel también actúa como una capa protectora ante el daño fotoquímico de las radiaciones ultravioleta. Mediante un incremento de la actividad de los melanocitos, el número de melanosomas producidos y la velocidad de transferencia de la melanina a queratinocitos epidermales, disminuye la absorción de la radiación ultravioleta y además, el estrato córneo de la piel refleja la radiación y en consecuencia se la reduce dosis de exposición. La piel también cumple asi mismo, una función termorreguladora, por la vasodilatación y/o vasoconstricción de los vasos sanguíneos cutáneos superficiales y profundos. La sudoración producida por las glándulas sudoríparas también favorece el proceso termorregulador de la piel. Por otra parte, la piel desempeña una función importante en la percepción sensorial y la síntesis de vitamina D [11,13].

1.1.3. Factores fisicoquímicos que condicionan la penetración tópica de los fármacos.

La penetración de los fármacos a través de las membranas biológicas de la vía ocular y dérmica está determinada por las propiedades fisicoquímicas de los fármacos. En particular, el carácter lipófilo es el factor más importante para la penetración. El coeficiente de partición óptimo de un fármaco para la absorción corneal está en el rango de 10 a 100, lo que sugiere los fármacos lipófilos a traviesan más fácilmente dicha membrana [14,15].

Por otra parte, el coeficiente de partición lípido/ agua es uno de los factores más importantes en la penetración de los fármacos a través de la piel. El estrato córneo de la piel, debido a su naturaleza altamente lipofílica, limita la absorción de fármacos hidrófilos. Sin embargo, la dermis es más hidrófila que el estrato córneo, por lo que constituye una barrera para la absorción de compuestos hidrofóbicos. En consecuencia, para una absorción óptima a través de la vía dérmica las sustancias deben poseer una polaridad intermedia [16].

Las propiedades fisicoquímicas del fármaco tales como, solubilidad, peso molecular y el grado de ionización, también modifican la biodisponibilidad de los fármacos administrados por la vía tópica [6,17,18]. La penetración de un fármacos ionizables depende del equilibrio químico entre la fracción ionizada y sin ionizar del mismo en la dosis instilada y eventualmente en el fluido lagrimal. La parte no ionizada usualmente penetra más fácilmente a través de la membrana de lípidos que la parte ionizada de la molécula [19]. En el caso de la molécula ionizada, no solamente el grado de ionización sino que también la carga de la molécula pueden afectar la penetración del fármaco a través de la córnea [20]. En consecuencia, compuestos catiónicos penetran más fácilmente a través de la córnea que las especies aniónicas, disminuyendo la penetración de los fármacos cargados negativamente.

1.2. FARMACOTERAPIA ANTIINFLAMATORIA OCULAR Y DÉRMICA.

1.2.1. Mecanismos de la inflamación.

Los eicosanoides y el factor activador de las plaquetas son los mediadores más importantes de los procesos biológicos y patológicos. Los eicosanoides se forman a partir del ácido araquidónico (AA) por tres vías enzimáticas: las ciclooxinagenas (COX), lipooxigenasas (LOX) y citocromo P-45O (CYP)-monooxigenasa. Estímulos mecánicos, inmunológicos, etc., conducen a la activación de las fosfolipasas y la elevación del Ca^{2+} citosólico, liberándose el ácido araquidónico, el cual por acción de las ciclooxigenasas, forma endoperóxidos inestables tales como, prostagladinas G_2 ($PGG_{2)}$ y prostagladinas H_2 ($PGH_{2)}$, de los cuales derivan los tromboxanos y las PG; lipooxigenasas, que catalizan la oxidación del ácido araquidónico a sus correspondientes ácidos hidroperoxieicosatrienoico (HPETE) de los cuales derivan los leucotrienos, las lipoxinas y las hepoxilinas; y finalmente, el citocromo P-450-monooxigenasa metaboliza el ácido araquidónico a los ácido epoxieicosatrienoicos (EET) o epóxidos y a los HETE (Figura 4) [21].

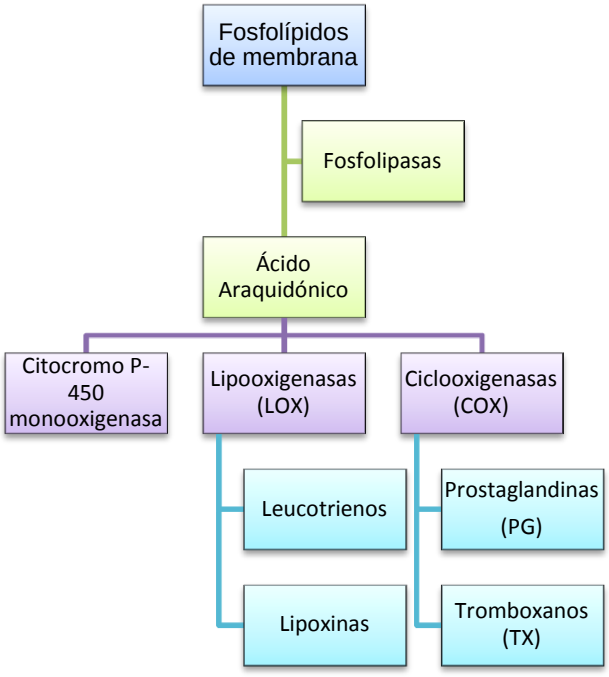

Figura 4. Biosíntesis de los eicosanoides, EET: ácidos epoxieicosatrienoicos; HETE: ácido hidroxieicosatetraenoicos

1.2.2. Mecanismo de acción de los fármacos antiinflamatorios no esteroideos (AINEs) en la inflamación.

Los AINEs se encuentran entre los fármacos más utilizados en todo el mundo. Estos fármacos producen alivio sintomático del dolor y de la inflamación en las artropatías crónicas, como ocurre en la artrosis y la artritis reumatoide, así como en enfermedades inflamatorias aguda. Su farmacología esencial se relaciona con su capacidad de inhibir la enzima COX de ácidos grasos, impidiendo de esta forma la producción de prostaglandinas y tromboxanos.

Existen dos isoformas comunes de la enzima COX: COX-1 y COX-2. Ambas están relacionadas íntimamente y catalizan la misma reacción. Sin embargo, la COX-1 es una enzima constitutiva que existe en la mayor parte de los tejidos, incluidas las plaquetas sanguíneas. Tiene una función de mantenimiento en el cuerpo, de modo que participa en la hemostasis de los tejidos y es responsable de la producción de prostaglandinas. Existen tres modos de unión la COX-1: unión rápida y reversible; unión rápida de baja afinidad, reversible, seguida de una unión más lenta, dependiente del tiempo, de gran afinidad y lentamente reversible; unión rápida, reversible, seguida de una modificación irreversible, covalente.

Por otra parte, la COX-2 es inducida en células inflamatorias cuando son lesionadas, infectadas o activadas, por ejemplo las citosinas inflamatorias, como la interleucina y el factor de necrosis tumoral. Así la isoforma COX-2 es responsable principalmente, de la producción de los mediadores de la inflamación de la familia de los prostanoides. Sobre la COX-2, los agentes específicos producen una inhibición reversible dependiente del tiempo.

La enzima tiene los siguientes activos: ciclooxigenasa y peroxidasa, denominados conjuntamente prostaglandina endoperóxidosintetasa [22]. El grupo peróxidasa es necesaria para que se active los grupos hemos, que participan en la reacción ciclooxigenasa. El complejo enzimático es un dímero, así que en total posee dos sitios ciclooxigenasa y dos sitios peróxidasa. Cada subunidad tiene un canal que se une a las membranas celulares internas o externas. El sitio activo está dentro del complejo, a modo de túnel que actúa guiando al acido araquidónico, liberado por la fosfolipasa A_2 (PLA_2), tras

estímulos diversos de los fosfolípidos de membrana. Tras su unión a dos moléculas de oxígeno, penetran en el canal, se anclan a diversos aminoácidos y liberan productos intermedios inestables como PGG_2 y posteriormente PGH_2 por acción de la peróxidasa. La PGH_2 se convierte por acción de enzimas específicas de células en prostaglandinas estables que salen de la célula. Por lo general, estos fármacos inhiben la enzima COX-1, mientras que la inhibición de la COX-2 es más lenta y, a menudo irreversible. Para inhibir estas enzimas, los AINEs entran en el canal hidrófobo y forman enlaces de hidrógeno con el residuo de arginina de la posición 120, lo que impide el acceso de los ácidos grasos que actúan como sustrato en el dominio catalítico. En la COX-2, tanto la apertura como la zona de unión de los AINEs es un 20% mayor, debido a la existencia de un bolsillo lateral hidrófilo y a ciertas variaciones en los aminoácidos (Figura 5). Los AINEs selectivos COX-2 poseen un lateral hidrófilo que encaja en el bolsillo.

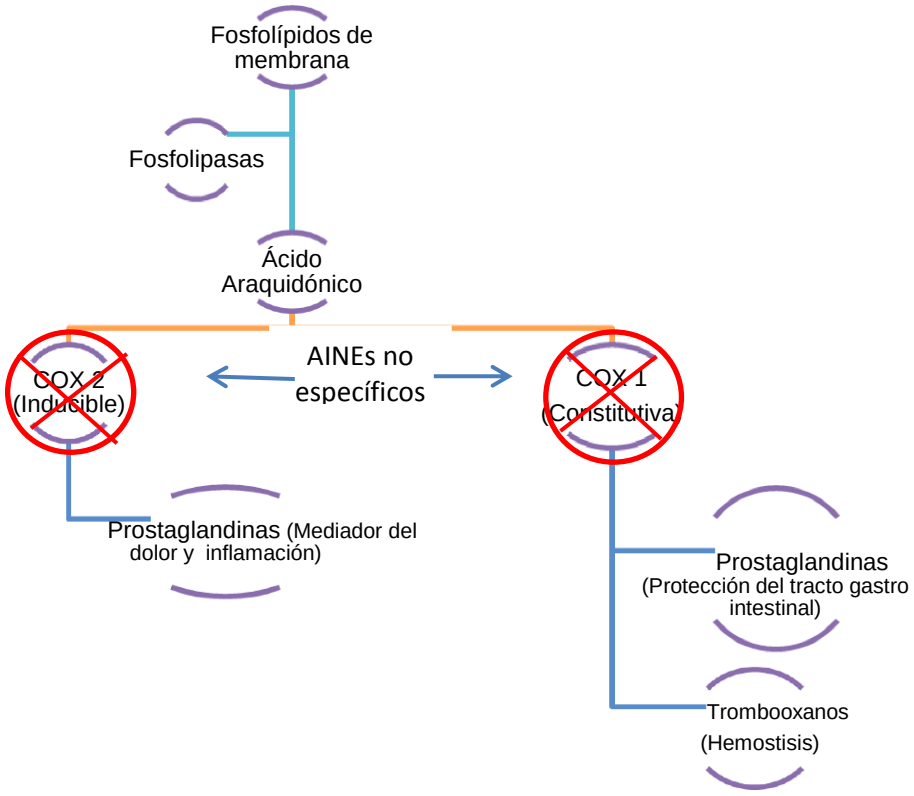

Figura 5. Mecanismo de acción de los AINEs.

La COX-1 y COX-2 tienen el mismo peso molecular y son muy similares. Ambas se encuentran en la membrana plasmática y cada una de ella tiene un canal. La única diferencia es que el canal es más ancho en la COX-2 que en la COX-1. Esto significa que casi todos los AINEs inhibidores de la COX-1, también inhiben la COX-2 pero que muchos inhibidores de la COX-2 poseen escaso poder bloqueante de la COX-1.

La mayor parte de las acciones analgésicas y antipiréticas de las AINEs se relaciona con la inhibición de la COX-2 de ácido araquidónico. La acción antiinflamatoria de los AINEs se lleva a cabo mediante la disminución de la prostaglandina E_2 y la prostaciclina y por la disminución de la vasodilatación.

Por otra parte, el efecto analgésico de los AINEs se debe a una disminución de la generación de prostaglandinas, lo que significa que hay menos sensibilización de las terminaciones nerviosas nociceptivas a los mediadores inflamatorios como la bradicinina y la 5-hidroxitriptamina.

Los AINEs poséen una potencia antiinflamatoria moderada, sin presentar los efectos secundarios oculares que caracterizan a los corticoides. Los efectos adversos más frecuentes tras su aplicación oftálmica, se deben a la irritación ocular transitoria que produce quemazón, lagrimeo e hiperemia conjuntival. Por otra parte, los AINEs constituyen el grupo terapéutico más importante para el tratamiento de procesos inflamatorios y dolorosos de la vía dérmica [21].

1.2.3. Pranoprofeno.

El Pranoprofeno (PF) es un fármaco analgésico no esteroideo, derivado del ácido propiónico. Es conocido químicamente como (2*RS*)-2-(10H–9-Oxa-1-azaantraceno-6-il) ácido propiónico (Figura 6). El peso molecular de este fármaco es 255.27 g/mol y se presenta como un polvo fino blanco e inodoro. Es libremente soluble en N,N dimetill formamida, soluble en ácido acético, poco soluble en metanol, escasamente soluble en anhídrido acético y prácticamente insoluble en agua [23].

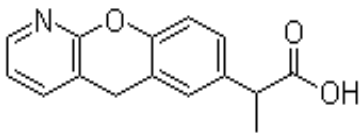

Figura 6. Estructura química de pranoprofeno.

El pranoprofeno es ampliamente metabolizado por glucuronidación en el hígado y posteriormente, es excretado por la orina.

Los parámetros farmacocinéticos de este fármaco han sido evaluados en sujetos jóvenes y geriátricos después de la administración oral de 75 mg de pranoprofeno por vía oral. Los resultados de este estudio revelaron que la semivida del fármaco es más prolongada en los sujetos geriátricos, lo que podria ser originado por una disminución en el metabolismo hepático y/o una reducción en la eliminación renal. La concentración plasmática terapéutica de PF para sujetos jóvenes y geriátricos es 4.89 ± 1.29 $\mu g/cm^3$ y 10.19 ± 2.43 $\mu g/cm^3$, respectivamente; determinada posterior a la administración oral del fármaco [24].

El PF, se ha utilizado recientemente como un fármaco alternativo, seguro y eficaz en el tratamiento de la inflamación producida después de la cirugía de estrabismo y cataratas [25 - 27]. Este fármaco, tiene un efecto beneficioso en la reducción de los signos oculares y los síntomas del ojo seco y disminuye los marcadores inflamatorios de las células epiteliales de la conjuntiva [28]. Su eficacia antiinflamatoria, es equivalente a los corticosteroides de potencia moderada, pero con un mejor perfil de seguridad. Por ello, puede ser considerado para el tratamiento de la conjuntivitis crónica de origen no bacteriano [29] y en el tratamiento agudo y a largo plazo de osteoartritis y artritis reumatoide [30].

A pesar de que el PF, ha demostrado una elevada eficacia anti-inflamatoria y analgésica, su uso farmacéutico está limitado debido a su inadecuado perfil biofarmacéutico, ya que tiene una vida media plasmática corta, baja solubilidad en agua y es inestable en solución acuosa, particularmente cuando se expone a la luz [31 - 32].

1.3. SISTEMAS DE LIBERACIÓN CONTROLADA DE FÁRMACOS.

La administración de fármacos antiinflamatorios no esteroideos a través de la vía tópica ofrece numerosas ventajas, entre ellas se evita el efecto del primer paso del metabolismo de los fármacos, se reducen los daños gastrointestinales y se favorece el efecto local los fármacos. Sin embargo, la relativa

impermeabilidad de las barreras biológicas de la vía tópica, limitan la penetración de los fármacos al lugar de acción. Adicionalmente, las características fisicoquímicas y las propiedades farmacocinéticas de los fármacos modifican la penetración de estos a través de las barreras biológicas del ojo y la piel [33]. Teniendo en cuenta estas consideraciones, en las últimas décadas se ha estudiado ampliamente diferentes sistemas de liberación controlada de fármacos. Algunos de los sistemas nano-estructurados más comúnmente usados en la vía tópica son los liposomas, nanoemulsiones, nanopartículas (poliméricas y lipídicas) [34, 35].

1.3.1. Nanopartículas poliméricas.

Los sistemas coloidales no tóxicos y biodegradables constituyen uno de los sistemas nanoestructurados más estudiados en las últimas décadas con el objetivo de mejorar la focalización de los fármacos en los tejidos y órganos, aumentar la biodisponibilidad de los principios activos, a través de las membranas biológicas y reducir su toxicidad. Las nanopartículas (NPs) son sistemas coloidales, cuyo tamaño de partícula oscila entre 10 y 1000 nm [36]. Los sistemas nanoestructurados formados a base de polímeros abarcan a las nanoesferas y nanocápsulas. Estos sistemas vesiculares, frecuentemente se utilizan para vehiculizar fármacos que, por su naturaleza lipófila, son escasamente solubles en el agua o completamente insolubles en medio acuoso. Las nanoesferas son sistemas con una estructura matricial en el que el fármaco puede concentrarse adsorbido en la superficie, atrapado en el interior y/o disuelto en la matriz polimérica. Por otra parte, las nanocápsulas poseen una cubierta polimérica con un núcleo interno. En estos sistemas de carga el fármaco puede localizarse disuelto en el núcleo oleoso de la partícula. Sin embargo, el fármaco también puede ser absorbido en su superficie (Figura 7).

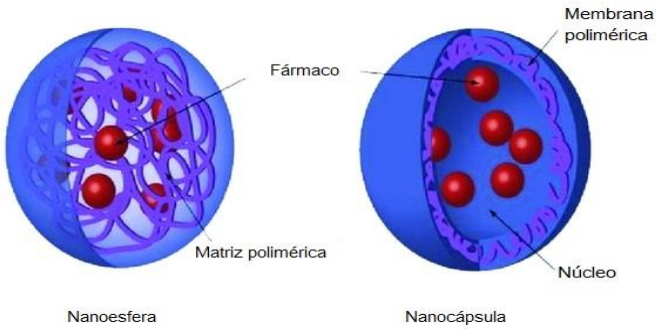

Figura 7. Clasificación de las Nanopartículas poliméricas.

Las nanopartículas poliméricas han sido consideradas como un importante sistema para la liberación controlada de fármacos, ya que permiten una liberación sostenida del principio activo, aumentando su biodisponibilidad en el sitio de acción.

1.3.1.1. Polímeros usados en la preparación de nanopartículas.

Diferentes polímeros han sido utilizados como matriz de las nanopartículas, con el objetivo de garantizar una liberación controlada del fármaco, favorecer la biodisponibilidad de la sustancia administrada, facilitar la vehiculización de macromoléculas con perfiles biofarmacéutico inadecuados y mejorar la liberación local de los fármacos reduciendo los efectos adversos. En general, los polímeros pueden ser clasificados como biodegradables (naturales o sintéticos) y no biodegradable. Entre los polímeros más comúnmente usados en la preparacion de las NPs están: el ácido poli-láctico (PLA), el ácido poli-láctico-co-glicólico (PLGA), poli-ε-caprolactona (PCL), poli-β-hidroxibutirato (PHB), acido poli-β,L-málico, N-2-hidroxipropil metacrilato (HPMA).

Entre ellos, el PLGA ha sido extensamente utilizado en el diseño de sistemas de liberación controlada de fármacos, debido a sus propiedades biodegradables y biocompatibles, lo que permite suministrar eficazmente el fármaco en el de acción y, por lo tanto, aumentar el beneficio terapéutico, y reducir al mínimo efectos adversos [37]. Adicionalmente, la creciente utilización de este polímero en la preparación de los sistemas nanoestructurados, también es debida a que el PLGA ha sido aprobado por el FDA para uso en humano, ya

que permite suministrar eficazmente el fármaco en el órgano o tejido diana, con una degradación controlada de la matriz polimérica [38].

El PLGA está formado por unidades monoméricas de ácido láctico y ácido glicólico. La relación molar de ácido láctico y ácido glicólico en el PLGA puede modificar la resistencia mecánica, el hinchamiento de la matriz, la hidrólisis, la velocidad de degradación, el peso molecular, el grado de cristalinidad y la temperatura de transición vítrea del PLGA.

Un incremento en la proporción molar de ácido glicólico respecto al ácido láctico, conduce una un aumento en la velocidad de degradación del polímero debido a que el ácido glicólico le confiere propiedades altamente hidrófilas al co-polímero formado. Por lo que, de acuerdo al porcentaje de los monómeros que conforman la estructura del PLGA, la velocidad de degradación del copolímero, puede ser descrita de la siguiente manera:

PLGA 65:35 > PLGA 75:25 > PLGA 85:15 [39].

La relación molar del ácido láctico y ácido glicólico del PLGA, también pueden modificar la transición vítrea y la cristalinidad del polímero, y consecuentemente, modular la degradación del PLGA. Durante el proceso de degradación, la cristalinidad aumenta gradualmente, dando como resultado un material altamente cristalino, más resistente a la hidrólisis que el polímero de partida. El incremento de la cristalinidad es atribuido a un aumento de la movilidad de las cadenas poliméricas parcialmente degradadas debido a un mayor grado de entrelazamiento. El realineamiento de las cadenas de polímero conduce a un estado cristalino más ordenada. Adicionalmente, el proceso de degradación del polímero, también puede ser modificado por la distribución del peso molecular. Los grupos carboxílicos terminales facilitan la autolisis del polímero, por lo que velocidad de degradación se produce lentamente cuando menor sea la cantidad de estos grupos en el polímero y viceversa. Las propiedades fisicoquímicas del fármaco, así como la concentración de este encapsulado en la matriz del polímero pueden modificar la velocidad de degradación. Cuanto mayor es el porcentaje de encapsulación del fármaco en el polímero, mayor es el porcentaje de fármaco que es liberado de forma rápida en la etapa inicial del proceso de liberación [40].

El tamaño y la forma de la matriz determinan en gran medida la velocidad de degradación del polímero. En general, un área de superficie grande conduce a un rápida degradación de la matriz polimérica [41].

La porosidad de la matriz, también modifica la biodegradación del polímero y la liberación del fármaco encapsulado en la matriz. Al mismo tiempo, la porosidad puede aumentar la difusión de oligómeros y productos de degradación de bajo peso molecular, cuyos grupos carboxílicos terminales puede facilitar la degradación auto-catalítica del polímero [40].

A pesar de que el PLGA es insoluble en agua, las cadenas de ésteres que conforman su estructura polimérica pueden hidrolizarse en condiciones fisiológicas. El mecanismo de degradación propuesto para el PLGA comprende tres etapas: inicialmente se produce la ruptura aleatoria de las cadenas del copolímero y el peso molecular del polímero disminuye continuamente con la degradación. En la fase intermedia, el peso molecular del polímero se reduce significativamente, este proceso se acompaña de una pérdida rápida de la masa y la formación de unidades monoméricas solubles. En la etapa final, los monómeros obtenidos a partir de la fragmentación del copolímero se solubilizan completamente, pudiendo ser absorbidos por el cuerpo o excretados a través de las vías metabólicas [42]. Las unidades monoméricas del PLGA entran en el ciclo del ácido tricarboxílico, en donde son metabolizadas y posteriormente, son eliminadas del cuerpo en forma de dióxido de carbono y agua. El ácido glicólico, también puede ser excretado sin cambios a través del riñón [43, 44].

Por otra parte, la biodegradación enzimática de PLGA ocurre principalmente en la superficie del polímero a través de la hidrólisis de las cadenas. Enzimas tales como, las esterasas tisulares, pronasas y bromelina han sido investigadas para determinar su efecto en la degradación del PLGA. Entre ellas, la proteinasa bacterial K es capaz de acelerar la degradación del PLA. En contraste, muchas otras enzimas parece que son inactivas. En este sentido, el rol de las enzimas en la degradación del PLGA aún no está completamente claro. Mientras, algunos autores sugieren que las enzimas contribuyen sustancialmente a la degradación de los polímeros biodegradables; otros investigados consideran que las enzimas tienen un rol secundario en este proceso [45 - 47].

1.3.1.2. Métodos de preparación.

Los métodos más comunes para preparar la preparación de las nanopartículas poliméricas son: nanoprecipitación o desplazamiento de disolvente, evaporación del disolvente, <<Salting out>> y difusión del disolvente. La elección de la técnica de preparación depende de las propiedades fisicoquímicas del fármaco.

Método de Nanoprecipitación o desplazamiento del disolvente. Esta técnica involucra el uso de un solvente orgánico, el cual es miscible en agua. El polímero preformado y el fármaco se disuelven conjuntamente en un solvente orgánico de polaridad intermedia y miscible con el agua. La solución orgánica se adiciona gota a gota, bajo agitación magnética, sobre una solución acuosa (no-solvente) en presencia o ausencia de un estabilizante (polivinil alcohol o poloxamer). Una vez en contacto con el agua, el polímero hidrofóbico y el fármaco precipitan instantáneamente, auto ensamblándose el fármaco en la matriz polimérica (Figura 8). Una suspensión coloidal se forma inmediatamente por una rápida difusión del disolvente al medio acuoso. Posteriormente, el disolvente se elimina a presión reducida [48]. La formación instantánea de las partículas es atribuida a las turbulencias interfaciales entre las fases liquidas generadas durante el desplazamiento del disolvente.

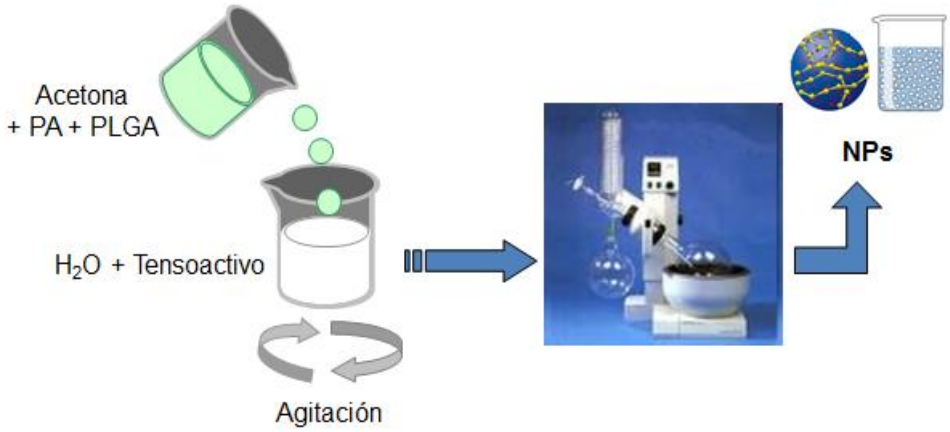

Figure 8. Representación esquemática de la preparación de nanopartículas por el método de desplazamiento del disolvente.

Las nanocápsulas, también pueden prepararse a través de esta técnica, mediante la adición de un volumen de aceite en la fase orgánica, el cual debe ser compatible con el polímero y al mismo tiempo, debe solubilizar el fármaco. Por lo que, una de las ventajas de esta técnica es que es útil para encapsular fármacos lipófilos e hidrófilos. Entre las desventajas del uso de esta técnica están: una baja eficiencia de encapsulación del fármaco en la matriz del polímero, comparado con otras técnicas y adicionalmente, la dificultad para eliminar completamente el solvente orgánico, una vez se han formado las nanopartículas [49].

Evaporación del disolvente. En este método, el polímero es disuelto en un solvente orgánico y volátil. Esta solución es emulsificada en una solución acuosa de un agente estabilizante. La emulsión se transforma en una suspensión coloidal por la evaporación del solvente orgánico que difunde a través de la fase continua de la emulsión (Figura 9). La emulsión puede prepararse en forma individual (agua / aceite y viceversa) o como doble emulsión ((agua/aceite)/agua, etc.). En esta técnica de preparación de nanopartículas se utiliza homogenización o ultrasonidos para reducir el tamaño de la gotícula de la emulsión, seguido de la evaporación del solvente orgánico, ya sea por agitación magnética continua a temperatura ambiente o bajo presión reducida, seguida de varios lavados con agua destilada para remover los aditivos tales como, los tensoactivos [50].

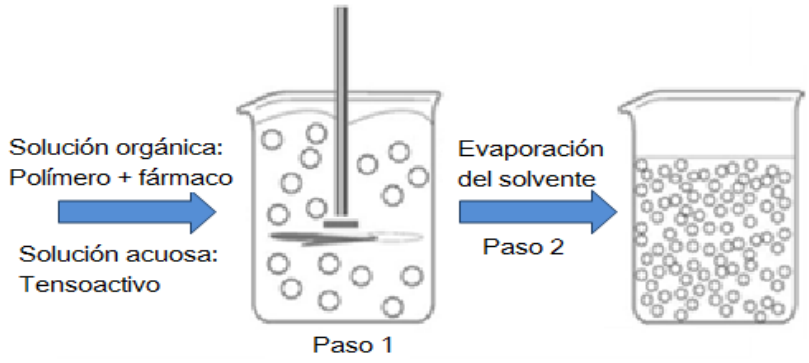

Figura 9. Representación esquemática de la preparación de nanopartículas por el método de evaporación del solvente.

<<Salting out>>. Este método se basa en la separación de un solvente miscible en agua de una solución acuosa enriquecida con electrolitos. Este

método es considerado como una modificación del método de difusión del disolvente. El polímero y el fármaco se disuelven en un solvente orgánico. Esta solución se emulsifica bajo agitación en un gel acuoso que contiene el agente de desplazamiento (electrolitos tales como, cloruro de magnesio, cloruro de calcio y acetado de magnesio y/o no electrolitos tales como, azúcar) y un estabilizante. Esta emulsión aceite/agua es diluida con suficiente volumen de agua o solución acuosa para aumentar la difusión de la acetona dentro de la fase acuosa, conduciendo a la formación de las nanoesferas [51]. El disolvente y los electrolitos se eliminan por filtración de flujo transversal (Figura 10).

El electrolito determina la eficacia de asociación del fármaco en la matriz del polímero. Este método puede ser usado para preparar sistemas coloidales de fármacos termosensibles, ya que no requiere incrementar la temperatura durante el proceso de preparación. Sin embargo, esta técnica es exclusiva para la encapsulación de fármacos lipófilos y adicionalmente, las nanopartículas formadas deben ser sometidas a numerosos lavados [52].

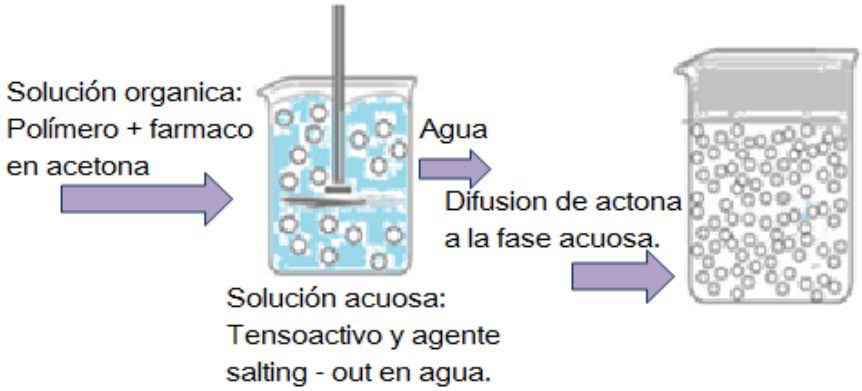

Figura 10. Representación esquemática de la preparación de nanopartículas por el método <<salting out>>.

Difusión del disolvente. Este método es una versión modificada de la técnica de evaporación del solvente. El polímero es disuelto en un solvente parcialmente soluble en agua previamente saturado con agua para asegurar el equilibrio termodinámico entre ambos líquidos. La fase de solvente - agua saturada de polímero se emulsifica bajo agitación, en una solución acuosa que contiene el agente estabilizante (Figura 11). La suspensión de nanopartículas

se forma por la difusión del solvente a la fase externa. Finalmente, el solvente se elimina por evaporación o filtración, de acuerdo con su punto de ebullición.

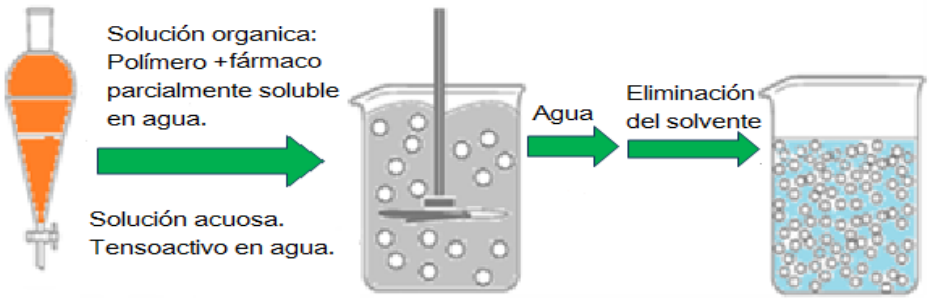

Figura 11. Representación esquemática de la preparación de nanopartículas por el método de difusión del solvente.

En los métodos de preparación de los sistemas poliméricos antes mencionados, factores tales como, el solvente, la solubilidad del fármaco, el tiempo de agitación y/o de mezcla del solvente acuoso y orgánico, el tensoactivo, la concentración de polímero en la fase orgánica, la proporción de la fase orgánica respecto a la acuosa, entre otros, pueden modificar las propiedades fisicoquímicas de las nanopartículas [53].

1.3.1.3. Caracterización de los nanosistemas poliméricos.

Las propiedades fisicoquímicas de los sistemas nanoparticulares tales como, el tamaño y morfología de las nanopartículas, el índice de polidispersión, la carga superficial, la eficiencia de encapsulación del fármaco en la matriz polimérica y el perfil de liberación del fármaco, determinan la eficacia terapéutica del fármaco vehiculizado en estos sistemas. Para caracterizar fisicoquímicamente a las nanopartículas, diferentes técnicas de análisis han sido desarrolladas y utilizadas.

El tamaño de partícula de los sistemas nanoparticulares destinados a la aplicación tópica, tiene una importancia crucial en las formulaciones que son destinadas a la instilación ocular. Este no debe exceder a las 10 micras para evitar una sensación de malestar en el ojo [54,55]. Otra consideración importante en la tamaño de las partículas es: que las partículas muy pequeñas poseen un área superficial grande, lo que puede conducir a una liberación más

rápida del fármaco, y también puede desempeñar un papel muy importante en la internalización celular [56,57]. El diámetro de nanopartículas puede ser determinado a través de técnicas tales como, espectroscopia de correlación de fotones (PCS), difracción laser (LD) y microscopia electrónica. Las técnicas de PCS y LD se utilizan habitualmente para una determinación rápida del tamaño de partícula y su distribución.

Entre las técnicas microscópicas utilizadas para determinar el tamaño y la morfología de las partículas están: la microscopia electrónica de barrido (SEM), la microscopia electrónica de transmisión (TEM) y la microscopia de fuerza atómica (AFM).

Por otra parte, el potencial zeta es una medida de la carga eléctrica de la superfície de las NPs, que puede influir en la mucoadhesion de estos sistemas, y al mismo tiempo, es una medida indirecta de la estabilidad física de las mismas. La formación de agregados suele ocurrir cuando las fuerzas de van der Waals son dominantes, lo que resulta en una reducción de los valores del potencial zeta y la pérdida de estabilidad del sistema [58]. Esta propiedad de las NPs se determina a través de técnicas analíticas tales como, anemometría láser Doppler y/o técnicas electroforéticas, empleando la ecuación de Helmholtz-Smoluchowski [59].

Otra propiedad fisicoquímica de las nanopartículas es la eficiencia de encapsulación. Esta se expresa en términos porcentuales, relacionando la cantidad de fármaco atrapado en sistema nanopartícular y la concentración total del fármaco adicionado en la preparación de las NPs. Previo a la cuantificación del fármaco encapsulado en las nanopartículas, las suspensiones de estos sistemas, frecuentemente son diluidos en un solvente adecuado, seguidamente se someten a filtración/centrifugación y/o ultracentrifugación. Existen diferentes técnicas analíticas que permiten cuantificar la concentración del fármaco encapsulado en las NPs.

La evaluación del perfil de liberación del fármaco desde la matriz, es otra característica fisicoquímica de las nanopartículas.

El fármaco encapsulado en los sistemas coloidales exhibe un perfil de liberación en dos fases: inicialmente el fármaco depositado en la superficie de la matriz polimérica en contacto con el medio, es liberado en función de la

solubilidad y de la penetración del agua dentro de la matriz. Seguidamente, el agua en el interior de la matriz, hidroliza el polímero en sus unidades monoméricas, lo que permite la formación de pasajes entre los cuales el fármaco puede ser liberado [60]. En términos generales, la liberación del fármaco a partir de la matriz polimérica puede ocurrir a través de la difusión, erosión del polímero o una combinación de ambos (Figura 12) [61]. Si la difusión del fármaco es más rápido que la degradación de la matriz, el mecanismo de liberación del fármaco se produce principalmente por difusión. Una liberación rápida del fármaco puede ser atribuida, a la fracción del fármaco que esta adsorbido o débilmente unido a la superficie de la matriz polimérica [62].

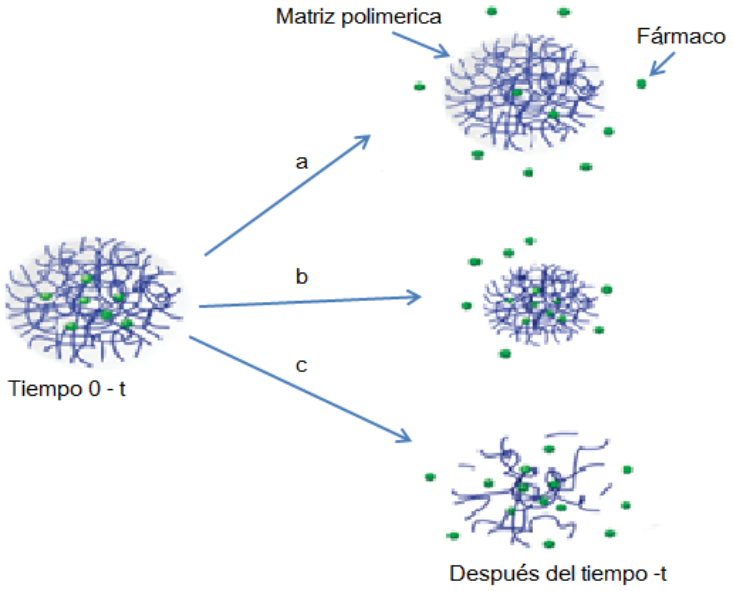

Figura 12. Mecanismo de liberación del fármaco a partir de las nanopartículas poliméricas: (a) difusión, (b) erosión/degradación de la matriz polimérica y (c) biodegradación del polímero por degradación hidrolítica [63], [64].

Además de las determinaciones fisicoquímicas antes mencionadas, técnicas de análisis tales como, espectroscopia infrarroja con transformada de Fourier (FTIR), difracción de rayos X, espectroscopia de fotoelectrones generado por rayos X (XPS), se usan habitualmente para evaluar el estado físico del fármaco (cristalino o amorfo) en la matriz polimérica y/o para determinar interacciones entre el fármaco y el polímero. Adicionalmente, la técnica de calorimetría

diferencial de barrido (DSC), se utiliza para determinar las propiedades físicas de los compuestos, por ejemplo la naturaleza cristalina o amorfa. Esta técnica, proporciona datos cuantitativos sobre el cambio de capacidad exotérmica, endotérmica y calor en función de la temperatura o el tiempo. Esta técnica, también puede demostrar cualquier posible interacción entre diferentes compuestos en mezcla [65,66].

1.3.1.4. Conservación de las nanopartículas

La inestabilidad de las NPs, después de un largo período de almacenamiento, es uno de los principales problemas que limita el uso de estos sistemas coloidales. Para asegurar la conservación de las NPs, evitar los problemas de inestabilidad física, así como variaciones químicas (disminución del fármaco encapsulado) y garantizar su integridad fisicoquímica, el agua contenida la formulación debe ser eliminada. La liofilización, es uno de los procedimientos más comúnmente empleados para este fin.

La congelación es la primera etapa del proceso de liofilización. Durante este paso, la suspensión líquida se enfría y el agua se congela formándose cristales de hielo. A medida que continúa el proceso de congelación, más cantidad de agua contenida en el líquido se congela. Esto se traduce en un aumento de la concentración en el líquido restante. A medida que la suspensión líquida se vuelve más concentrada, su viscosidad aumenta, lo que conduce a una inhibición de la cristalización. El producto congelado puede presentar una estructura cristalina o amorfa y/o una combinación de ambas. Seguidamente, el producto congelado se somete a la etapa del secado primario. La temperatura se eleva para favorecer la sublimación del hielo y el vapor de agua formado pasa a través del producto a la superficie de la muestra y, luego al condensador, donde es solidificado en forma de hielo. Al final de la etapa de sublimación se forma un tapón poroso. Sus poros corresponden a los espacios que fueron ocupados por los cristales de hielo. El secado secundario consiste en la eliminación del agua residual absorbida del producto. Esta agua es la que no se separó en forma de hielo durante la etapa de la congelación. El agua residual es extraída por desorción. La liofilización puede generar estrés en las partículas, desestabilizándolas y en consecuencia, podrían producirse

modificaciones en las características fisicoquímicas. Los crioprotectores o lioprotectores son frecuentemente añadidos a la formulación con la finalidad de proteger a las partículas durante el proceso de liofilización [67].

El polivinil alcohol (PVA), es uno de los tensoactivos más comúnmente usados en la preparación de NPs estables [68]. Este compuesto, forma una capa hidrófila en la superfície de las partículas, que proporciona estabilidad al sistema coloidal y mejorara su resistencia a la congelación y su redispersión después de la liofilización [69,70].

1.4. ESTRATEGIAS PARA FAVORECER LA BIODISPONIBILIDAD DE LOS FÁRMACOS DE ADMINISTRACIÓN TÓPICA.

1.4.1. Vehiculización de nanopartículas en hidrogeles bioadhesivos.

Los hidrogeles son redes poliméricas con una configuración tridimensional capaz de captar grandes cantidades de agua o fluidos biológica. Su afinidad para absorber el agua es atribuida a la presencia de numerosos grupos hidrófilos tales como, -OH, -CONH, -CONH2 y –SO3H en su estructura polimérica [71].

En general, los hidrogeles pueden clasificarse en bases a sus características, incluyendo la naturaleza de los grupos laterales (neutrales o iónicos), características mecánicas y estructurales, método de preparación (homopolímero o copolímero), estructura cristalina (amorfo, semicristalino, unido por puentes de hidrogeno, supramolecular e hidrocoloidal), y por su capacidad de respuesta al estímulo del entorno (pH, fuerza iónica, temperatura, etc.). Los hidrogeles poliméricos, también pueden clasificarse en dos grupos: geles preformados y geles de formación *in situ*. Adicionalmente, los geles hidrofílicos, de acuerdo a su origen pueden dividirse en: naturales, semisintéticos y sintéticos.

El carbomero es un hidrogel preformado de origen sintético, ampliamente utilizado en las preparaciones farmacéuticas, debido a que es química y biológicamente inerte y presenta excelentes características mucoadhesivas, mecánicas, organolépticas y biocompatibles.

Este polímero muestra una estructura en espiral en estado seco. Sin embargo, cuando es dispersado en agua, las cadenas del polímero se hidratan formándose uniones estrechas entre ellas por puentes de hidrogeno. Este gel hidrofílico presenta una elevada viscosidad a bajas concentraciones (0.5 – 1.0% p/v). Para obtener el máximo efecto espesante, la solución del polímero puede ser neutralizada con sustancias alcalinas tales como, hidróxido de sodio y/o trietanolamina. Las fuerzas repulsivas entre dos grupos adyacentes cargados negativamente a lo largo de las cadenas del polímero permiten que la espiral de la cadena se desenrolle, y en consecuencia que el polímero se humecta y se forme un gel con una estructura uniforme. El máximo espesor se obtiene generalmente cuando el pH de la solución del polímero está en el rango de 6 a 10 [72,73].

El mecanismo principal de liberación de los fármacos a partir de los hidrogeles es por difusión pasiva. La difusión del fármaco fuera de la matriz del hidrogel depende principalmente del tamaño de la malla dentro de la matriz del gel, el cual es afectado por factores tales como, el grado de reticulación, la estructura química de la composición de los monómeros y/o la intensidad de los estímulos externos [74].

Los sistemas nanoparticulares son considerados como vehículos apropiados para mejorar la biodisponibilidad de los fármacos. Sin embargo, una de las limitantes para la administración tópica de estos sistemas radica en la baja viscosidad de las suspensiones coloidales, lo que conduce a una rápida eliminación del fármaco después de la administración sobre la superficie ocular y/o dérmica. En este sentido, los suspensiones de nanopartículas frecuentemente son incorporadas en agentes gelifícantes, con el fin de incrementar la viscosidad de las suspensiones coloidales y obtener formulaciones con características reológicas apropiadas para prolongar el tiempo de contacto de fármaco en la superficie aplicada, favoreciendo la absorción del mismo, prolongando la duración del efecto terapéutico y reduciendo la frecuencia de aplicación. Por lo que, diferentes sistemas nanoparticulares destinados a la aplicación ocular y/o dérmica han sido incorporados en hidrogeles [75 - 77].

1.4.2. Promotores de la permeación de fármacos.

La estructura anatómica de las vías ocular y dérmica, constituyen una barrera importante, que limita la entrada o salida de los compuestos a través de estas estructuras. Promotores de la permeación de fármacos (también conocidos como, potenciadores o aceleradores de la absorción) han sido utilizados como una estrategia para disminuir de forma reversible, la resistencia de las barreras biológicas y favorecer la penetración de un gran número de fármacos. Aunque muchos productos químicos han sido evaluados como potenciadores de la penetración de los fármacos en piel humana o animales, hasta la fecha ninguno ha demostrado ser ideal. Algunas de las propiedades más deseables para los promotores de la penetración destinados a la aplicación tópica son:

- no tóxico, no irritante y no alergénico.

- No deben ejercer una actividad farmacológica dentro del cuerpo, es decir no debe unirse a los sitios receptores.

- Poseer una acción promotora reversible. Una vez, retirado de la superficie tópica, las propiedades de barreras biológicas deben recuperarse de manera rápida y completa.

- Los potenciadores de la penetración deben ser apropiados para la formulación en diversas preparaciones tópicas, por lo tanto debe ser compatible con excipientes y fármacos [78].

Entre los promotores de la permeación comúnmente usados se encuentran: el agua, sulfóxidos y químicos similares, azona, pirrolidona, ácidos grasos, alcoholes y glicoles, surfactantes, urea, aceites esenciales y terpenos y/o terpenoides y fosfolípidos. Entre ellos, la azona (1-dodecilazaciclohептan-2-ona o Laurocapram), fue la primer molécula diseñada como promotor de la permeación de la vía dérmica. La azona es un líquido incoloro, inodoro, con un punto de fusión de - 7°C, es suave y oleosa al tacto. Su estructura química, le

confiere un carácter lipofílico con un Log P octanol /agua cercano a 6.2. Es incompatible con la mayoría de los solventes orgánicos, incluyendo alcoholes y propilenglicol. La irritación y toxicidad causada por la azona es muy baja (La DL_{50} determinada en ratas por vía oral es de 9 g/Kg).

La azona ha sido utilizada en la vía tópica para incrementar el flujo de fármacos lipófilos e hidrófilos entre ellos: esteroides, antibióticos, antiinflamatorios y antivirales, etc. [79]. Así como otros potenciadores de la permeación, la eficacia de la azona como promotor de la permeación depende tanto de la concentración en la que se usa, como del vehículo desde donde se aplica. La azona puede ser usada en el ser humano de manera segura y efectiva en el rango de 1 al 10% [80], sin embargo, ha demostrado ser más eficaz a bajas concentraciones (0.1 – 5%). Aunque la azona ha sido utilizada por más de 25 años, su mecanismo de acción como promotor de la permeación aún sigue siendo investigado. Teniendo en cuenta que la estructura química de la azona posee numerosos grupos de cabeza polar y una cadena alquílica de lípidos, es probablemente que este compuesto pueda ejercer su efecto como potenciador de la absorción de los fármacos, a través de interacciones de los grupos lipídicos de su estructura con los estratos lipídicos de la superficie tópica. Así, las moléculas de azona puede disponerse de manera dispersa dentro de las capas lipídicas de las estructuras anatómicas de la vía tópica [79]. El extenso uso de azona como promotor de la permeación de fármacos, se pone de manifiesto en numeras investigaciones llevadas a cabo con diversos fármacos destinados a ser aplicados en las vías ocular y dérmica [77, 81 - 83].

2. OBJETIVOS

PLGA nanoparticles are one of the colloidal systems that have been most widely studied over the past few decades with the objective of improving drug targeting of tissues and organs and increasing drug bioavailability across biological membranes or reducing its toxicity. The growing use of these systems is due to their ability to improve the biopharmaceutical profile of the drug entrapped within the polymeric matrix of the NPs and, also due to the biodegradable and biocompatible properties of the PLGA. This polymer has been approved by the FDA for use in humans and they can effectively deliver the drug to a target site with a controllable degradation.

Pranoprofen is the drug that has been studied in this research. Although this drug has shown high anti-inflammatory and analgesic efficiency, the pharmaceutical use of pranoprofen is limited due to its inadequate biopharmaceutical profile. Therefore, the main purpose of the present investigation was to develop and optimize a new delivery system for PF- loaded PLGA NPs, suitable for the ocular and dermal route in the treatment and prevention of edema.

To reach this objective, this research has been developed as described below:

1. Preparation of the PF-loaded PLGA NPs by the solvent displacement technique and the optimization of these systems using a factorial design.

2. Physicochemical characterization of the polymeric NPs containing PF, analyzing their morphological and morphometric properties (average particle size and polydispersity index), the electrical charge of the nanospheres surface and the entrapment efficiency of the drug in the polymer.

3. To assess the physical stability of the optimized nanostructured systems over a short time period.

4. Freeze-drying of the optimized pranoprofen-loaded nanoparticles to ensure the long- term stability of these systems and to avoid the possible chemical instabilities (drug leakage) during storage.

5. Evaluation of the physical state of the PF and the possible interactions between drug and polymer of the nanospheres before and after freeze - drying, using X-ray spectroscopy, FTIR spectral measurements and DSC analysis.

6. Incorporation of the optimized nanoparticles containing PF into carbomer hydrogel in presence or absence of azone as penetration enhancer to obtaine a topical dosage form with a desired semisolid consistency, improve the biopharmaceutical profile of PF. Also, to facilitate the prolonged contact of the PF on biological membranes of the ocular and skin surface and improve its topical retention, thus enhancing anti-inflammatory and analgesic efficiency and improving patient compliance by reducing application frequency.

7. Physicochemical, morphological and rheological characterization of the semisolid formulations of pranoprofen.

8. To determine the *in vitro* release profile of pranoprofen from the optimized nanospheres (before and after freeze-drying) and from the semisolid formulations.

9. To evaluate *ex vivo* the corneal permeation, *in vivo* anti-inflammatory efficacy and *in vitro e in vivo* ocular tolerance of pranoprofen from the optimized nanostructured systems and from the formulation of the nanoparticles incorporated into hydrogel.

10. To assess *ex vivo* the skin permeation, *in vivo* anti-inflammatory efficacy and *in vivo* skin tolerance of pranoprofen from the optimized nanoparticles and from the semisolid formulation.

3. RESULTADOS

.

Los resultados obtenidos a través de los diferentes análisis llevados a cabo en la presente investigación, permitieron generar tres publicaciones científicas, en forma de artículos. Los títulos y autores de los mismos, se describen a continuación y al mismo tiempo, cada uno de estos artículos se acompaña de un breve resumen:

Artículo 1:

G. Abrego, H.L. Alvarado, M.A. Egea, E. Gonzalez-Mira, A.C. Calpena, M.L. García.

Design of nanosuspension and freeze-dried PLGA nanoparticles as a novel approach for ophthalmic delivery of pranoprofen. Journal of Pharmaceutical and Sciences 103 (2014) 3153 – 3164

Artículo 2:

G. Abrego, H.L. Alvarado, E. Souto, B. Guevara, L.H. Bellowa, A. Parra, A.C. Calpena, M.L. García.

Biopharmaceutical profile of pranoprofen-loaded PLGA nanoparticles containing hydrogels for ocular administration. European Journal of Pharmaceutics and Biopharmaceutics. http://dx.doi.org/10.1016/j.ejpb.2015.01.026

Artículo 3:

G. Abrego, H.L. Alvarado, E. Souto, B. Guevara, L.H. Bellowa, M.L. Garduño, M.L. García, A.C. Calpena.

Pranoprofen-loaded polymeric nanoparticles hydrogels for skin administration: *in vitro*, *ex vivo* and *in vivo* characterization. Nanotechnology.

Design of nanosuspensions and freeze-dried PLGA nanoparticles as a novel approach for ophthalmic delivery of pranoprofen

G. Abrego, H.L. Alvarado, M.A. Egea, E. Gonzalez-Mira, A.C. Calpena, M.L. Garcia. **Journal of Pharmaceutical and Sciences 103 (2014) 3153 – 3164.**

3.1. Design of nanosuspensions and freeze-dried PLGA nanoparticles as a novel approach for ophthalmic delivery of pranoprofen (Artículo 1).

Resumen

Se prepararon formulaciones de pranoprofeno asociado a una matriz de ácido poli-láctico-co-glicólico (PLGA) por la técnica de desplazamiento del disolvente, con la finalidad de mejorar el perfil biofarmacéutico de este fármaco. Las nanopartículas conteniendo pranoprofeno fueron optimizadas a través de un diseño factorial, evaluando la influencia de algunos factores (pH de la fase acuosa, la concentración del polímero, tensoactivo y fármaco) en las propiedades fisicoquímicas de las partículas. A partir de los resultados obtenidos, las formulaciones optimizadas fueron aquellas que se prepararon con un pH de la fase acuosa de 4.5 y 5.5; una concentración de pranoprofeno de 1.0 ó 1.50 mg/mL; tensoactivo 5, 10 ó 25 mg/mL y PLGA 9.0 ó 9.5 mg/mL. En estas condiciones, los sistemas nanoestructurados mostraron un tamaño de partícula apropiado para la administración ocular (alrededor de 350 nm) y una eficiencia de encapsulación del fármaco del 80%.

El ensayo de estabilidad a corto plazo de las NPs optimizadas reveló pequeñas variaciones en el perfil de retrodispersión, poniendo de manifiesto una ligera sedimentación de las NPs en el fondo del vial. La inestabilidad de las NPs, después de un largo período de almacenamiento, es uno de los principales problemas que limitan el uso de los sistemas coloidales. En este sentido, las NPs se liofilizaron con el objetivo de preservar las propiedades fisicoquímicas de las mismas. Las características morfométricas y el potencial zeta de las NPs (antes y después de liofilizar) fueron determinadas y comparadas. Los resultados obtenidos no mostraron modificaciones significativas entre los valores obtenidos para las NPs antes o después de liofilizar. Adicionalmente, las interacciones fármaco - polímero se determinaron a través de difracción de rayos X, espectroscopia infrarroja con transformada de Fourier (FTIR) y calorimetría diferencial de barrido (DSC), cuyos resultados revelaron la ausencia de interacciones y confirmaron que el fármaco se dispersó en el interior de la matriz polimérica.

Los perfiles de liberación *in vitro* de pranoprofeno desde las nanopartículas antes o después de liofilizar fueron similares entre sí, exhibiendo una liberación sostenida del fármaco, con una liberación rápida al inicio, debido a la cantidad PF presente en la superfície de las NPs, seguido por una fase de liberación lenta, correspondiente a la difusión del fármaco atrapado en el interior de las mismas.

Los resultados obtenidos a través del HET-CAM revelan una tolerancia ocular óptima para la NPs optimizadas, ya que no se detectó ninguna reacción de irritación a los 5 minutos de la prueba.

RESEARCH ARTICLE – *Pharmaceutics, Drug Delivery and Pharmaceutical Technology*

Design of Nanosuspensions and Freeze-Dried PLGA Nanoparticles as a Novel Approach for Ophthalmic Delivery of Pranoprofen

GUADALUPE ABREGO,[1,2] HELEN L. ALVARADO,[1,2] MARIA A. EGEA,[1] ELIZABETH GONZALEZ-MIRA,[1] ANA C. CALPENA,[2] MARIA L. GARCIA[1]

[1]Department of Physical Chemistry, Faculty of Pharmacy, University of Barcelona, Barcelona 08028, Spain
[2]Department of Biopharmacy and Pharmaceutical Technology, Faculty of Pharmacy, University of Barcelona, Barcelona 08028, Spain

Received 12 February 2014; revised 23 June 2014; accepted 3 July 2014

Published online 4 August 2014 in Wiley Online Library (wileyonlinelibrary.com). DOI 10.1002/jps.24101

ABSTRACT: Pranoprofen (PF)-loaded poly (lactic-*co*-glycolic) acid (PLGA) nanoparticles (NPs) were optimized and characterized as a means of exploring novel formulations to improve the biopharmaceutical profile of this drug. These systems were prepared using the solvent displacement technique, with polyvinyl alcohol (PVA) as a stabilizer. A factorial design was applied to study the influence of several factors (the pH of the aqueous phase and the stabilizer, polymer and drug concentrations) on the physicochemical properties of the NPs. After optimization, the study was performed at two different aqueous phase pH values (4.50 and 5.50), two concentrations of PF (1.00 and 1.50 mg/mL), three of PVA (5, 10, and 25 mg/mL), and two of PLGA (9.00 and 9.50 mg/mL). These conditions produced NPs of a size appropriate particle size for ocular administration (around 350 nm) and high entrapment efficiency (80%). To improve their stability, the optimized NPs were lyophilized. X-ray, FTIR, and differential scanning calorimetry analysis confirmed the drug was dispersed inside the particles. The release profiles of PF from the primary nanosuspensions and rehydrated freeze-dried NPs were similar and exhibited a sustained drug delivery pattern. The ocular tolerance was assessed by an HET-CAM test. No signs of ocular irritancy were detected (score 0). © 2014 Wiley Periodicals, Inc. and the American Pharmacists Association J Pharm Sci 103:3153–3164, 2014

Keywords: pranoprofen; polymeric drug delivery system; nanoparticles; factorial design; poly (lactic/glycolic) acid (PLGA); freeze-drying/lyophilization; stability; biodegradable polymers

INTRODUCTION

Pranoprofen (PF) is a nonsteroidal anti-inflammatory drug that can be used as a safe and effective alternative anti-inflammatory treatment following strabismus and cataract surgery.[1–3] PF has the beneficial effect of reducing the ocular signs and symptoms of dry eye and decreasing the inflammatory markers of conjunctival epithelial cells.[4] Its efficacy is equivalent to moderate-potency corticosteroids, but it has a better safety profile. It should be considered for the treatment of chronic conjunctivitis of presumed nonbacterial origin.[5] Although this drug has shown high anti-inflammatory and analgesic efficiency, the pharmaceutical use of PF is limited because of its inadequate biopharmaceutical profile. PF has a short plasmatic half-life, low water solubility, and is unstable in aqueous solution, particularly when exposed to light.[6,7] PF is commercially available such as eye drops (PF 0.1%). However, this conventional dosage form cannot be considered optimal in the treatment of ocular diseases because of the fact that most of the drug is removed from the surface of the eye, following the instillation, by various mechanisms (tear dilution and tear turn over). Moreover, the relatively impermeable corneal barrier restricts the entry of foreign substances. As a result, less than 5% of the administered drug penetrates the cornea and reaches intraocular tissues.[8] Polymeric nanoparticles (NPs) are one of the colloidal systems that have been most widely studied over the past few decades with the objective of improving drug targeting of tissues and organs and increase drug bioavailability across biological membranes. Biodegradable polymers, such as poly (lactic-*co*-glycolic) acid (PLGA), have been widely used in drug delivery research, in part due to their approval by the United States Food and Drug Administration for use in humans and they can effectively deliver the drug to a target site with a controllable degradation.[9]

The instability of the NPs after a long storage period is one of the main problems that limit the use of these systems. To ensure the long-term preservation of the physicochemical integrity of these colloidal systems, the water contained in the formulations must be removed. Lyophilization or freeze-drying is one of the procedures commonly employed to this end. Freezing is the first step of the lyophilization process. The liquid suspension is frozen and then the water is removed by sublimation and desorption under vacuum. Lyophilization could generate considerable stresses that could destabilize NPs, and modify their physicochemical characteristics. Thus, to avoid such possible modifications, cryoprotectants or lyoprotectants are usually added to the formulation.

Polyvinyl alcohol (PVA) is a hydrophilic, biocompatible polymer used as surfactant to produce stable NPs.[10] PVA forms a hydrophilic layer at the NP surface, which provides stability to the colloidal system and improves their resistance to freezing as well as their redispersion after freeze-drying.[11–13]

The objective of this study was to develop and optimize a new delivery system for PF-loaded PLGA NPs, suitable for the ocular route, prepared by the solvent displacement technique.[14] After selecting the critical formulation variables that affect mean particle size, zeta potential (ZP), and drug loading

Correspondence to: Ana C. Calpena (Telephone: +34-934024560; Fax: +34-934024563; E-mail: anacalpena@ub.edu)

Journal of Pharmaceutical Sciences, Vol. 103, 3153–3164 (2014)

efficiency, a four-factor five-level central rotatable composite design was employed to plan and perform the experiments. The physical stability of the NPs was also evaluated. As an attempt to improve the stability of the systems, lyophilization studies were carried out. Furthermore, the physical state of the PF and possible interactions between the drug and the polymer were studied, as well as *in vitro* release and ocular tolerance of the optimized vehicle.

MATERIALS AND METHODS

Materials

Pranoprofen and Oftalar® were kindly supplied by Alcon Cusi (Barcelona, Spain); PLGA Resomer® 753S was obtained from Boehringer Ingelheim (Ingelheim, Germany); PVA with 90% hydrolization was obtained from Sigma–Aldrich (St. Louis, Missouri). The purified water used in all the experiments was obtained from a MilliQ System. All the other chemicals and reagents used in the study were of analytical grade.

Methods

Preparation and Optimization of PLGA NPs

The NPs were obtained by the solvent displacement technique described by Fessi et al.[14] PLGA (80–100 mg) and PF (0–20 mg) were dissolved in 5 mL of acetone. This organic phase was poured, under moderate stirring into 10 mL of an aqueous solution of PVA (5–25 mg/mL) adjusted to the desired pH value (2.5–6.5). The acetone was then evaporated, and the NPs dispersed were concentrated to 10 mL under reduced pressure (Büchi B-480 Flawil, Switzerland).

A factorial design is frequently used to plan research because it provides maximum information, requiring the minimum number of experiments.[15] A four factor, five-level central composite rotatable design 2^4 + principal was used to study the main effects and interactions of four factors on average particle size (*Z* Ave), polydispersity index (PI), ZP, and entrapment efficiency (EE). This central composite design consisted of three groups of design points, including two-level factorial axial and center design points. The factors or independent variables studied were PF concentration (cPF), PVA concentration (cPVA), PLGA concentration (cPLGA), and aqueous phase pH. They were studied at five different levels coded as $-\alpha$, -1, 0, 1, and $+\alpha$. The value of alpha (2) was calculated to meet the design rotatability (Table 1).

Effects and interactions between factors were calculated. To determine the effect of a factor, x, (Ex) the following expression was used:

$$Ex = \frac{\sum x(+) - \sum x(-)}{n/2} \quad (1)$$

Table 1. Factors and their Corresponding Levels in Experimental Design

Factor	−2	−1	0	+1	+2
cPF (mg/mL)	0.00	0.50	1.00	1.50	2.00
cPVA (mg/mL)	5.00	10.00	15.00	20.00	25.00
cPLGA (mg/mL)	8.00	8.50	9.00	9.50	10.00
Aqueous phase pH	2.50	3.50	4.50	5.50	6.50

where Σx (+) is the sum of the factors at their highest level (+2), Σx (−) is the sum of the factors at their lowest level (−2), and $n/2$ is half of the number of measurements used in the calculation.

Interactions between factors were also calculated. To estimate an interaction between two factors, one has to calculate the effect of the first factor at the lowest level of the second factor and subtract this from the effect of the first factor at the highest level of the second factor. An interaction between two factors is symbolized as factor1 × factor2.

The experimental responses studied were the result of the individual influences and interactions of the four factors. The responses were modeled by the following polynomial equation:

$$\begin{aligned} Y = {} & \beta_0 + \beta_1 X_1 + \beta_2 X_2 + \beta_3 X_3 + \beta_4 X_4 \\ & + \beta_{11} X_1^2 + \beta_{22} X_2^2 + \beta_{33} X_3^2 + \beta_{44} X_4^2 \\ & + \beta_{12} X_1 X_2 + \beta_{14} X_1 X_4 + \beta_{23} X_2 X_3 \\ & + \beta_{24} X_2 X_4 + \beta_{34} X_3 X_2 \end{aligned} \quad (2)$$

where Y is the measured response, β_0 is the intercept term, β_is (for i = 1–4) are the linear effects, β_{ij}s the quadratic effects, β_{ij}s (for ij = 1–4, $i < j$) the interaction between the ith and jth variables.

ANOVA identified the significance of the effects and the interactions between them. p Values of less than 0.05 were considered to be statistically significant.

According to the composite central design matrix, generated by Statgraphics Plus 5.1 (Sigma Plus) Software, a total of 26 experiments, including 16 factorial points, eight axial points, and two replicated center points, are summarized in Table 2.

Physicochemical Characterization of the NPs

Particle Size and ZP. Z Ave and ZP of the NPs were determined by photon correlation spectroscopy (PCS) with a Zetasizer Nano ZS (Malvern Instruments, Malvern, UK) at 25°C using disposable quartz cells and disposable folded capillary zeta cells (Malvern Instruments), respectively. In all the determinations, the samples were diluted with MilliQ water (1:20). The reported values are the mean ± SD of at least three different batches of each formulation. PCS is referred to as dynamic light scattering and quasi-elastic light scattering when it is used to determine rapidly the particle diameter and size distribution expressed as the PI. The movement of particles in water is inversely proportional to their size, which can therefore be identified by analyzing the time dependency of the light intensity fluctuations caused by scattering off the particles when they are illuminated with a laser beam.[16] The ZP of NPs is a measure of the electrical charge at the surface of nanospheres, and is an indirect measure of their physical stability. ZP was calculated using the Helmholtz–Smoluchowski equation.[17]

Entrapment Efficiency. The EE of PF in the NPs was determined indirectly by measuring the concentration of the free drug in the dispersion medium. The nonentrapped PF was separated using a filtration/centrifugation technique with Ultracel–100K (Amicon® Ultra; Milipore Corporation, Billerica, Massachusetts) centrifugal filter devices at 1814 g. for 30 min at 4°C (Heraeus, Multifuge 3 L-R, Centrifuge. Osterode, Germany). Each sample was diluted with MilliQ water (1:20) prior to filtration/centrifugation. The EE was calculated using the following

 DOI 10.1002/jps.24101

Table 2. Coded Values and Measured Responses of the Four Factors: cPF, cPVA, cPLGA, and Aqueous Phase pH

	Coded Levels of Factors				Measured Responses			
Factorial	cPF (mg/mL)	cPVA (mg/mL)	cPLGA (mg/mL)	pH	Mean Size (nm) ± SD	Polidispersity Index ± SD	Zeta Potential (mV) ± SD	Entrapment Efficiency (%) ± SD
F1	−1	−1	−1	−1	566.50 ± 8.05	0.286 ± 0.02	−8.28 ± 0.71	87.69 ± 0.13
F2	1	−1	−1	−1	597.60 ± 3.12	0.335 ± 0.01	−8.17 ± 0.32	90.26 ± 1.18
F3	−1	1	−1	−1	605.00 ± 6.28	0.256 ± 0.01	−6.00 ± 0.48	82.57 ± 2.01
F4	1	1	−1	−1	611.20 ± 7.21	0.368 ± 0.02	−6.80 ± 0.18	90.85 ± 1.25
F5	−1	−1	1	−1	539.00 ± 8.11	0.227 ± 0.03	−9.27 ± 0.31	85.14 ± 1.82
F6	1	−1	1	−1	532.10 ± 6.70	0.231 ± 0.03	−7.31 ± 0.07	89.29 ± 0.51
F7	−1	1	1	−1	784.30 ± 5.63	0.391 ± 0.02	−5.91 ± 0.06	89.93 ± 1.98
F8	1	1	1	−1	641.50 ± 6.26	0.363 ± 0.01	−5.99 ± 0.36	89.01 ± 0.56
F9	1	1	1	1	348.30 ± 2.12	0.106 ± 0.03	−7.50 ± 0.16	66.50 ± 0.07
F10	−1	1	1	1	280.10 ± 1.50	0.098 ± 0.03	−7.92 ± 0.15	49.79 ± 0.62
F11	1	−1	1	1	324.30 ± 4.03	0.091 ± 0.01	−7.41 ± 0.56	80.02 ± 1.33
F12	−1	−1	1	1	265.40 ± 5.75	0.073 ± 0.02	−9.61 ± 0.31	62.05 ± 2.18
F13	1	1	−1	1	408.90 ± 4.67	0.216 ± 0.01	−6.68 ± 0.15	45.54 ± 0.23
F14	−1	1	−1	1	318.40 ± 3.11	0.207 ± 0.02	−7.44 ± 0.19	39.79 ± 1.77
F15	1	−1	−1	1	327.60 ± 1.91	0.095 ± 0.01	−7.22 ± 0.54	69.51 ± 0.32
F16	−1	−1	−1	1	269.90 ± 1.25	0.096 ± 0.01	−11.20 ± 0.53	72.74 ± 1.15
F17	2.0	0	0	0	433.90 ± 5.15	0.224 ± 0.01	−6.97 ± 0.14	77.23 ± 0.52
F18	−2.0	0	0	0	326.70 ± 2.78	0.013 ± 0.03	−8.54 ± 0.12	00.00 ± 0.00
F19	0	2.0	0	0	368.20 ± 2.65	0.097 ± 0.01	−6.25 ± 0.34	80.29 ± 1.25
F20	0	−2.0	0	0	343.80 ± 2.74	0.085 ± 0.03	−8.50 ± 0.61	80.34 ± 0.32
F21	0	0	2.0	0	421.00 ± 3.99	0.153 ± 0.02	−7.63 ± 0.15	77.15 ± 1.29
F22	0	0	−2.0	0	340.40 ± 4.66	0.118 ± 0.01	−8.06 ± 0.30	68.48 ± 2.45
F23	0	0	0	2.0	321.40 ± 1.47	0.224 ± 0.01	−12.92 ± 0.29	58.70 ± 0.25
F24	0	0	0	−2.0	611.80 ± 3.29	0.301 ± 0.04	−2.15 ± 0.13	86.39 ± 1.36
F25	0	0	0	0	354.60 ± 2.62	0.146 ± 0.02	−6.90 ± 0.15	62.01 ± 0.85
F26	0	0	0	0	357.80 ± 3.40	0.147 ± 0.02	−6.58 ± 0.22	62.09 ± 1.30

equation:

$$\text{EE}\,(\%) = \frac{\text{Total amount of PF} - \text{free PF}}{\text{Total amount of PF}} \times 100 \qquad (3)$$

The EE (%) was determined by HPLC using a method previously validated in our laboratory. The HPLC system consisted of a Waters 1525 pump (Waters, Milford, Connecticut) with a UV-Vis 2487 detector (Waters), a flow rate of 1 mL/min and wavelength of 245 nm were used with a (Kromasil®, 100–5C18, 4.6 × 100 mm^2) column. The mobile phase consisted of methanol:glacial acetic acid 5% (45:55, v:v).

Determination of Residual PVA

The amount of PVA associated with the NPs was determined by a colorimetric method, through the formation of a stable complex between two adjacent hydroxyl groups of PVA and an iodine molecule in the presence of boric acid.[18] Briefly, 7 mL of the NP suspension was ultracetrifuged at 99276 g for 2 h (Optima L90K ultracentrifuge; Beckman Coulter. USA). The NP pellet was washed twice with 6 mL of purified water. Then, the pellet was dried to constant weight, treated with 2 mL of 2 N NaOH for 12 h under stirring, and neutralized with 2 N HCL. A volume of 3 mL of boric acid solution (4% w/w) and 0.5 mL of iodine solution (1.27% iodine and 2.5% potassium iodide in water w/v) was added and the volume was made up to 10 mL with water. A standard PVA solution was prepared under the same conditions. The absorbance of these samples was measured at wavelength of 640 nm.

Storage Stability

The physical stability of the NPs was assessed after 1, 8, 15, and 30 days of storage at 4°C. The determinations were performed at 25°C, three times over a period of 10 min, measuring the variations of the backscattering (BS) signal in a TurbiScanLab® (Formulaction, L'Union, France). This instrument is able to detect destabilization phenomena much earlier than the operator's naked eye, especially for concentrated and optically dense media. Each undiluted formulation (15 mL) was placed in a cylindrical glass measuring cell, which was completely scanned by a reading head. The reading head consists of a pulsed near-infrared light source (λ = 880 nm) and two synchronous transmission (T) and BS detectors. The T detector receives the light transmitted through the sample (135° from the incident radiation), whereas the BS detector receives the light scattered backward by the sample.

The TurbiScanLab®, based on the measurement of the BS and T signals, provides information on the type of destabilization process occurring: particle migration (creaming or sedimentation) and particle size variation (flocculation or coalescence), reversible and irreversible processes, respectively. The BS signal is graphically reported as a positive (BS increase) or negative (BS decrease) peak. The migration of particles to the top of the cell leads to a concentration decrease at the bottom, shown as a decrease in the BS signal (negative peak) and vice versa for the phenomenon occurring at the top of the cell. If the BS profiles have a deviation of $\leq \pm 2\%$, it can be considered that there are no significant variations in particle size. Variations more than ±10 indicate unstable formulations.[19]

Freeze-Drying NPs

An aliquot of 2.0 mL of the optimized NP suspension was transferred to a glass vial. The sample was frozen at –40°C for 4 h. To remove the frozen water by sublimation (primary drying), the samples were heated to 5°C for 25 h. Once, the primary drying was completed, secondary drying was performed at 30°C for 4 h. The NPs were lyophilized using a freeze-drying system (A Telstar Lyobeta, equipped with Pirani and capacitance vacuum gauges and a SCADA system) at 1.3×10^{-3} mbar. The freeze-dried cake was rehydrated with 2 mL of water by manual shaking and then the properties of the NPs were measured as described above.

Interaction Studies

The physical state of the PF and the possible interactions between the drug and the polymer were assessed by X-ray spectroscopy, FTIR spectral measurements, and differential scanning calorimetry (DSC) analysis.

In order to remove the water, the suspensions of the NPs were ultracentrifuged at 99276 g for 2 h (Optima L90K, ultracentrifuge; Beckman, Coulter. USA). The pellet was then dried to constant weight in a desiccator. This procedure was not applied to the freeze-dried NPs because the water was had been removed during the lyophilization process.

X-ray spectroscopy was used to analyze the state (amorphous or crystalline) of the PF-loaded NPs before and after the lyophilization process. Powder of PF, PVA, PLGA, and NPs was sandwiched between 3.6 μm films of polyester and exposed to CuKα radiation (45 kV, 40 mA, $\lambda = 1.5418$ Å) in the range (2θ) from 2° to 60° with a step size of 0.026° and a measuring time of 200 s per step.

FTIR spectra of PF, PVA, PLGA, and PF-loaded NPs before and after the lyophilization process were obtained using a Thermo Scientific Nicolet iZ10 with an ATR diamond and DTGS detector. The scanning range was 525–4000 cm^{-1}.

Differential scanning calorimetry analysis was performed using a DSC823e System (Mettler-Toledo, Barcelona, Spain). A pan with indium (purity ≥ 99.95%; Fluka, Switzerland) was used to check the calibration of the calorimetric system and an empty pan was used as a reference. The DSC measurements were carried out on the PF-loaded NPs before and after lyophilization. Samples (2.32–2.95 mg) of the NPs were heated from 10°C to 225°C at 2°C/min under a nitrogen atmosphere. Data were evaluated from the peak areas using the Mettler STARe V 9.01 DB software (Mettler-Toledo).

In Vitro Release Study

An *in vitro* release study of PF from the primary nanosuspensions and rehydrated freeze-dried NPs was performed in Franz diffusion cells.[20] These cells consist of a donor and a receptor chamber between which a membrane is positioned. A dialysis membrane (Dialysis Tubing Visking; Medicell International Ltd., London, UK) was used. The membrane was hydrated for 24 h before being mounted in the Franz diffusion cell. The experiment was performed under "sink condition". The F11 (PF 1.5 mg/mL), F19 (1.0 mg/mL), and F20 (1.0 mg/mL) formulations were compared with commercial eye drops (Oftalar®, PF 1 mg/mL) and the free drug (1 mg/mL) in phosphate buffer solution (PBS) at pH 7.4. A volume of 200 μL of these samples was placed in the donor compartment and the receptor compartment was filled with PBS at pH 7.4 kept at 32°C ± 0.5°C and stirred continuously. Samples of 300 μL were withdrawn from the receptor compartment at fixed times and replaced by an equivalent volume of fresh PBS at the same temperature. The concentration of PF released was measured as described previously for EE. Values are reported as the mean ± SD of three replicates.

The amount of PF released was fitted to the following kinetic models[21]:

$$\text{Zero} - \text{Order} : \%R_t/R_\infty = k \times t \tag{4}$$

$$\text{First} - \text{Order} : \ \%R_t/R_\infty = 1 - e^{-k \times t} \tag{5}$$

$$\text{Higuchi} : \ \%R_t/\%R_\infty = k \times t^{1/2} \tag{6}$$

$$\text{Korsmeyer} - \text{Peppas} : \ \%R_t/\%R_\infty = k \times t^n \tag{7}$$

where $\%R_t$ is the percentage of the drug released at time t, $\%R_\infty$ is the total percentage of drug released, $\%R_t/\%R_\infty$ is the fraction of drug released at time t, k is the release rate constant, and n is the diffusion release exponent that can be used to characterize the different release mechanisms; $n \leq 0.5$ (Frickian diffusion), $0.5 < n < 1.0$ (anomalous transport), and $n \geq 1$ (case II transport, i.e., zero-order release). A nonlinear least-squares regression was performed using the WinNonLin® software (WinNonLin® professional edition version 3.3 and Graphpad prism version 6 Demo) and the model parameters were calculated. Akaike's information criterion (AIC) was determined for each model as an indicator of the model's suitability for a given dataset.[22] The kinetic models used to adjust the amount of PF released in this study were selected as they are the most common models used in the literature of drug delivery system.

In Vitro Ocular Tolerance

The ocular tolerance of the NPs was assessed by the HET-CAM test. This is an alternative to animal testing (Draize test) described by Luepke.[23] To perform it, the shell and the inner membrane of 10-day-oldchicken eggs were previously removed, so that the CAM that separates the embryo from the air chamber was visible, according to the Invittox protocol[24] and the Journal officiel de la République Française.[25] Tolerance was assessed by testing six eggs for each sample, using two eggs treated with 0.1 N NaOH and two treated with 1% sodium lauryl sulfate solution as positive controls. After exposing the CAM and rinsing it with PBS at pH 7.4, 300 μL of the test solution was applied to the CAM. The intensity of the reaction was semi-quantitatively assessed on a scale from 0 (no reaction) to 3 (strong reaction). The time of the appearance and the intensity of any reactions that occurred within 5 min were recorded. The ocular irritation index (OII) was then calculated using the following equation:

$$\text{OII} = \frac{(301 - h) \times 5}{300} + \frac{(301 - l) \times 7}{300} + \frac{(301 - c) \times 9}{300} \tag{8}$$

where h is the time (in seconds) until the start of a hemorrhage, l until the start of lysis, and c until the coagulation. The following

DOI 10.1002/jps.24101

Table 3. *p* Value Obtained from ANOVA Statistical Analysis of Effect of Independent Variables on the Physicochemical Properties of the NPs

Evaluated Factors and their Interactions	*p* Value			
	Z Ave	PI	ZP	EE
A: PF	0.34	0.68	0.24	0.03
B: PVA	0.16	0.19	0.00	0.36
C: PLGA	0.64	0.64	0.90	0.57
D: pH	0.00	0.00	0.00	0.01
AB	0.67	0.92	0.39	0.91
AC	0.60	0.64	0.71	0.73
AD	0.24	0.77	0.57	0.74
BC	0.59	0.77	0.87	0.57
BD	0.44	0.95	0.97	0.25
CD	0.56	0.56	0.58	0.69

classification was used: OII ≤ 0.9: slightly irritating; 0.9 ≤ OII ≤ 4.9: moderately irritating; 4.9 ≤ OII ≤ 8.9: irritating; 8.9 ≤ OII ≤ 21: severely irritating.

RESULTS AND DISCUSSION

Physicochemical Characterization of the NPs

Using a 2^4 central composite factorial design, the effect of the independent variables on the physicochemical properties of the NPs was studied (Tables 1 and 2).

The particle size of formulations intended for ocular instillation is of crucial importance and should not exceed 10 μm, larger sizes may cause a scratching feeling of a foreign body in the eye and, would therefore, jeopardize patient comfort.[26,27] There are other considerations regarding particle size, such as the fact that smaller particles have relatively more surface area, which can lead to faster release of the entrapped drug, and can also play an important role in the cellular uptake.[28,29] The Z Ave and PI values of the 26 formulations varied from 265.40 ± 5.75 to 784.30 ± 5.63 nm and from 0.013 ± 0.02 to 0.391 ± 0.02, respectively (Table 2), indicating that they are suitable for ocular administration.

ANOVA statistical analysis was performed to identify the effect of the independent variables on Z Ave, PI, ZP, and EE. Table 3 displays the *p* values obtained from the ANOVA analysis.

Quadratic polynomial equations were generated to establish the relationship between the independent variables and the properties of the NPs. Figures 1 and 2 show the response surface plots as a graphical representation of these equations.

According to Table 3, the only factor that had a significant effect (p value < 0.05) on Z Ave and PI was the aqueous phase pH (Figs. 1a and 1b, respectively). There was a trend toward smaller particle and a lower PI as pH varied from 4.5 to 6.5, whereas a significant increase in particle size and PI was observed (Table 2) at pH values lower than p*Ka* (4.35).

Another important physicochemical property of NPs is ZP. This is a measure of the particle charge and can influence both the stability of the particle and its mucoadhesion. Electrostatic repulsion between particles with the same polarity of electrical charge prevents aggregation.[30] All the formulations had a net negative charge with ZP values ranging from –2.15 ± 0.13 to –12.92 ± 0.29 mV (Table 2). The ANOVA (Table 3) revealed the

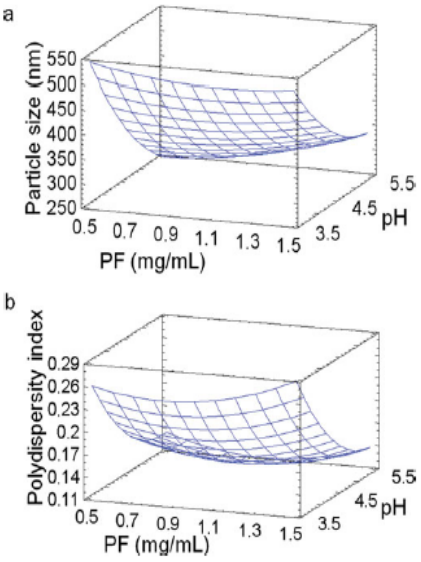

Figure 1. Response surface plot of the effect of the aqueous phase pH on the Z Ave and PI. (cPLGA = 9.0 mg/mL; cPVA = 15.0 mg/mL), (a) Z Ave (nm) = 1962.42–340.55 cPF – 525.31 pH + 70.68 cPF^2 + 39.24 pH^2 + 51.74 cPF pH. (b) PI = 1.19–0.12 cPF – 0.37 pH + 0.10 cPF^2 + 0.04 pH^2 –0.01 cPF pH.

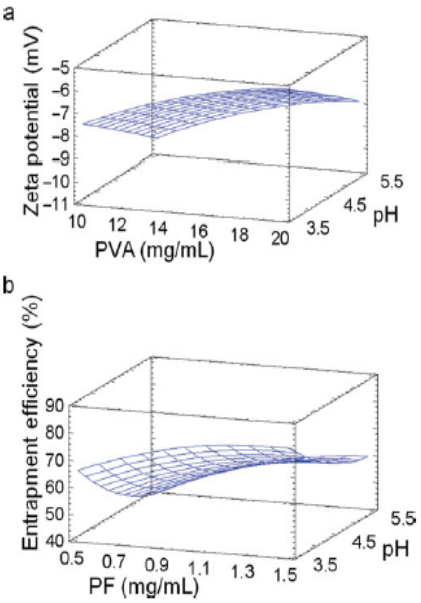

Figure 2. Response surface plot of the (a) effect of the aqueous phase pH and cPVA on the ZP. (cPLGA = 9.0 mg/mL; cPF = 1.0 mg/mL), ZP (mV) = –9.25 + 0.73 cPVA – 1.01 pH – 0.02 $cPVA^2$ + 0.04 pH^2 + 0.01 cPVA pH. (b) effect of the aqueous phase pH and cPF on entrapment efficiency. (cPLGA = 9.0 mg/mL; cPVA = 15.0 mg/mL). EE (%) = 173.24 + 39.72 cPF – 50.63 pH – 17.79 cPF^2 + 4.04 pH^2 + 2.89 cPF pH.

significant influence ($p < 0.05$) of PVA and the aqueous phase pH on ZP, but there was no significant interaction between them. Figure 2a shows the change in the ZP values of the NPs with regard to different cPVA and aqueous phase pH values, it can be observed that the ZP of the formulations increased by increasing cPVA at lower pH values.

The ZP values could be attributed to the effective adsorption of PVA onto the NP surface, as well as the uncapped carboxyl groups of the PLGA polymer. PLGA NPs are known to be negatively charged as a result of the presence of these ionized carboxyl groups. The presence of an amphiphilic polymer, such as PVA, forms a stable network on the polymer surface. This network shields the surface charge and moves the shear plane outward from the particle surface resulting in a slightly negative ZP.[31]

Regarding the EE of the formulations containing PF, ranged from 40% to 91% of PF incorporated into the PLGA NPs (Table 2). The ANOVA (Table 3) shows that both, aqueous phase pH and cPF, have a significant effect ($p < 0.05$) on the EE, but their interaction is not statistically significant. As can be observed in Figure 2b, increasing cPF at a pH value lower than p*Ka* lead to higher EE. Such a high incorporation could be explained by the fact that at pH values lower than p*Ka*, the drug entrapped within the NPs is in its nondissociated form that exhibits greater polymer affinity, resulting in higher drug retention in the hydrophobic NP matrix.[32] Otherwise, when the pH values increase, probably there are more ionized molecules. For this reason, less drug could be retained in the hydrophobic NP matrix, leading to a slight decrease in the EE of PF.[27] Therefore, the determination of an optimal pH value of the water phase is crucial because it can affect the drug ionization and, consequently, its polymer affinity, as well as, according to the factorial design results, modifying the Z Ave and PI of the NPs.[33,34]

In accordance with the objective of this study and the factorial design results, the F11, F19, and F20 formulations showed the best Z Ave and PI values with a percentage of incorporated PF in the polymeric matrix (EE) of around 80%. These formulations were selected to carry out studies of physical stability, lyophilization, physicochemical interactions, *in vitro* PF release from the NPs and, finally, *in vitro* ocular tolerance tests to confirm their safety.

Determination of Residual PVA

The F11, F19, and F20 NPs were prepared with a cPVA of 10, 25, and 5 mg/mL, respectively. The amount of PVA remaining on the NP surface was determined in the NP pellet after two washes. The PVA percentages associated with F11, F19, and F20 NPs were 1.84%, 4.27%, and 0.64%, respectively. These results suggest that the amount of PVA adsorbed onto the NP surface increased as the aqueous phase cPVA increased. The same trend has been reported by other authors.[31,35] It has been described that a fraction of the PVA used in the formulation remains associated with the NP surface, despite repeated washing. This could be attributed to that the hydroxyl groups of the PVA molecules being fixed to the acetyl groups of the PLGA via hydrophobic bonding.[36] Those segments of PVA would penetrate into the organic phase and remain trapped within the polymeric matrix of the NPs. The binding of PVA to the particle surface is likely to occur when the organic solvent is removed from the interface at which interpenetration of PVA and PLGA molecules takes place.[31]

Storage Stability

The physical stability of the optimized formulations was assessed at 25°C, after 1, 8, 15, and 30 days storage at 4°C. A TurbiScanLab® was used to determine destabilization processes, such as particle migration and particle size variation. Figure 3 shows the BS profile of the formulations assayed.

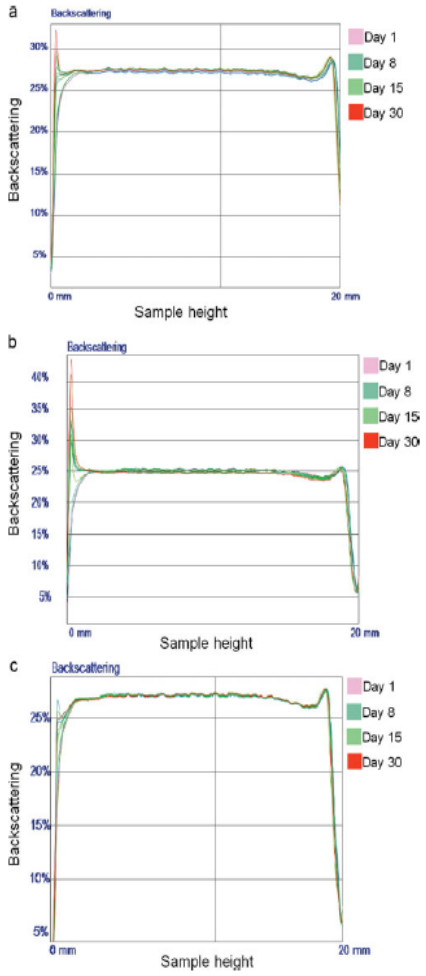

Figure 3. Backscattering profiles of (a) F11, (b) F19, and (c) F20 NPs as a function of time, measured through the height (mm) of the sample cell, analyzed at 1, 8, 15, and 30 days storage at 4°C.

A change in BS, specifically an increase on the left of the graph for the F11, F19, and F20 formulations, was observed (Fig. 3), which indicates particle migration to the bottom of the cell: a sedimentation process. This slight destabilization observed in the profiles of F11 (Fig. 3a) and F20 (Fig. 3c) was reversible and quickly disappeared after shaking. In contrast, the BS profiles of F19 (Fig. 3b), revealed variations of more than to ±10%, 30 days after production, indicating the low stability of this formulation.

In an attempt to overcome these physical instability problems as well as possible chemical instabilities (drug leakage) during storage, the freeze-drying technique was used.

Freeze-drying NPs

After lyophilization, the samples did not show any sign of collapse and all the freeze-dried cakes were white and easily rehydrated by manual shaking. The physicochemical properties of the primary nanosuspensions and rehydrated freeze-dried

DOI 10.1002/jps.24101

Table 4. Physicochemical Characterization of the NPs Before and After Freeze-Drying

	Before Freeze-Drying			After Freeze-Drying		
Formulation	Mean Size (nm) ± SD	Polidispersity Index ± SD	Zeta Potential (mV) ± SD	Mean Size (nm) ± SD	Polidispersity Index ± SD	Zeta Potential (mV) ± SD
F11	324.30 ± 4.03	0.091 ± 0.01	−7.41 ± 0.56	317.1 ± 0.98	0.096 ± 0.02	−6.86 ± 0.62
F19	368.20 ± 2.65	0.097 ± 0.01	−6.25 ± 0.34	360.7 ± 1,32	0.098 ± 0.03	−5.07 ± 0.23
F20	343.80 ± 2.74	0.085 ± 0.03	−8.50 ± 0.61	338.5 ± 1.90	0.132 ± 0.01	−3.43 ± 0.28

formulations were evaluated to study their physical stability (Table 4).

The results given in Table 4 show that the Z Ave of the rehydrated freeze-dried NPs were similar to those of the primary formulations, with PI values remaining in the range for monodisperse systems (PI < 0.1). Slight variations in the ZP values of the F11 and F20 NPs assessed before and after the lyophilization process were observed; however, due to the presence of PVA that provides a steric stabilization, these changes were not considered to impair the physical stability of these systems.

According to these data, optimal freeze-dried NPs were obtained as there were no signs of collapse or aggregation. These results suggest that the PVA used in the preparation of the formulations as a steric stabilizer also has cryoprotective properties afforded by its high molecular weight and, thus, the steric stabilizer layer is large enough to prevent NP agglomeration during the freezing process, which is the most critical step in the lyophilization. In addition, the presence of PVA on the NP surface favors the appropriate rehydration; this can be attributed to the hydrophilicity of PVA molecules.[11]

Interaction Studies

Since the physical state of the drug and the polymer will have an influence on the *in vitro* and *in vivo* release characteristics of the drug, the physical state of the PF within the NPs and the possible interactions between drug and polymer was assessed by X-ray spectroscopy, FTIR spectral measurements, and DSC analysis.

Figure 4 shows the X-ray diagrams of PF, PLGA, PVA, and PF-loaded NPs before and after freeze-drying.

The X-ray spectrum of PLGA shows it is amorphous, whereas PVA is a semipartially crystaline polymer with a broad peak at $2\theta = 19.5^\circ$ and weak bulges at $2\theta = 11.02^\circ$ and 40.6°.[37] Pure PF is a crystalline substance; in Figure 4, it has sharp peaks in the range of $2\theta = 8^\circ$–32°. The analysis of the pattern of PF in the NPs (F11, F19, and F20) shows that they consist of a combination of two structures (PF and part of the polymer), although the original structure of the polymer is amorphous (Fig. 4). The intensity of some of the peaks of crystalline PF present in the NPs before freeze-drying slightly increased when cPF increased from 1.0 mg/mL (F19 and F20) to 1.5 mg/mL (F11). Some authors have reported that when the amount of drug surpasses drug solubility in the polymer, part of the drug precipitates as nanocrystals.[38–40] The diffractograms for all the lyophilized NPs (Fig. 4) reveal an amorphous shape; there are many small peaks and an amorphous protuberance that could be attributed to the PVA layer on the surface of the NPs forming an amorphous glass state at low temperature during the lyophilization process and hydrogen bonds forming between the polymer and water molecules that prevent aggregation during freeze-drying.

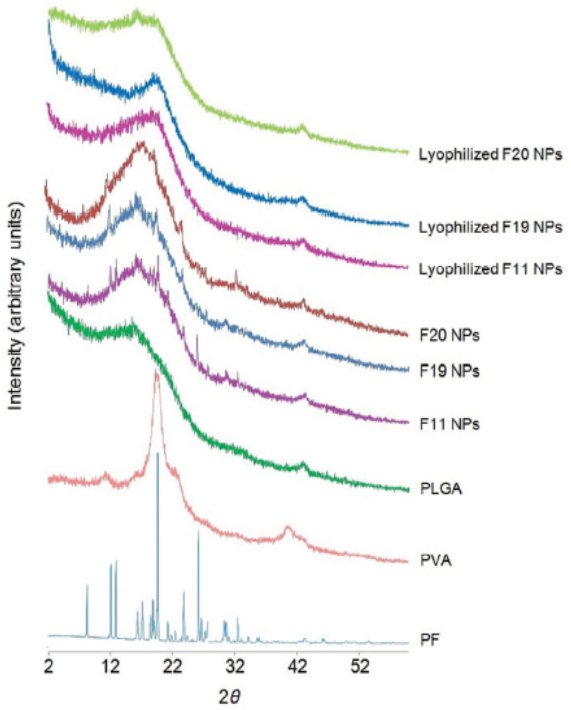

Figure 4. X-ray spectra of PF, PVA, PLGA, F11, F19, and F20 NPs before and after being freeze-dried.

This hydrophilic layer on the surface on the NPs favors redispersion of the lyophilized NPs after rehydration.[18]

FTIR analysis was used to study the interactions between the drug and polymer. The FTIR spectra of PF, PLGA, PVA, and PF-loaded NPs before and after lyophilization are shown in Figure 5.

In Figure 5, the FTIR spectra of PF shows strong peaks at 1700 cm^{-1} due to C=O stretching, and aromatic C=C stretching at 1432, 1497, and 1582 cm^{-1}. The PLGA spectrum displays a characteristic peak at 1746 cm^{-1}. PVA exhibits a number of absorption peaks at 2912, 1324, 843 and 1084, and 3237 cm^{-1} attributed to the C–H stretching, C–H bending and C–O stretching, and O–H streaching frequencies, respectively.[41] Before freeze-drying in Figure 5, the NPs show a FTIR spectrum similar to that of PLGA, whereas the lyophilized NPs show a combination of PLGA and PVA in the FITR spectrum (Fig. 5). The results obtained from FTIR analysis suggest there is no evidence of any chemical interaction or strong bond formation between PF and PLGA.

Differential scanning calorimetry is a thermal analytical technique, which provides information about the physical

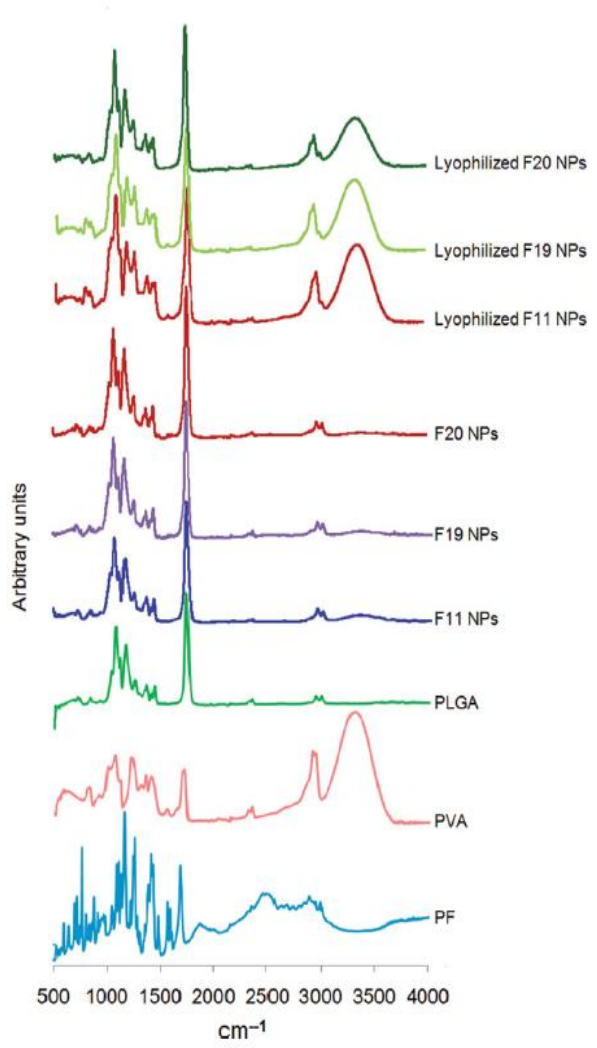

Figure 5. FTIR spectra of PF, PVA, PLGA, F11, F19, and F20 NPs before and after lyophilization.

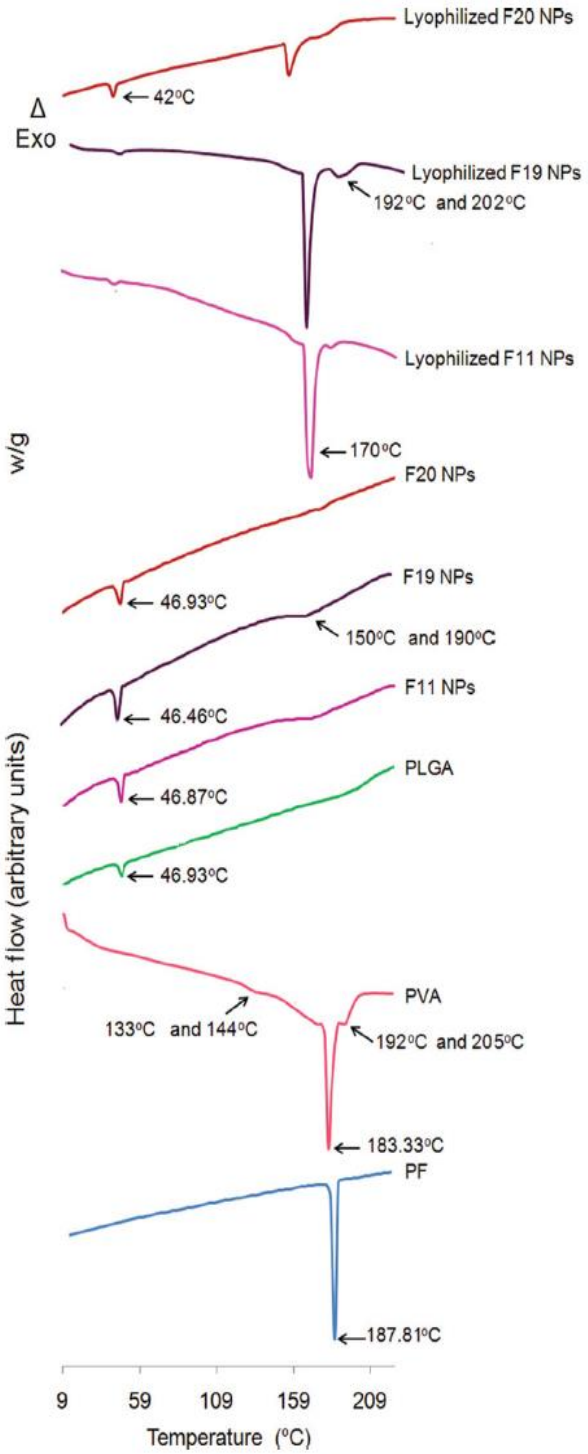

Figure 6. DSC curves of PF, PVA, PLGA, F11, F19, and F20 NPs before and after lyophilization.

properties of products, for example, the crystalline or amorphous nature of samples. Quantitative information regarding exothermic, endothermic, and heat capacity change as a function of temperature or time is also provided. DSC is a rapid and sensitive technique that has been successfully used for evaluating interactions between different the compounds of a mixture.[42,43]

Differential scanning calorimetry curves of PF, PLGA, PVA, and PF-loaded NPs before and after freeze-drying are displayed in Figure 6.

As can be observed in Figure 6, pure PF shows a crystalline state and exhibits a melting point peak at 187.81°C. PLGA was amorphous with a glass transition temperature of 46.93°C. The DSC curve of PVA shows one peak between 133°C and 144°C attributed to the glass transition temperature, another peak at 183.33°C, due to the loss of bound water and another small thermal event between 192°C and 205°C, attributed to the structural decomposition of the PVA.[44]

As shown the Figure 6, the shape of the thermograms of the optimized NPs before lyophilization is very similar to each other and quite similar to that of pure PLGA. They also exhibit thermal events around the glass transition temperature of PLGA (46.87°C, 46.46°C, and 46.93°C, respectively). The peak corresponding to the melting of the drug was not visible in the thermograms of the NPs before lyophilization. Nevertheless,

DOI 10.1002/jps.24101

a thermal event between 150°C and 190°C appeared in DSC curve of the F11 and F19, whereas in DSC curve of the F20, this thermal event is smaller compared with the other two formulations. This can be attributed can be attributed to the amount of PVA adsorbed onto the NP surface. The amount of PVA bound to the surface being greater for F11 and F19 than for F20 (Table 1).

Moreover, the results obtained by X-ray diffraction technique showed that the intensity of some of the peaks of crystalline PF present in these NPs before lyophilization slightly increased when cPF increased from 1.0 mg/mL (F19 and F20) to 1.5 mg/mL (F11). Taking into account these results, the thermal event observed between 150°C and 190°C in the thermograms of the NPs before freeze-drying also could be due to the melting point of free crystalline drug or a possible formation of an eutectic mixture of PF and PVA. These compounds exhibit melting point close to each other. In order to separate close thermal events, the DSC experiments were carried out at a rate of at 2°C/min. Although a low heating rate was used in DSC, it was not possible identify the correspondence of the thermal events with the free drug or PVA. Probably the intensity signal PVA masks the melting point of the free drug, as the cPVA is greater than cPF in the NPs formulation. These results are in agreement with those obtained by Vega et al.[38] for flurbiprofen-loaded PLGA Nanospheres.

Otherwise, the thermograms of the NPs after lyophilization (Fig. 6) show that when the PF was formulated in NPs, the peak corresponding to the melting of the drug totally disappeared, which could be attributed to the PVA layer on the surface of the NPs forming an amorphous glass state at low temperature during the lyophilization process, as well as demonstrated the X-ray spectrum of the freeze-dried NPs (Fig. 4). In Figure 6, the thermograms of the NPs after freeze-drying reveal only characteristic peaks corresponding to PLGA and PVA. The intensity of the PVA peaks in the lyophilized NPs is directly related with the amount of PVA used in the preparation of the NPs. Figure 6 also exhibits a peak at 42°C corresponding to the PLGA matrix and two additional peaks, one at 170°C and the other between 192°C and 202°C, which could be attributed to the presence of PVA. However, all these thermal events in the lyophilized NPs are recorded at lower temperatures than those obtained in the thermograms of pure PLGA and pure PVA. This could be due to the PLGA NPs retaining significant quantities of water after a typical manufacturing process, which could have a plasticizing effect on the NPs. Otherwise, this effect also could be due to the drying conditions used during the process of lyophilization.[45] Additionally, the insertion of a hydrophilic backbone PVA into hydrophobic PLGA chain lead to an important flexibility of PLGA chains. As previously reported, in the dry state PVA-graft-PLGA revealed only small differences in their glass transition temperature, whereas the wet state caused a reduction of glass transition, which is due to that the PVA exhibit a higher affinity to polar solvents and rapid water uptake.[46,47]

In Vitro Release Study

The *in vitro* release study of PF from the primary nanosuspensions and rehydrated freeze-dried F11, F19, and F20 NPs was performed in Franz diffusion cells. The NPs were compared with commercial eye drops (Oftalar®, 1.0 mg/mL) and the free drug (1.0 mg/mL) dissolved in PBS pH 7.4.

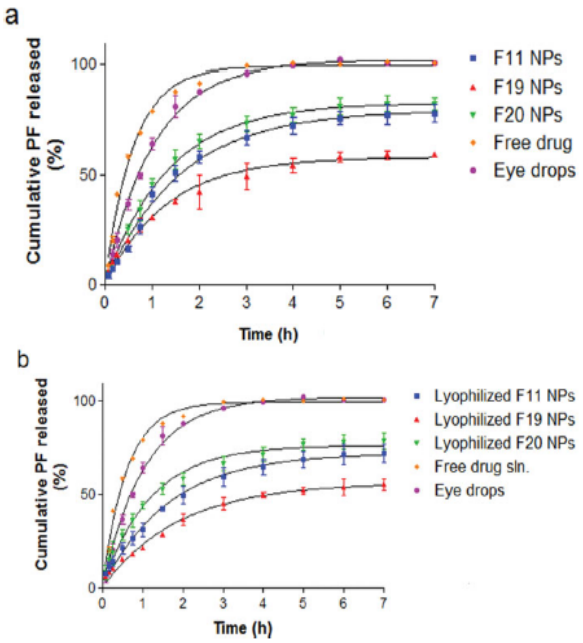

Figure 7. *In vitro* release profiles of PF from commercial eye drops, free drug solution and primary nanosuspensions (a) and rehydrated freeze-dried NPs (b) (mean ± SD, $n = 3$).

As can be observed in Figure 7, the release profile of PF from the solution and the commercial eye drops shows faster release than from the NPs; after 3 h, 100% of the drug was released.

The drug can be released from PLGA particles via diffusion, polymer erosion or a combination of both.[48] If drug diffusion is faster than the matrix degradation, then drug release occurs mainly by diffusion. A burst in the release profile is attributed to the fraction of the drug, which is adsorbed or weakly bound to the large surface area of the NPs.[49] The release profile of PF from the primary nanosuspensions (Fig. 7a) and rehydrated freeze-dried NPs (Fig. 7b) shows a sustained release behavior, with an initial burst attributed to the PF adsorbed to the NP surface, followed by a slower release phase while the trapped PF slowly diffuses out of the polymeric matrix into the release medium. The accumulative amount of PF released from F11, F19, and F20 nanosuspensions after 7 h was 78.18%, 59.33%, and 82.17%, respectively (Fig. 7a). Over the same period of time, rehydrated freeze-dried F11, F19, and F20 NPs showed values of 71.88%, 55.10%, and 78.62%, respectively (Fig. 7b). Figure 7 also shows that the amount of PF released from F19 before or after lyophilization was less than from F11 and F20, whereas for the latter two the accumulated percentages at 7 h were similar.

These results might be attributed to the fact that the viscosity increases when there is an increase in the cPVA. This viscosity increase could result in a more compact polymer matrix leading to slower degradation of the polymer or slower diffusion of the encapsulated PF from the NPs.[31]

Despite this, the release profiles of PF from primary NP nanosuspensions and rehydrated freeze-dried NPs were comparable and they could offer sustained release of the drug as there was no strong bond formation between PF and PLGA, as the FITR results showed.

Table 5. Mean Parameter Obtained after Fitting the Release Data from PF-Loaded NPs Before and After Freeze-Drying, Free Drug Solution, and Eye Drops to Different Release Models

		Before Lyophilization			After Lyophilization				
Models	Parameter	F11	F19	F20	F11	F19	F20	Free Drug	Eye Drops
Zero Order	AIC	101.98	86.58	106.47	92.63	83.83	96.05	115.50	114.85
First Order	AIC	53.22	70.31	52.16	58.87	54.52	65.82	67.01	56.51
Higuchi	AIC	87.05	66.70	93.61	72.94	64.22	78.99	107.85	104.52
Korsmeyer–	n	0.46	0.48	0.42	0.45	0.48	0.40	0.28	0.38
Peppas	AIC	86.35	58.77	91.55	70.90	63.87	73.49	102.10	101.26

n, diffusional release exponent; AIC, Akaike's information criterion.

Table 6. Mean Parameter Obtained after Fitting the Release Data from PF-Loaded NPs Before and After Lyophilization, Free Drug Solution, and Eye Drops to First Order Equation

	Before Lyophilization			After Lyophilization				
Parameters	F11	F19	F20	F11	F19	F20	Free Drug	Eye Drops
Best-fit values								
Y_{max} (%)	79.57	58.17	82.86	71.94	56.14	76.12	99.31	101.90
K (h^{-1})	0.63	0.75	0.74	0.61	0.53	0.84	1.64	0.95
$t_{1/2}$ (h)	1.11	0.92	0.93	1.14	1.32	0.83	0.42	0.73
Standard error								
Y_{max} (%)	1.68	1.39	0.91	1.67	1.61	1.65	1.43	1.01
K (h^{-1})	0.04	0.05	0.02	0.04	0.04	0.06	0.09	0.03
95% CI								
Y_{max} (%)								
Lower	75.88	55.11	80.85	68.27	52.59	72.48	96.16	99.68
Upper	83.25	61.22	84.87	75.60	59.69	79.75	102.40	104.10
K (h^{-1})								
Lower	0.54	0.63	0.69	0.52	0.44	0.71	1.40	0.88
Upper	0.71	0.88	0.80	0.70	0.62	0.96	1.85	1.02
$t_{1/2}$ (h)								
Lower	1.28	1.09	1.01	1.33	1.58	0.98	0.48	0.79
Upper	0.98	0.79	0.87	0.99	1.12	0.72	0.38	0.68
Goodness of Fit								
DF	11	11	11	11	11	11	11	11
R^2	0.9976	0.9952	0.9991	0.9968	0.9961	0.9955	0.9966	0.9991
ASS	24.05	21.74	9.25	22.71	16.24	34.84	42.47	14.88
Sy.x	1.48	1.41	0.92	1.44	1.22	1.78	1.97	1.16

Y_{max}, total percentage drug released; K, release rate constant; $t_{1/2}$, half-life; CI, confidence intervals; DF, degrees of freedom; ASS, absolute sum of squares; Sy.x, covariance.

The amount of PF released from the primary nanosuspensions and rehydrated freeze-dried F11, F19, and F20 NPs, as well as the commercial eye drops and free drug solutions was fitted to different kinetic models: zero-order equation, first-order equation, Higuchi and Korsmeyer–Peppas equation. The AIC was determined for each model. This parameter is an indicator of the suitability of the model for a given dataset. The smaller the value of AIC, the better the model fits the data. From the AIC values presented in Table 5, it can be concluded that the release curves of PF from the free drug solution, and eye drops, as well as from the primary nanosuspensions and rehydrated freeze-dried F11 and F20 NPs fitted to the first order kinetic model very well. The drug release mechanism of the rehydrated freeze-dried F19 NPs, which also fitted to first-order model, differed from that of the F19 primary nanosuspension, which followed the Korsmeyer–Peppas model.

These models had the smallest AIC values (Table 5) and, therefore, statistically, best described the drug release mechanism. Taking into account the diffusional exponent value (n) that is used to characterize different release mechanisms, n values of less than 0.5 were obtained in all the formulations studied. This suggest that the release of PF from the NPs occurs by passive diffusion, mainly through the pores of the matrix.[50]

As a result of this release study, it was confirmed that the NPs (primary nanosuspensions and rehydrated freeze-dried formulations) could offer sustained release of the drug compared with the conventional dosage forms. These results are in accordance with the statistically significant differences (p value < 0.05) found between the NP half-life ($t_{1/2}$) values and those of the free drug solution or the eye drops. There were not statistically significant differences between the half-life ($t_{1/2}$) values of the NPs (primary nanosuspension and rehydrated freeze-dried NPs. However, statistically significant differences were found between the NPs (primary nanosuspension and freeze-dried NPs) and the eye drops or free drug solution, with the exception of the freeze-dried F20 NPs with respect to free drug solution (Table 6).

DOI 10.1002/jps.24101

From the results of the release study, it could be conclude that the main factor that governs the release rate of the drug from the NPs is the amount of PVA present in the formulation, and additionally, this process is influenced by presence of PF in crystalline form as the drug in crystalline form should dissolve first before being transported out to the matrix by diffusion. All the NPs formulation show sustained release of the drug compared with the conventional dosage forms. Nevertheless, the freeze-dried F20 NPs not shows statistically significant differences between the half-life ($t_{1/2}$) values with respect to free drug solution. This may be explained due to the amount of PVA in F20 NPs is less than other NPs formulations. Therefore, in the F20 NPs, a less compact polymer matrix was formed, which lead to faster degradation of the polymer or faster diffusion of the encapsulated PF from the freeze-dried F20 NPs.

Ocular Tolerance

The HET-CAM assay is based on the direct application of the sample onto the choriollantoic membrane and the observation of reactions, such as hemorrhage, intravasal coagulation, or lysis of blood vessels. It, provides a suitable alternative to the Draize test for ocular irritation analysis.[51]

The results of the HET-CAM test revealed optimal ocular tolerance of the PF-loaded NPs (F11, F19, and F20) as no irritation reactions were detected within 5 min of the assay (score 0). These results are in accordance with those obtained by Araujo et al.[32]

CONCLUSIONS

In this study, a factorial design proved to be a useful tool to develop and optimize polymeric NPs using solvent displacement technique. Mathematical analysis of the results lead to polynomial equations that suitably describe the influence of pH and the initial concentration of the stabilizer, drug, and polymer used to prepare the NPs. According to the results of the factorial design the optimum formulations were those prepared at two different aqueous phase pH values (4.50 and 5.50), two cPFs (1.00 and 1.50 mg/mL), two cPLGAs (9.00 and 9.50 mg/mL), and three cPVAs (5, 10, and 25 mg/mL). The optimized formulations showed an average size appropriate for ophthalmic administration (around 350 nm) and high EE (80%). These NPs also showed good physicochemical stability, as revealed by the results over a short time period (30 days). Lyophilization assays was performed to ensure the long-term stability. The physicochemical properties of the rehydrated freeze-dried NPs were similar to those of the primary formulations and no sign of collapse or aggregation was observed. X-ray diffraction, infrared spectroscopy, and thermal methods showed that the drug was dispersed inside the particles. The release behavior of PF from the primary nanosuspensions and rehydrated freeze-drying NPs was similar for each other formulation and exhibited a sustained release pattern. The optimized NPs showed no irritation. All these results suggest that the optimized NPs could be an effective system for the delivery and controlled release of PF. These systems can improve the biopharmaceutical profile of this drug. In addition, the optimized freeze-dried NPs provide protection to the drug, avoiding the degradation of PF or PLGA in aqueous dispersion. Nevertheless, additional studies, related to *in vitro* and *in vivo* PF permeation profiles and anti-inflammatory efficacy are necessary for clinical applications.

ACKNOWLEDGMENTS

G. Abrego wishes to acknowledge the Spanish Ministry of Foreign Affairs and Cooperation and the Spanish Agency for International Development Cooperation (MAEC-AECID) for a research scholarship. Also, the authors would like to acknowledge the financial support of the Spanish Ministry of Science and Innovation (grant MAT2011–26994) and the kind help of Dr. Saša Nikolić and Gladys Ramos from the Reig Jofre, S.A laboratory for their valuable technical assistance in conducting the lyophilization assays. The authors would like to thank the *Serveis Lingüístics* of the University of Barcelona for the assistance in translation.

REFERENCES

1. Akyol-Salman I, Lece-Sertoz D, Baykal O. 2007. Topical pranoprofen 0.1% is as effective anti-inflammatory and analgesic agent as diclofenac sodium 0.1% after strabismus surgery. J Ocul Pharmacol Ther 23:280–283.
2. Sawa M, Masuda K, Nakashima M. 1999. Anti-inflamatory effect of diclofenac sodium eye drops on cataract surgery. Double masked study with pranoprofen eye drops. J Ocul Pharmcol Ther 13:193–200.
3. McColgin AZ, Heier JS. 2000. Control of intraocular inflammation associated with cataract surgery. Curr Opin Ophthalmol 11:3–6.
4. Liu X, Wang S, Kao AA, Long Q. 2012. The effect of topical pranoprofen 0.1% on the clinical evaluation and conjunctival HLA-DR expression in dry eyes. Cornea 31:1235–1239.
5. Notivol R, Martinez M, Bergamini M. 1994. Treatment of chronic nonbacterial conjunctivitis with a cyclo-oxygenase inhibitor or a corticosteroid. Pranoprofen study group. Am J Ophthalmol 117(5):651–656.
6. Narashino M, Ichikawa H, Narita S, Yotsukaido AS. 1993. Patent US005225206A.
7. Kobe K, Otsu H, kobe Y, Kakogawa Y. 1999. Patent US005856345A.
8. Araújo J, Gonzalez E, Egea MA, Garcia ML, Souto EB. 2009. Nanomedicines for ocular NSAIDs: Safety on drug delivery. Nanomedicine 5:394–401.
9. Nair LS, Laurencin CT. 2007. Biodegradable polymers as biomaterials. Prog Polym Sci 32:762–798.
10. Laurent S, Forge D, Port M, Roch A, Robic C, Vander Elst L, Muller R.2008. Magnetic iron oxide nanoparticles: Synthesis, stabilization, vectorization, physicochemical characterizations, and biological applications. Chem Rev 108:2064–2110.
11. Abdelwahed W, Degobert G, Stainmesse S, Fessi H. 2006. Freeze-drying of nanoparticles: Formulation, process and storage considerations. Adv Drug Deliv Rev 58:1688–1713.
12. Layre A, Couvreur P, Richard J, Requier D, Eddine Ghermani N, Gref R. 2006. Freeze-drying of composite core–shell nanoparticles. Drug Dev Ind Pharm 32:839–846.
13. Panyam J, Williams D, Dash A, Leslie-Pelecky D, Labhasetwar V. 2004. Solid-state solubility influences encapsulation and release of hydrophobic drugs from PLGA/PLA nanoparticles. J Pharm Sci 93:1804–1814.
14. Fessi H, Puisieux F, Devissaguet JP, Ammoury N, Benita S. 1989. Nanocapsule formation by interfacial polymer deposition following solvent displacement. Int J Pharm 55:R1-R4.
15. Fangueiro JF, Andreani T, Egea Ma, Garcia ML, Souto SB, Souto EB. 2012. Experimental factorial design applied to mucoadhesive lipid nanoparticles via multiple emulsion process. Colloids Surf B Biointerfaces 100:84–89.

16. Yegin BA, Lamprecht A. 2006. Lipid nanocapsule size analysis by hydrodynamic chromatography and photon correlation spectroscopy. Int J Pharm 320:165–170.
17. Teeranachaideekul V, Junyaprasert VB, Souto EB, Müller RH. 2008. Development of ascorbyl palmitate nanocrystals applying the nanosuspension technology. Int J Pharm 354:227–234.
18. Allémann E, Leroux J, Gurny R, Doelker E. 1993. In vitro extended-release properties of drug-loaded poly(D,L-lactic acid) nanoparticles produced by a salting-out procedure. Pharm Res 10:1732–1737.
19. Celia C, Trapasso E, Cosco D, Paolino D, Fresta M. 2009. Turbiscan Lab® Expert analysis of the stability of ethosomes® and ultradeformable liposomes containing a bilayer fluidizing agent. Colloids Surf B Biointerfaces 72:155–160.
20. Franz TJ. 1975. Percutaneous absorption. On the relevance of in vitro data. J Investig Dermatol 64:190–195.
21. Costa P, Sousa Lobo JM. 2001. Modeling and comparison of dissolution profiles. Eur J Pharm Sci 13:123–133.
22. Yamaoka K, Nakagawa T, Uno T. 1978. Application of Akaike's information criterion (AIC) in the evaluation of linear pharmacokinetic equations. J Pharmacokinet Biopharm 6:165–175, 1978;1978.
23. Luepke NP. 1985. Hen's egg chorioallantoic membrane test for irritation potential. Food Chem Toxicol 23:287–291.
24. Invittox-Protocol N.15. 1990. The Ergatt/Frame data bank of in vitro techniques in toxicology. Heng´s egg test.
25. Journal Officiel de la République Française. 1996. Méthode Officiel d'evaluation du potentiel irritant par application sur la membrane chorioallantoidienne de l'oeuf de poule. Annexe IV 1937–1938.
26. Zimmer A, Kreuter J. 1995. Microspheres and nanoparticles used in ocular delivery systems. Ocul Drug Deliv Rev 16:61–73.
27. Song X, Zhao Y, Hou S, Xu F, Zhao R, He J, Cai Z, Li Y, Chen Q. 2008. Dual agents loaded PLGA nanoparticles: Systematic study of particle size and drug entrapment efficiency. Eur J Pharm Biopharm 69:445–453.
28. Win K, Feng S. 2005. Effects of particle size and surface coating on cellular uptake of polymeric nanoparticles for oral delivery of anticancer drugs. Biomaterials 26:2713–2722.
29. Anand P, Nair HB, Sung B, Kunnumakkara A, Yadav V, Tekmal R,Aggawal B.2010. Design of curcumin-loaded PLGA nanoparticles formulation with enhanced cellular uptake, and increased bioactivity in vitro and superior bioavailability in vivo. Biochem Pharmacol 79:330–338.
30. Feng S, Huang G. 2001. Effects of emulsifiers on the controlled release of paclitaxel (Taxol®) from nanospheres of biodegradable polymers. J Control Release 71:53–69.
31. Sahoo SK, Panyam J, Prabha S, Labhasetwar V. 2002. Residual polyvinyl alcohol associated with poly (D,L-lactide-co-glycolide) nanoparticles affects their physical properties and cellular uptake. J Control Release 82:105–114.
32. Araujo J, Vega E, Lopes C, Egea MA, Garcia ML, Souto EB. 2009. Effect of polymer viscosity on physicochemical properties and ocular tolerance of FB-loaded PLGA nanospheres. Colloids Surf. B Biointerfaces 72:48–56.
33. Vega E, Egea MA, Valls O, Espina M, García ML. 2006. Flurbiprofen loaded biodegradable nanoparticles for ophtalmic administration. J Pharm Sci 95:2393–2405.
34. Jiang B, Hu L, Gao C, Shen J. 2005. Ibuprofen-loaded nanoparticles prepared by a co-precipitation method and their release properties. Int J Pharm 304:220–230.
35. Zambaux MF, Bonneaux F, Gref R, Maincent P, Dellacherie E, Alonso MJ, Labrude P, Vigneron C. 1998. Influence of experimental parameters on the characteristics of poly(lactic acid) nanoparticles prepared by a double emulsion method. J Control Release 50:31–40.
36. Murakami H, Kobayashi M, Takeuchi H, Kawashima Y. 1999. Preparation of poly (D,L-lactide-co-glycolide) nanoparticles by modified spontaneous emulsification solvent diffusion method. Int J Pharm 187:143–152
37. Zhao X, Zhang Q, Chen D, Lu P. 2010. Enhanced mechanical properties of graphene-based poly(vinyl alcohol) composites. Macromolecules 43:2357–2363.
38. Vega E, Gamisans F, Garcia ML, Chauvet A, Lacoulonche F, Egea MA. 2008. PLGA nanospheres for the ocular delivery of flurbiprofen: Drug release and interactions. J Pharm Sci 97:5306–5317.
39. Zeng J, Yang L, Liang Q, Zhang X, Guan H, Xu X, Chen X, Jing X. 2005. Influence of the drug compatibility with polymer solution on the release kinetics of electrospun fiber formulation. J Control Release 105:43–51.
40. Konno H, Taylor LS. 2006. Influence of different polymers on the crystallization tendency of molecularly dispersed amorphous felodipine. J Pharm Sci 95:2692–2705.
41. Jayasekara R, Harding I, Bowater I, Christie GBY, Lonergan GT. 2004. Preparation, surface modification and characterization of solution cast starch PVA blended films. Polym Test 23:17–27.
42. Dillen K, Vandervoort J, Van den Mooter G, Verheyden L, Ludwig A. 2004. Factorial design, physicochemical characterization and activity of ciprofloxacin-PLGA nanoparticles. Int J Pharm 275:171–187.
43. Toscani S, Cornevin L, Burgot G. 2012. Weak interactions in clobazam–lactose mixtures examined by differential scanning calorimetry: Comparison with the captopril–lactose system. Thermochim Acta 543:197–204.
44. Kumar RV, Koltypin Y, Cohen YS, Cohen Y, Aurbach D, Palchik O, Felner I. 2000. Preparation of amorphous magnetite nanoparticles embedded in polyvinyl alcohol using ultrasound radiation. J Mater Chem 10:1125–1129.
45. Passerini N, Craig DQM. 2001. An investigation into the effects of residual water on the glass transition temperature of polylactide microspheres using modulated temperature DSC. J Control Release 73:111–115.
46. Pistel KF, Breitenbach A, Zange-volland R, Kissel T. 2001. Brush-like branched biodegradable polyesters, part III Protein release from microspheres of poly(vinyl alcohol)-graft-poly (D,L-lactic-co-glycolic acid). J Control Release 73:7–20.
47. Westedt U, Wittmar M, Hellwig M, Hanefeld P, Greiner A, Schaper AK, Kissel T. 2006. Paclitaxel releasing films consisting of poly (vinyl alcohol)-graft-poly(lactide-co-glycolide) and their potential as biodegradable stent coatings. J Control Release 111:235–246.
48. Faisant N, Siepmann J, Benoit JP. 2002. PLGA-based microparticles: Elucidation of mechanisms and a new, simple mathematical model quantifying drug release. Eur J Pharm Sci 15:355–366.
49. Niwa T, Takeuchi H, Hino T, Kunou N, Kawashima Y. 1993. Preparations of biodegradable nanospheres of water-soluble and insoluble drugs with D,L-lactide/glycolide copolymer by a novel spontaneous emulsification solvent diffusion method, and the drug release behavior. J Control Release 25:89–98.
50. Ford JL, Rubinstein MH, McCaul F, Hogan JE, Edgar PJ. 1987. Importance of drug type, tablet shape and added diluents on drug release kinetics from hydroxypropylmethylcellulose matrix tablets. Int J Pharm. 40:223–234.
51. Tavaszi J, Budai P. 2007. The use of HET-CAM test in detecting the ocular irritation. Commun Agric Appl Biol Sci 72:137–141.

Biopharmaceutical profile of pranoprofen-loaded PLGA nanoparticles containing hydrogels for ocular administration (Aceptado)

G. Abrego, H.L. Alvarado, E. Souto, B. Guevara, L.H. Bellowa, A. Parra, A.C. Calpena, M.L. García.

European Journal of Pharmaceutics and Biopharmaceutics. http://dx.doi.org/10.1016/j.ejpb.2015.01.026

3.2. Biopharmaceutical profile of pranoprofen-loaded PLGA nanoparticles containing hydrogels for ocular administration (Artículo 2).

Resumen

En un estudio previo, pranoprofeno fue asociado a una matriz de ácido poli-láctico-co-glicólico (PLGA). Las nanopartículas optimizadas (PF-F1NPs y PF-F2NPs) fueron seleccionadas para llevar a cabo estudios adicionales en la presente investigación. Los sistemas optimizados fueron incorporados en un hidrogel de carbomero (HG_PF-F1NPs y HG_PF-F2NPs) o hydrogel en presencia de un 1% de azona (HG_PF-F1NPs-Azona y HG_PF-F2NPs-Azona), con la finalidad de obtener formulaciones semisólidas que permitan prologar el tiempo de contacto del fármaco en la superficie ocular, favoreciendo la retención del fármaco en este el órgano e incrementando la eficacia analgésica y antiinflamatoria de pranoprofeno.

Los resultados obtenidos a partir del análisis morfológico de las NPs incorporadas en el hidrogel llevado a cabo por microscopía elecronica de transmisión (TEM) reveló un diámetro de partícula similar al observado para estas en suspensión. Adicionalmente, estas formulaciones exhibieron propiedades fisicoquímicas apropiadas para la aplicación ocular, lo que sugiere que el agente gelificante no modifió notablemente la morfología y/o tamaño de las partículas.

Por otra parte, la caracterización reologica de las formulaciones semisólidas en presencia o ausencia de azona, puso en evidencia que las formualciones ensayadas presentan un comportamiento no-Newtoniano y pseudoplástico, con una prevalencia del comportamiento elástico sobre el viscoso ($G´ > G´´$) para todas las formulaciones testadas.

El perfil de liberación de pranoprofeno desde las formulaciones de hidrogel en presencia o ausencia de azona exhibió una liberación sostenida del fármaco comparado con el colirio comercial (®Oftalar) y/o con la solucion de farmaco libre.

Los resultados obtenidos a partir del ensayo de permeación transcorneal *ex vivo* y la evaluación *in vivo* de la eficacia antiinflamatoria de pranoprofeno contenido en las formulaciones semisólidas sugieren que la aplicación ocular de las nanopartículas incorporadas en el hidrogel en presencia de azona

pueden ser un sistemas más efectico que las mismas formulaciones en ausencia de promotor para tratar el edema de la superficie ocular. Finalmente, la irritación ocular de las formulaciones semisólidas con o sin promotor se evaluó *in vitro* a través del metodo HET-CAM e *in vivo* mediante el test de Draize. Ningun signo de irritacion fue detectado durante la realización del ensayo.

EJPB 11820
16 February 2015
ARTICLE IN PRESS
No. of Pages 10, Model 5G

European Journal of Pharmaceutics and Biopharmaceutics xxx (2015) xxx–xxx

Contents lists available at ScienceDirect

European Journal of Pharmaceutics and Biopharmaceutics

journal homepage: www.elsevier.com/locate/ejpb

Research paper

Biopharmaceutical profile of pranoprofen-loaded PLGA nanoparticles containing hydrogels for ocular administration

Guadalupe Abrego[a,b], Helen Alvarado[a,b], Eliana B. Souto[c,d,*], Bessy Guevara[b], Lyda Halbaut Bellowa[e], Alexander Parra[a,b], Ana Calpena[b], María Luisa Garcia[a,*]

[a] Department of Physical Chemistry, Faculty of Pharmacy, University of Barcelona, Barcelona, Spain
[b] Department of Biopharmacy and Pharmaceutical Technology, Faculty of Pharmacy, University of Barcelona, Barcelona, Spain
[c] Department of Pharmaceutical Technology, Faculty of Pharmacy, University of Coimbra (FFUC), Pólo das Ciências da Saúde, Coimbra, Portugal
[d] Center for Neuroscience and Cell Biology & Institute for Biomedical Imaging and Life Sciences (CNC-IBILI), University of Coimbra, Pólo das Ciências da Saúde, Coimbra, Portugal
[e] Department of Pharmacy and Pharmaceutical Technology, Faculty of Pharmacy, University of Barcelona, Barcelona, Spain

ARTICLE INFO

Article history:
Received 24 November 2014
Accepted in revised form 28 January 2015
Available online xxxx

Chemical compounds:
Pranoprofen (PubChem CID:4888)

Keywords:
Pranoprofen
Nanoparticles
Hydrogel
Ocular tolerance
Physical stability
Corneal permeation
Anti-inflammatory efficacy
Azone
Non-steroidal anti-inflammatory drug

ABSTRACT

Two optimized pranoprofen-loaded poly-L-lactic-co glycolic acid (PLGA) nanoparticles (PF-F1NPs; PF-F2NPs) have been developed and further dispersed into hydrogels for the production of semi-solid formulations intended for ocular administration. The optimized PF-NP suspensions were dispersed in freshly prepared carbomer hydrogels (HG_PF-F1NPs and HG_PF-F2NPs) or in hydrogels containing 1% azone (HG_PF-F1NPs-Azone and HG_PF-F2NPs-Azone) in order to improve the ocular biopharmaceutical profile of the selected non-steroidal anti-inflammatory drug (NSAID), by prolonging the contact of the pranoprofen with the eye, increasing the drug retention in the organ and enhancing its anti-inflammatory and analgesic efficiency. Carbomer 934 has been selected as gel-forming polymer. The hydrogel formulations with or without azone showed a non-Newtonian behavior and adequate physicochemical properties for ocular instillation. The release study of pranoprofen from the semi-solid formulations exhibited a sustained release behavior. The results obtained from *ex vivo* corneal permeation and *in vivo* anti-inflammatory efficacy studies suggest that the ocular application of the hydrogels containing azone was more effective over the azone-free formulations in the treatment of edema on the ocular surface. No signs of ocular irritancy have been detected for the produced hydrogels.

1. Introduction

Pranoprofen is a non-steroidal anti-inflammatory drug (NSAID) which can be used as a safe and effective alternative anti-inflammatory treatment following strabismus and cataract surgery [1–3]. This drug has the beneficial effect of reducing the ocular signs and symptoms of dry eye and decreasing the inflammatory markers of conjunctival epithelial cells [4]. Its efficacy is equivalent to moderate-potency corticosteroids, but it has improved safety profile. It should be considered for the treatment of chronic conjunctivitis of presumed nonbacterial origin [5]. Although this drug has shown high anti-inflammatory and analgesic efficiency, the pharmaceutical use of pranoprofen is limited due to its inadequate biopharmaceutical profile. Pranoprofen has a short plasmatic half-life, low water solubility and is unstable in aqueous solution, particularly when exposed to light [6,7]. Pranoprofen is commercially available as eye-drops (0.1% m/V). However, this conventional dos-

Abbreviations: PF, pranoprofen; NPs, nanoparticles; HG, hydrogel; PF-F1NPs and PF-F2NPs, optimize pranoprofen nanoparticles; HG_PF-NPs-Azone and HG_PF-NPs, nanoparticles incorporated into hydrogel with and without azone, respectively; Z-Ave, average particle size; PI, polydispersity index; ZP, zeta potential; EE, entrapment efficiency; PVA, polyvinyl alcohol; cPF, PF concentration; cPVA, PVA concentration; PLGA, poly-L-lactic-co glycolic acid; cPLGA, PLGA concentration; SA, arachidonic acid sodium; PBS, phosphate buffer solution; BR, Bicarbonate Ringer; Q_P, amounts of drug permeated across cornea; Q_R, amounts of drug retained in the cornea.

* Corresponding authors. Department of Pharmaceutical Technology, Faculty of Pharmacy, University of Coimbra (FFUC), Pólo das Ciências da Saúde, Azinhaga de Santa Comba, 3000-548 Coimbra, Portugal. Tel.: +351 239 488 400; fax: +351 239 488 503 (E.B. Souto). Department of Physical Chemistry, Faculty of Pharmacy, University of Barcelona, Av. Joan XXIII s/n, 08028 Barcelona, Spain. Tel.: +34 934 021 220; fax: +34 934 021 231 (M.L. Garcia).
E-mail addresses: ebsouto@ff.uc.pt (E.B. Souto), marisagarcia@ub.edu (M.L. Garcia).

http://dx.doi.org/10.1016/j.ejpb.2015.01.026
0939-6411/

EJPB 11820
16 February 2015
ARTICLE IN PRESS
No. of Pages 10, Model 5G

age form cannot be considered optimal in the treatment of ocular diseases due to the fact that upon instillation most of the drugs are removed from the surface of the eye, by various mechanisms (tear dilution and tear turn over). Moreover, the relatively impermeable corneal barrier restricts the entry of foreign substances. As a result, less than 5% of the administered drug penetrates the cornea and reaches intraocular tissue [8]. Polymeric NPs are one of the colloidal systems that have been most widely studied over the past few decades with the objective of improving drug targeting of tissues and organs and increase drug bioavailability across biological membranes. Biodegradable polymers, such as poly (lactic-co-glycolic) acid (PLGA), have been widely used in drug delivery research, in part due to their approval by the FDA for use in humans and they can effectively deliver the drug to a target site with a controllable degradation [9]. PLGA can be used such as matrix to load different drugs for topical administration [10–12].

Different drug delivery systems have been studied in order to improve drug targeting of tissues, increase drug bioavailability across biological membranes or reducing its toxicity. For topical application of nanoparticle suspensions, several of these systems have been dispersed in semi-solid vehicles such as hydrogels or cream [13,14]. Among the gelling agents, carbomer has been extensively used for design topical formulations [15–17]. In addition, to improve the permeability of drugs through the ocular barriers, different enhancers have also been tested. Azone is one of the most widely studied penetration enhancers which can be used as a safe and effective penetration enhancer for human use in the range of 1–10% [18]. In previous studies, we have formulated pranoprofen in PLGA nanoparticles (PF-NPs) using the solvent displacement technique [19]. A 2^4 central composite factorial design has been applied to study the main effects and interactions of four factors on average particle size (Z-Ave), polydispersity index (PI), zeta potential (ZP) and entrapment efficiency (EE). The factors studied were PF concentration (cPF), PVA concentration (cPVA), PLGA concentration (cPLGA) and aqueous phase pH. From a total of 26 formulations obtained by factorial design, two optimum formulations (PF-F1NPs and PF-F2NPs) were selected for further investigation here [20]. The aim of this study was designed semi-solid formulations containing pranoprofen loaded-PLGA nanoparticles for ocular administration. Carbomer 934 was selected to disperse the optimized PF-NP suspension because of the bioadhesive properties, low or no toxicity, rheological characteristics and biocompatibility of the hydrophilic polymer. Polyacrylic acid hydrogels such as Carbomer 934, polycarbophil and carboxymethylcellulose have been reported as the most appropriate bioadhesive polymers for ocular drug delivery [21]. Additionality, the high viscosity of the carbomer hydrogels ensures the prolonged retention improving the ocular bioavailability of some drugs [22]. The optimized PF-F1NP and PF-F2NP suspensions were dispersed into blank hydrogels (HG_PF-F1NPs and HG_PF-F2NPs) or in hydrogels containing 1% azone (HG_PF-F1NPs-Azone and HG_PF-F2NPs-Azone) in order to improve the biopharmaceutical profile of pranoprofen in the eye, by increasing is ocular retention and improving the anti-inflammatory and analgesic efficiency. The ultimate aim of the developed formulations is to improving the patient's compliance to the pharmacological treatment by reducing the application frequency. In this study, azone was selected as permeation enhancer with the purpose to improve the permeability of pranoprofen from PF-NPs based HG through the ocular barriers. Azone is one of the most widely studied penetration enhancers for hydrophilic and lipophilic drugs. As a penetration enhancer, azone is more effective at low percentages (1–3%), and it has also been reported to be of low irritancy and very low toxicity [23]. The mechanism of azone may be related to some changes in the epithelial cell junctions of the cornea, which are nevertheless reversible in cornea structure [24,25].

The physicochemical properties and the rheological behavior of HG_PF-NP formulations have been characterized. The physical stability of the nanoparticles incorporated into hydrogels has also been evaluated. *In vitro* release profile and *ex vivo* corneal permeation of pranoprofen from the semi-solid formulations, as well as their *in vitro e in vivo* ocular tolerance and the anti-inflammatory efficacy have also been assayed.

2. Materials and methods

2.1. Materials

Pranoprofen and Oftalar® were kindly supplied by Alcon Cusi (Barcelona, Spain); PLGA Resomer® 753S was obtained from Boehringer Ingelheim (Ingelheim, Germany). Polyvinyl alcohol (PVA) with 90% hydrolyzation and Arachidonic acid sodium (SA) were obtained from Sigma Aldrich (St. Louis, USA). Gel-forming polymer (Carbomer 934) was obtained from Fagron Ibérica. The purified water used in all the experiments was obtained from a MilliQ System. All the other chemicals and reagents used in the study were of analytical grade.

2.2. Methods

2.2.1. Preparation of pranoprofen-loaded nanoparticles

The nanoparticles have been produced by the solvent displacement technique, described by Fessi et al. [19]. PLGA (90 mg or 95 mg) and pranoprofen (10 mg or 15 mg) were dissolved in 5 mL of acetone. This organic phase was poured, under moderate stirring into 10 mL of an aqueous solution of PVA (5 mg/mL or 10 mg/mL) adjusted to the desired pH value (4.5 or 5.5). The acetone was then evaporated and the dispersed nanoparticles were concentrated to 10 mL under reduced pressure (Büchi B-480 Flawil, Switzerland). Table 1 shows the composition of the optimized pranoprofen-loaded nanoparticles.

2.2.2. Mean particle size and zeta potential

The mean particle size (Z-Ave) and the zeta potential (ZP) of the nanoparticles were determined by photon correlation spectroscopy (PCS) with a Zetasizer Nano ZS (Malvern Instruments, Malvern, UK) at 25 °C using disposable quartz cells and disposable folded capillary zeta cells (Malvern Instruments, Malvern, UK), respectively. For all measurements, the samples were diluted with MilliQ water (1:20). The reported values are the mean ± SD of at least three different batches of each formulation.

2.2.3. Encapsulation efficiency

The encapsulation efficiency (EE) of pranoprofen in the nanoparticles was determined indirectly by measuring the concentration of the free drug in the dispersion medium. The non-encapsulated pranoprofen was separated using a filtration/centrifugation technique with Ultracel-100K (Amicon® Ultra, Millipore Corporation, Billerica, MA) centrifugal filter devices at 3000 rpm for 30 min at 4 °C (Heraeus, Multifuge 3 L-R, centrifuge. Osterode, Germany). Each sample was diluted with MilliQ water (1:20) prior to filtration/centrifugation. The EE was calculated using the following equation:

Table 1
Composition of the optimized pranoprofen-loaded nanoparticles.

PF-NPs	cPF (mg/mL)	cPVA (mg/mL)	cPLGA (mg/mL)	pH
PF-F1NPs	1.5	10.0	9.5	5.5
PF-F2NPs	1.0	5.0	9.0	4.5

Please cite this article in press as: G. Abrego et al., Biopharmaceutical profile of pranoprofen-loaded PLGA nanoparticles containing hydrogels for ocular administration, Eur. J. Pharm. Biopharm. (2015), http://dx.doi.org/10.1016/j.ejpb.2015.01.026

EJPB 11820
16 February 2015
ARTICLE IN PRESS
No. of Pages 10, Model 5G

$$EE(\%) = \frac{\text{Total Amount of pranoprofen} - \text{Free drug}}{\text{Total Amount of pranoprofen}} \times 100 \quad (1)$$

The assay was carried out by high performance liquid chromatography (HPLC) using a method previously validated in our laboratory. The detection and quantification limits (LOD and LOQ) found for the validated method were 1.05 ± 0.70 μg/mL and 3.17 ± 2.12 μg/mL, respectively. The HPLC system consisted of a Waters 1525 pump (Waters, Milford, USA) with a UV–Vis 2487 detector (Waters), a flow rate of 1 mL/min and wavelength of 245 nm were used with a (Kromasil®, 100-5C18, 4.6 × 100 mm) column. The mobile phase consisted of methanol: glacial acetic acid 5% (45: 55, v: v).

2.3. Preparation of pranoprofen-loaded nanoparticles dispersed in hydrogels

The blank hydrogels were prepared with carbomer (1% w/v), dispersed in purified water and allowed to hydrate for 24 h. Subsequently, glycerol (3% w/w) and azone (0% or 1% w/w) were incorporated into the hydrogel by stirring for 5 min at 1000 rpm in a high speed stirred (Cito Unguator Konietzko, Bamberg, Germany) and then the pH was adjusted at 6.5 with 0.1 N NaOH. The HG was left to equilibrate for 24 h at room temperature before used. The optimized aqueous PF-NP suspensions were incorporated into HG with 0% or 1% azone using a high speed stirred by 3 min at 1000 rpm, in a concentration of 50% (w/w) of the nanoparticle dispersion into the hydrogel.

2.4. Physicochemical characterization of the hydrogels

The morphological examination of the NPs incorporated into HG was performed by Transmission Electron Microscopy (TEM). The sample was dispersed in MilliQ water using an Elma Transsonic Digital S T490 DH ultrasonic bath (Elma, Singen, Germany). A drop of this dispersion (10 μL) was placed on copper electron microscopy grids and stained with a 2% (w/v) uranyl acetate solution. After 1 min, the sample was washed with ultra-purified water and the excess fluid removed with a piece of filter paper. The dried sample was then examined.

The physical stability of the HG_PF-NP formulations was assessed after 1 day of the production and 90 days of storage at 25 °C. The Z-Ave and ZP of the particles were determined by photon PCS as described above. The diameter of the nanoparticles dispersed into the hydrogels also was measured by laser diffraction (LD) data, obtained with a Mastersizer Hydro 2000MU (Malvern Instruments Ltd., Malvern, UK), using the volume distribution as diameter values of LD 10%, LD 50% and LD 90%. The diameter values indicate the percentage of nanoparticles showing a diameter equal or lower than the given value. For all measurements, the samples were dispersed in MilliQ water using an Elma Transsonic Digital S T490 DH ultrasonic bath (Elma, Singen, Germany).

2.5. Rheological measurements of the hydrogels

The hydrogel samples were placed in glass vials with rubber top and aluminum capsule and storage at 25 °C ± 2 °C. The rheological characterization of each formulation was performed using a Haake Rheostress1 rheometer (Thermo Fisher Scientific, Karlsruhe, Germany) connected to a temperature control Thermo Haake Phoenix II + Haake C25P and equipped with parallel plate geometry (Haake PP60 Ti, 60 mm diameter, 0.5 mm gap between plates) or cone plate set-up with a fixed lower plate and a mobile upper cone (Haake C35/2° Ti, 35 mm diameter, 0.106 mm gap between cone-plate). The viscosity curves and flow curves were recorded under rotational runs at 25 °C for 3 min during the ramp-up period from 0 to 100 s^{-1}, 1 min at 100 s^{-1} (constant share rate period) and finally 3 min during the ramp-down period from 100 to 0 s^{-1}. Viscosity values at 100 s^{-1} were determined after 8 days of the production and 90 days of storage at 25 ± 2 °C, in three replicates. Oscillatory stress sweep tests were performed at a constant frequency of 1 Hz in a stress range of 0.1 and 200 Pa. Oscillation frequency tests were carried out from 0.01 to 10 Hz at a constant shear stress within the linear viscoelastic region, in order to determine the related variation of storage modulus (G') and loss modulus (G'') at 25 °C. The software Haake RheoWin®Job Manager V.3.3 and RheoWin®Data Manager V.3.3 (Thermo Electron Corporation, Karlsruhe, Germany) were used to carry out the test and analysis of the obtained data, respectively.

2.6. In vitro pranoprofen release from the hydrogels

In vitro release study of pranoprofen from the HG_PF-NP formulations was performed in Franz diffusion cells [26]. These cells consist of a donor and a receptor chamber between which a membrane is positioned. A dialysis membrane (MWCO 12,000–14,000 Da., Dialysis Tubing Visking, Medicell International Ltd., London, UK) was used. The membrane was hydrated for 24 h before being mounted in the Franz diffusion cell. The experiment was performed under "sink condition". The HG_PF-NP formulations were compared with the commercial eye drops (Oftalar®, pranoprofen 1 mg/mL) and the free drug (1 mg/mL) dissolved in phosphate buffer solution (PBS) at pH 7.4. A weight of 400 mg of the HG_PF-NP formulations or a volume of 200 μL of the free drug solution and commercial eye drops was placed in the donor compartment and the receptor compartment was filled with PBS at pH 7.4 kept at 37 ± 0.5 °C. A volume of 300 μL was withdrawn from the receptor compartment at fixed times and replaced by an equivalent volume of fresh PBS at the same temperature. The concentration of pranoprofen released was measured as described previously for EE. Values are reported as the mean ± SD of three replicates.

The amount pranoprofen release was adjusted to the following kinetic models [27]:

$$\text{Zero order}: \%R_t/\%R_\infty = k \times t \quad (2)$$

$$\text{First order}: \%R_t/\%R_\infty = 1 - e^{-k \times t} \quad (3)$$

$$\text{Higuchi}: \%R_t/\%R_\infty = k \times t^{1/2} \quad (4)$$

$$\text{Hyperbola}: \%R_t/\%R_\infty = R_\infty \times t/(k+t) \quad (5)$$

$$\text{Korsmeyer–Peppas}: \%R_t/\%R_\infty = k \times t^n \quad (6)$$

where $\%R_t$ is the percentage of the drug released at time t, $\%R_\infty$ is the total percentage of drug released, $\%R_t/\%R_\infty$ is the fraction of drug released at time t, k is the release rate constant and n is the diffusion release exponent that can be used to characterize the different release mechanisms; $n \leqslant 0.5$ (Frickian diffusion), $0.5 < n < 1.0$ (anomalous transport), and $n \geqslant 1$ (case II transport, i.e., zero-order release). A nonlinear least-squares regression was performed using the WinNonLin® software (WinNonLin® professional edition version 3.3 and Graphpad prism version 6 Demo) and the model parameters were calculated. Akaike's information criterion (AIC) was determined for each model as an indicator of the model's suitability for a given dataset [28].

2.7. Corneal permeation study

Ex vivo corneal permeation experiments were carried out with New Zealand rabbits (male, weighing 2.5–3.0 kg), under veterinary supervision and according to the Ethics Committee of Animals Experimentation at the University of Barcelona. The rabbits were anesthetized with intramuscular administration of ketamine HCl (35 mg/kg) and xylazine (5 mg/kg). The animals were euthanized

Please cite this article in press as: G. Abrego et al., Biopharmaceutical profile of pranoprofen-loaded PLGA nanoparticles containing hydrogels for ocular administration, Eur. J. Pharm. Biopharm. (2015), http://dx.doi.org/10.1016/j.ejpb.2015.01.026

EJPB 11820
16 February 2015
ARTICLE IN PRESS
No. of Pages 10, Model 5G

by an overdose of sodium pentobarbital (100 mg/kg) administered through marginal ear vein under deep anesthesia. The corneas, with 2 mm ring of sclera were excised and immediately transported to the laboratory in artificial tear solution. The assay was done using Franz diffusion Cells. The cornea was fixed between the donor and receptor compartment of Franz cell. The corneal area available for permeation was 0.64 cm^2. The receptor compartment was filled with freshly prepared Bicarbonate Ringer's (BR) solution. This compartment was kept at 37 ± 0.5 °C and stirred continuously. A weight of 1 g of the HG_PF-NP formulations or 1 mL of the commercial eye drops and free drug solution was placed in the donor compartment (covered with parafilm® in order to avoid evaporation). A volume of 300 µL was withdrawn from the receptor compartment at fixed times and replaced by an equivalent volume of fresh BR solution at the same temperature. The cumulative pranoprofen amount permeated through the cornea per unit area (µg/cm^2) was calculated, at each time point, from cPF in the receiving medium and plotted as function time (min).

2.8. Amount of pranoprofen retained in the cornea

At the end of the study, the cornea was used to determine the amount of drug retained. The cornea was carefully freed from the sclera ring, cleaned using a 0.05% solution of sodium lauryl sulfate and washed with distilled water, weighed and treated with methanol: water (50:50, V/V) under sonication during 30 min using an ultrasound bath. The amount of pranoprofen permeated and retained through the cornea was determined by HPLC as described previously for EE. The results are reported as the median ± SD and median value (minimum – maximum range) of six and three replicates for the amount of pranoprofen permeated and retained, respectively.

2.9. Ocular permeation parameter

Lag time T_L (h) values were calculated by plotting the cumulative pranoprofen permeating the cornea versus time, determining x-intercept by linear regression analysis. The corneal permeability coefficient K_P (cm/h), partition coefficient P_1 (cm) and diffusion coefficient P_2 (h^{-1}) were calculated from the following equations:

$$K_P = P_1 \times P_2 \quad (7)$$

$$P_1 = J/(A \times C_0 \times P_2) \quad (8)$$

$$P_2 = 1/(6 \times T_L) \quad (9)$$

where C_0 is the initial concentration of drug in the donor compartment, A (0.64 cm^2) is the exposed corneal surface. All the values are reported as median value (minimum – maximum range) of three replicates. Experimental data were processed using Graphpad prism software (version 6 Demo) and compared by the application of a non-parametric statistical Kruskal–Wallis Z test followed by the Dunn's multiple comparison tests. Values were considered to be significant at $p < 0.05$.

2.10. Corneal hydration levels

The corneal hydration level HL (%) of the cornea was determined at the end of the study of corneal permeation. The cornea was carefully freed from the sclera ring, washed, weighed (W_w) and dessicated at constant weight dried at 80 °C and then reweighed (W_d). The HL values are reported as median value (minimum – maximum range) of three replicates. HL was calculated using the following expression:

$$HL = [1 - (W_d/W_w) \times 100] \quad (10)$$

2.11. In vitro ocular tolerance

The ocular tolerance of the HG_PF-NP formulations with a 0% or 1% azone was assessed by the HET-CAM test. This is an alternative to animal testing (Draize test) described by Luepke [29]. To perform it, the shell and the inner membranes of 10-day-old chicken eggs were previously removed, so that the CAM that separates the embryo from the air chamber was visible, according to the Invittox protocol [30], and the Journal officiel de la République Française [31]. Tolerance was assessed by testing 6 eggs for each sample, using 2 eggs treated with 0.1 N NaOH and 2 treated with 1% sodium lauryl sulfate solution as positive controls. After exposing the CAM and rinsing it with PBS at pH 7.4, 300 µL of the test solution was applied to the CAM. The intensity of the reaction was semi-quantitatively assessed on a scale from 0 (no reaction) to 3 (strong reaction). The time of the appearance and the intensity of any reactions that occurred within 5 min were recorded. The ocular irritation index (OII) was then calculated using the following equation:

$$OII = \frac{(301-h)\times 5}{300} + \frac{(301-l)\times 7}{300} + \frac{(301-c)\times 9}{300} \quad (11)$$

where h is the time (in seconds) until the start of a hemorrhage, l until the start of lysis and c until the coagulation. The following classification was used: OII ⩽ 0.9: slightly irritating; 0.9 ⩽ OII ⩽ 4.9: moderately irritating; 4.9 ⩽ OII ⩽ 8.9: irritating; 8.9 ⩽ OII ⩽ 21: severely irritating.

2.12. In vivo ocular tolerance

The irritancy of the HG_PF-NP formulations with a 0% or 1% azone was evaluated in New Zealand white rabbits (2.5–3.0 kg) following the method described by Draize et al.[32,33] A single instillation of 50 µL of each HG_PF-NP formulation was instilled in one eye, using untreated contra-lateral eye as a control. Readings were performed 1 h after sample application, then after 1, 2, 3, 4 and 7 days. The method provided an overall scoring system for grading the severity of ocular lesions involving the cornea (opacity), iris (inflammation degree) and conjunctiva (congestion, swelling and discharge). The Draize score was determined by visual assessment of change in these ocular structures. The mean total score (MTS) was calculated as follows:

$$MTS = \frac{X_1(n)}{2} + \sum\frac{X_2(n)}{2} - \sum\frac{X_3(n)}{5} \quad (12)$$

where x_1 (n), x_2 (n) and x_3 (n) are the cornea, conjunctiva and iris scores, respectively, being n the number of rabbits included in the ocular tolerance assay.

2.13. In vivo anti-inflammatory efficacy

The anti-inflammatory efficacy of the HG_PF-NP formulations was assessed using the method described by Spampinato Santi et al. [34], the ocular inflammation was induced by ocular instillation of 50 µL SA (dissolved in PBS, 0.5% (w/v)) in the right eye of eight groups of six rabbits (including control group). A volume of 50 µL of each HG_PF-NP formulation or 0.9% (w/v) isotonic saline solution (control group) was instilled in the conjunctival sac of the right eye 30 min before induction of ocular inflammation by SA using left eye as an inflammation control. Inflammation was quantified 30 min after AS instillation, then after 60, 90, 120, and 150 min, according to a modified Draize scoring system [32]. The MTS was calculated as described previously in the ocular tolerance assay (Eq. (12)). Since corneal transparency was not affected by the instillation of SA, this parameter was not considered. The sum of the conjunctival and iris score is expressed by the mean ± SD.

Please cite this article in press as: G. Abrego et al., Biopharmaceutical profile of pranoprofen-loaded PLGA nanoparticles containing hydrogels for ocular administration, Eur. J. Pharm. Biopharm. (2015), http://dx.doi.org/10.1016/j.ejpb.2015.01.026

EJPB 11820
16 February 2015
ARTICLE IN PRESS
No. of Pages 10, Model 5G

3. Results and discussion

3.1. Physicochemical characterization of the HG_PF-NPs

In previous studies, we have formulated pranoprofen in PLGA nanoparticles as new delivery system suitable for the ocular route. The Z-Ave of the optimized PF-F1NP and PF-F2NP formulations was around 350 nm with PI values in the range of mono-disperse systems (PI < 0.1). Both formulations had net negative charge with ZP values of − 7.41 mV and − 8.5 mV for PF-F1NPs and PF-F2NPs, respectively. The percentage of encapsulated pranoprofen in the polymeric matrix for these formulations reached 80% [20]. For the present work, carbomer 934 was selected as hydrogel matrix to incorporate the optimized PF-F1NP and PF-F2NP suspensions in order to improve the biopharmaceutical profile of pranoprofen for the ocular application. The size and surface morphology of the optimized PF-NPs after incorporation into HG were determined by TEM. The mean diameters of HG_PF-NP formulations were around 300 nm.

TEM image depicted in Fig. 1 reveals that the optimized NPs after incorporation into HG were spherical shape and non-aggregated. The results obtained show that the Z-Ave of the NPs incorporated into HG was similar to those of the NP suspensions.

The stability of the nanoparticles dispersed into the hydrogels was assessed after 1 day of the production and after 90 days of storage at 25 °C. The results obtained by DL 1 day after the production reveal two peaks, one at about 400 nm and another small peak at 1 μm for all the HG_PF-NP formulations indicating an increase of the Z-Ave and PI of the PF-NPs after incorporated into the hydrogels (see Fig. a, c, e and g in Supplementary materials). After 90 days of storage at 25 °C, an increase in the Z-Ave values compared with the results obtained 1 day after the production (see Fig. b, d, f and h in Supplementary materials). The results given in Table 2 show that the Z-Ave values obtained by PCS were similar to those obtained by DL. This increase in the apparent particle size was attributed to the strong entrapment of the particles within the tridimensional gel structure, rather than real particle agglomerates. These results are in accordance with those obtained by Gonzalez-Mira et al. [35]. These results are also in agreement with those obtained by TEM (Fig. 1), since PF-NPs incorporated into HG showed similar particle size in comparison with PF-NP suspension and they were not aggregated. The particle size of formulations intended for ocular instillation is of crucial importance and it should not exceed 10 μm; larger sizes may cause a scratching feeling of a foreign body in the eye and it would therefore compromise patient's comfort [36,37]. The results obtained by PCS in Table 2 also revealed a significant increase of the ZP values of the PF-NPs after incorporated into hydrogels. These results were attributed to the adsorption of negatively charge of the jellifying agent molecules onto the surface of the particles [38]. All the results obtained from the stability study show that the HG_PF-NPs with or without azone formulations exhibit appropriates physicochemical properties for ocular administration, which indicates that the gel network of carbomer could not influence the morphology and size of the NPs notably.

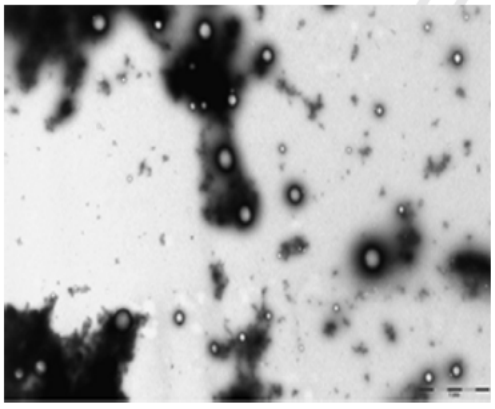

Fig. 1. Transmission electron microphotograph of the optimized NPs incorporated into hydrogel.

3.2. Rheological measurements

The results obtained from the rheological characterization of the HG_PF-NP formulations with or without azone are shown in Table 3.

The rheological characterization of the HG_PF-NP formulations with or without azone revealed a non-Newtonian behavior and the pseudo-plastic character. The spreading properties and the ability of controlling their viscosity showed for the HG_PF-NPs are desirable for the ocular application. The results obtained in Table 3 show that the HG_PF-NP formulations after 90 days of storage at 25 °C exhibited a decreased of the viscosity and Thixotropy values regarding to the values observed at 8 days of the production. Table 3 also reveals that the inclusion of azone in the HG_PF-NP formulations leads a significant viscosity increase in the HG_PF-F1NPs-Azone and HG_PF-F2NPs-Azone formulations. These results are in accordance with the increase of the Z-Ave and PI obtained after 90 days of storage at 25 °C obtained by LD (see Figure in Supplementary material) and PCS (Table 2) which could be explained by the fact that the NPs characterized by a wide polydispersity could pack better than those with a narrow polydispersity. The particles with a large polydispersity have more free space to move around, which means that it was easier for the sample to flow and a lower viscosity would be measured [39].

The oscillation frequency test was carried out from 0.01 to 10 Hz at a constant shear stress within the linear viscoelastic region, in order to determine the related variation of storage modulus (G') and loss modulus (G'') at 25 °C, where the G' describes the elastic properties whereas G'' describes the viscous properties of the sample.

With respect to the stress sweep test of the oscillatory study, the critical stress was found at 10 Pa for the semi-solid formulations assayed. These results suggest that none of the formulations showed a weak structure. From the results of oscillatory stress sweeps, a constant shear stress of 2 Pa (20% of the critical value) was selected to perform the frequency sweep tests. The oscillatory measurements applied to the formulations showed the prevalence

Table 2
Mean particle size (Z-Ave) and zeta potential (ZP) of the HG_PF-NP formulations 1 day after production and after 90 days of storage at 25 °C.

Time	HG_PF-F1NPs		HG_PF-F2NPs		HG_PF-F1NPs-Azone		HG_PF-F2NPs-Azone	
Day	Z-Ave (nm)	ZP (mV)	Z-Ave (nm)	ZP (mV)	Z-Ave (nm)	ZP (mV)	Z-Ave (nm)	ZP (mV)
1	385.20 ± 0.21	−27.50 ± 0.10	391.30 ± 0.22	−37.80 ± 0.13	428.07 ± 0.13	−34.20 ± 0.10	437.20 ± 0.10	−31.87 ± 0.01
90	495.70 ± 0.33	−28.80 ± 0.11	471.50 ± 0.41	−39.4 ± 0.12	549.63 ± 0.10	−37.77 ± 0.12	479.57 ± 0.12	−37.63 ± 0.11

Please cite this article in press as: G. Abrego et al., Biopharmaceutical profile of pranoprofen-loaded PLGA nanoparticles containing hydrogels for ocular administration, Eur. J. Pharm. Biopharm. (2015), http://dx.doi.org/10.1016/j.ejpb.2015.01.026

EJPB 11820
16 February 2015
ARTICLE IN PRESS
No. of Pages 10, Model 5G

Table 3
Rheological characterization of the HG_PF-NP formulations after 8 and 90 days of storage at 25 °C.

Time	HG_PF-F1NPs		HG_PF-F2NPs		HG_PF-F1NPs-Azone		HG_PF-F2NPs-Azone	
Days	Viscosity (Pa s)	Thixotropy (Pa/s)	Viscosity (Pa s)	Thixotropy (Pa/s)	Viscosity (Pa s)	Thixotropy (Pa/s)	Viscosity (Pa s)	Thixotropy (Pa/s)
8	1.64 ± 0.002	586.30	2.38 ± 0.001	1935.03	2.70 ± 0.002	3562.01	2.95 ± 0.002	3281.50
90	1.10 ± 0.001	542.45	0.93 ± 0.002	555.10	1.99 ± 0.001	3290.63	2.08 ± 0.002	3061.30

of the elastic over the viscous behavior ($G' > G''$) for all the HG_PF-NP formulations.

3.3. In vitro drug release

An *in vitro* release study of pranoprofen from the HG_PF-NP formulations, free drug solution (pranoprofen, dissolved in PBS) and commercial eye drops (Oftalar®, pranoprofen 1.0 mg/mL) was performed in Franz diffusion cell. As shown in Fig. 2, the release profile of pranoprofen from the free drug solution and the commercial eye drops exhibited faster release than from the HG_PF-NP formulations with or without azone. After 3 h, 100% of the drug was released from the free drug solution or commercial eye drops. Fig. 2 reveals that the HG_PF-NP formulations with or without azone exhibit a sustained release behavior. The accumulative amount of pranoprofen released from HG_PF-F1NPs, HG_PF-F2NPs, HG_PF-F1NPs-Azone and HG_PF-F2NPs-Azone after 24 h was 41.99%, 64.35%, 56.75% and 59.14%, respectively. Fig. 2 also shows that the amount released of pranoprofen from HG_PF-F1NPs and HG_PF-F1NPs-Azone was slightly smaller than HG_PF-F2NPs and HG_PF-F2NPs-Azone, respectively. These results might be attributed to the fact that during the preparation of the NPs the viscosity increases when there is an increase in the cPVA from 5 mg/mL (PF-F2NPs) to 10 mg/mL (PF-F1NPs). This viscosity increase could result in a more compact polymer matrix leading to slower degradation of the polymer or slower diffusion of the loaded pranoprofen from the nanoparticles [40].

In previous studies, we assessed the release profile of pranoprofen from the PF-F1NP and PF-F2NP formulations. The results obtained from this study revealed that both formulations showed a sustained release behavior, with an initial burst attributed to the pranoprofen adsorbed onto the nanoparticles' surface, followed by a slower release phase while the trapped pranoprofen slowly diffuses out of the polymeric matrix into the release medium [20]. However, the pranoprofen release rate was faster from the pranoprofen-loaded nanoparticles than from the hydrogel formulations with or without azone. All these results suggest that the diffusion velocity of pranoprofen from the nanoparticles can be modified due to higher viscosity of the hydrogels respect to the nanoparticle suspensions. Nevertheless, the pranoprofen-loaded nanoparticles or hydrogels with or without azone could offer sustained release of the drug in comparison with the free drug solution or commercial eye drops.

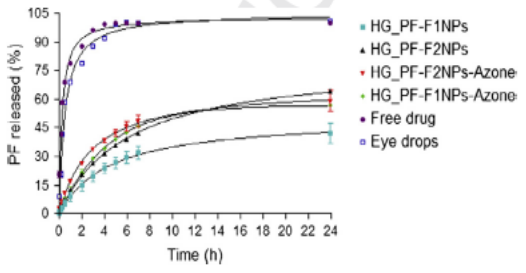

Fig. 2. *In vitro* release profiles of PF from HG_PF-F1NPs, HG_PF-F2NPs, HG_PF-F1NPs-Azone, HG_PF-F2NPs-Azone, commercial eye drops and free drug solution. Mean ± SD, $n = 3$. (For the interpretation of the references to color in this figure legend, the reader is referred to the web version of this article.)

The amount of pranoprofen released from the HG_PF-F1NPs, HG_PF-F2NPs, HG_PF-F1NPs-Azone, HG_PF-F2NPs-Azone, commercial eye drops and free drug solution was adjusted to various kinetic models, such as zero-order, first-order, Higuchi, Hyperbola and Korsmeyer–Peppas (Table 4). The AIC was determined for each model. This parameter is an indicator of the model's suitability for a given dataset. The smaller the value of AIC, the better the model adjusts the data.

From the AIC values (Table 4), it can be concluded that the release curves of pranoprofen from HG_PF-F1NPs, HG_PF-F2NPs, HG_PF-F2NPs-Azone, commercial eye drops and free drug solution fitted to the hyperbola model very well. The drug release mechanism of the HG_PF-F1NPs-Azone formulation differed respect to the other formulations, which adjusted to the first order model. These models had the smaller AIC value and, therefore, statistically, described best the drug release mechanism. Taking into account the diffusional exponent value (n) that is used to characterize different release mechanisms, n values $\leqslant 0.5$ were obtained in all the investigated HG_PF-NP formulations indicating that the release of pranoprofen from the semi-solid formulations occurs by passive diffusion. All these results suggest that the main factors that govern the release of the pranoprofen from the HG_PF-NP formulations with or without azone are the amount of PVA present in the formulation. Furthermore, the release rate is influenced by the presence of pranoprofen in crystalline form, since the drug in crystalline form should dissolve first before being transported out to the matrix by diffusion. As previously reported, in our study that the intensity of some of the peaks of crystalline pranoprofen present in the nanoparticles slightly increased when the concentration of the drug increased from 1.0 mg/mL (PF-F2NPs) to 1.5 mg/mL (PF-F1NPs) by X-ray diffraction technique [20]. Additionally, the drug diffusion out of a hydrogel matrix dependent on mechanical strength degradability, diffusivity, and other physical properties of hydrogel network [41].

3.4. Corneal permeation study

Ex vivo corneal permeation study has been carried out up to 6 h, to compare the permeation profile of pranoprofen from the hydrogel formulations with or without azone, commercial eye drops and free drug solution, and the results are shown in Fig. 3. The permeation parameter values are summarized in Table 5.

At the end of the corneal permeation study, the cornea was used to determine the amount of drug retained and the corneal hydration level. These results are exhibited in Table 6.

The corneal permeation parameters of pranoprofen calculated from the amounts of permeated across cornea from the hydrogel formulations with or without azone, commercial eye drops and free drug solution in Table 5 were compared by the application of a non-parametric statistical Kruskal–Wallis Z test followed by the Dunn's multiple comparison tests. From the statistical analysis of the K_P parameter obtained from these formulations, statistically significant differences ($p < 0.05$) were found between HG_PF-F1NPs and HG_PF-F2NPs, HG_PF-F1NPs and commercial eye drops,

Please cite this article in press as: G. Abrego et al., Biopharmaceutical profile of pranoprofen-loaded PLGA nanoparticles containing hydrogels for ocular administration, Eur. J. Pharm. Biopharm. (2015), http://dx.doi.org/10.1016/j.ejpb.2015.01.026

EJPB 11820
16 February 2015
ARTICLE IN PRESS
No. of Pages 10, Model 5G

Table 4
Mean parameter obtained after fitting the release data of HG_PF-F1NPs, HG_PF-F2NPs, HG_PF-F1NPs-Azone, HG_PF-F2NPs-Azone, commercial eye drops and free drug solution to different kinetic models.

Models	Parameters	HG_PF-F1NPs	HG_PF-F2NPs	HG_PF-F1NPs-Azone	HG_PF-F2NPs-Azone	Eye drops	Free drug
Zero order	AIC	75.35	80.67	86.52	88.03	110.78	109.76
First Order	AIC	9.40	33.32	−7.46	37.01	70.48	67.21
Higuchi	AIC	55.12	52.86	69.11	71.01	101.97	102.63
Hyperbola		7.35	−8.23	26.99	15.96	59.36	50.52
Korsmeyer-	*n*	0.50	0.50	0.50	0.50	0.38	0.28
Peppas	AIC	55.20	53.22	69.20	72.62	110.27	115.37

n, diffusional release exponent; AIC, Akaike information criterion.

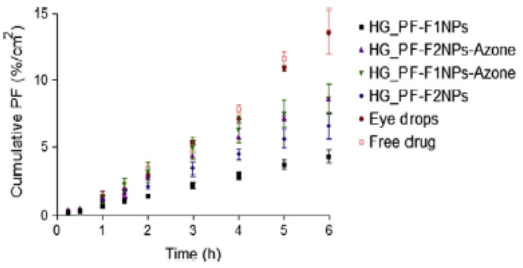

Fig. 3. *Ex vivo* corneal permeation profile of PF from the HG_PF-F1NPs, HG_PF-F2NPs, HG_PF-F1NPs-Azone, HG_PF-F2NPs-Azone formulations, commercial eye drops and free drug solution after 6 h. Mean ± SD, $n = 6$. (For the interpretation of the references to color in this figure legend, the reader is referred to the web version of this article.)

HG_PF-F1NPs-Azone and HG_PF-F2NPs, HG_PF-F1NPs-Azone and commercial eye drops. The HG_PF-F1NPs and HG_PF-F2NPs show the lowest and highest K_P value, respectively. Statistically significant differences ($p < 0.05$) were found between HG_PF-F1NPs and HG_PF-F2NPs, HG_PF-F1NPs and commercial eye drops, HG_PF-F1NPs and free drug, HG_PF-F2NPs-Azone and free drug, HG_PF-F1NPs-Azone and commercial eye drops, HG_PF-F1NPs-Azone and free drug for the P_1 parameter. As shown in Table 5 the free drug solution and HG_PF-F1NPs formulation exhibited the highest and lowest P_1 value, respectively. The statistical analysis of the P_2 and T_L parameters in Table 5 revealed a significant difference ($p < 0.05$) between HG_PF-F1NPs and commercial eye drops, HG_PF-F1NPs and free drug, HG_PF-F2NPs-Azone and free drug, HG_PF-F1NPs-Azone and commercial eye drops, HG_PF-F1NPs-Azone and free drug. The HG_PF-F1NP formulation exhibits the highest P_2 value and the lowest P_1 value, thus this formulation shows the lowest K_P value, since K_P depends directly of P_1 and P_2. The K_P values obtained for the HG_PF-F2NP formulation, commercial eye drops and free drug solution are directly related to the P_1 parameter. Otherwise, the P_2 values exhibited for the HG_PF-F1NPs-Azone and HG_PF-F2NPs-Azone suggest that the diffusion coefficient of a drug is influenced by the presence of azone in the formulation. The T_L values obtained in Table 5 for the HG_PF-NPs with or without azone are lower than those obtained for the commercial eye drops and free drug solution. Therefore, these formulations reach faster the steady state equilibrium than the commercial eye drops and free drug solution.

The Q_P and Q_R values obtained for the commercial eye drops and free drug solution are greater than those obtained for the hydrogel

Table 5
Corneal permeation parameters of PF from HG_PF-NP formulations, commercial eye drops and free drug solution after 6 h.

Samples	$K_P \times 10^2$ (cm/h)	$P_1 \times 10^1$ (cm)	$P_2 \times 10^1$ (h^{-1})	$TL \times 10^1$ (h)
HG_PF-F1NPs	1.50 (1.32–1.72)[b,e]	0.05 (0.04–0.05)[b,e,f]	32.64 (24.61–40.67)[e,f]	0.54 (0.41–0.68)[e,f]
HG_PF-F2NPs	5.56 (4.10–7.03)[a,c]	0.61 (0.53–0.69)[a]	8.98 (7.80–10.16)	1.90 (1.64–2.14)
HG_PF-F1NPs-Azone	2.68 (2.62–2.72)[b,e]	0.11 (0.08–0.14)[e,f]	25.87 (18.09–33.66)[e,f]	0.71 (0.50–0.92)[e,f]
HG_PF-F2NPs-Azone	3.26 (3.27–3.29)	0.20 (0.16–0.24)[f]	16.93 (13.39–20.47)[f]	1.03 (0.81–1.25)[f]
Eye drops	3.46 (3.42–3.62)[a,c]	0.89 (0.77–0.91)[a,c]	3.98 (3.87–4.47)[a,c]	4.19 (3.73–4.31)[a,c]
Free drug	3.32 (3.28–3.56)	1.00 (0.93–1.07)[a,d,c]	3.30 (3.06–3.84)[a,d,c]	5.00 (4.34–5.45)[a,d,c]

Results are reported as median value (minimum–maximum range) $n = 6$.
[a] Differences with HG_PF-F1NPs.
[b] Differences with HG_PF-F2NPs.
[c] Differences with HG_PF-F1NPs-Azone.
[d] Differences with HG_PF-F2NPs-Azone.
[e] Commercial eye drops.
[f] Free drug solution.

Table 6
Amounts of PF permeated (Q_P) and retained (Q_R) across cornea and corneal hydration level (HL) from the HG_PF-NP formulations, commercial eye drops and free drug solution after 6 h.

Samples	Q_P (%/cm²)	Q_R (%/cm² g)	HL (%)
HG_PF-F1NPs	4.28 (3.6–4.93)	18.23 (15.21–19.61)	79.87 (76.18–80.03)
HG_PF-F2NPs	6.58 (5.35–7.08)	16.32 (16.17–16.64)	77.56 (77.25–79.80)
HG_PF-F1NPs-Azone	8.57 (7.20–9.59)	24.56 (23.38–25.57)	76.98 (76.57–78.87)
HG_PF-F2NPs-Azone	6.61 (8.51–8.17)	20.71 (16.64–24.60)	78.19 (77.87–79.67)
Eye drops	13.53 (11.12–13.57)	52.55 (51.23–53.62)	77.44 (78.23–79.87)
Free drug	13.62 (11.58–15.46)	50.41 (49.91–50.19)	78.12 (76.67–79.98)

Results are reported as median value and minimum – maximum range values (Q_P, $n = 6$; Q_R, $n = 3$; HL, $n = 3$).

Please cite this article in press as: G. Abrego et al., Biopharmaceutical profile of pranoprofen-loaded PLGA nanoparticles containing hydrogels for ocular administration, Eur. J. Pharm. Biopharm. (2015), http://dx.doi.org/10.1016/j.ejpb.2015.01.026

EJPB 11820
16 February 2015
ARTICLE IN PRESS
No. of Pages 10, Model 5G

formulations with or without azone (Table 6). Nevertheless, the free drug solution is inherently irritating to the eye and additionally, pranoprofen is unstable in aqueous solution [42]. Otherwise, the increased in the corneal permeation of pranoprofen showed for the commercial eye drops can be explained due to this conventional dosage form has a combination of benzalkonium chloride (BAK) and edetate disodium (EDTA). The BAK produces an increase of the amount of drug permeating the cornea by disruption of the corneal epithelium. Additionally, it can also emulsify the corneal epithelium, leading to increased partitioning of the drug [43]. Moreover, EDTA also increases the corneal permeability of different drugs, by removing the extracellular calcium ions increasing tight junction permeability [22,44,45].

Table 6 also shows that the Q_P and Q_R values of pranoprofen in the cornea from the HG_PF-F1NPs-Azone and HG_PF-F2NPs-Azone formulations are greater than those obtained from HG_PF-F1NPs and HG_PF-F2NPs, respectively. The results suggest that the inclusion of azone into HG formulation leads to the increase in the amount of drug permeated and retained. Azone is one of the most widely studied penetration enhancers of hydrophilic and lipophilic drugs, which can be used as a safe and effective penetration enhancer for human. Azone as a penetration enhancer is most effective at low percentages; values ranging from 1% to 3% had been reported in the literature. Although azone has been used for over 25 years, several researchers continue to investigate its mechanism of action. The mechanism of azone may be related with modifications in the epithelial cell junctions and enhanced the influx of water and the transcorneal penetration of hydrophilic drugs but delayed the apparent drug permeation of lipophilic drugs through the cornea [22,23]. Regarding the corneal hydration analysis, the healthy corneal has a hydration level of 76–80% [46]. According to the results obtained in Table 6 for the HG_PF-NP formulations with or without azone, commercial eye drops and free drug solution, it can be concluded that during the assay the cornea was no damage.

3.5. In vitro ocular tolerance

The studies using the HET-CAM are based on the direct application of the sample onto the chorioallantoic membrane and the observation of reactions, such as hemorrhage, intravasal coagulation or lysis of blood vessels [47]. The results of the HET-CAM test revealed optimal ocular tolerance of the HG_PF-NPs with or without azone since no irritation reactions were detected within 5 min of the assay (score 0).

3.6. In vivo ocular tolerance

Durand-Cavagna et al. evaluated in rabbits the ocular irritation potential of 1% or 2% azone incorporated in ophthalmic vehicles, such as poloxamer 188, hydroxyl-ethylcellulose, benzalkonium chloride and phosphate buffer. Signs of ocular irritation were detected. However, the reported results were inconclusive since irritation could not be attributed to the presence of azone or benzalkonium chloride [48]. In the present work, the irritancy of the optimized HG_PF-NP formulations with or without azone was evaluated in New Zealand white rabbits. The results of Draize test showed good ocular tolerance of HG_PF-NPs with a 0% or 1% azone. No signs of ocular irritancy were detected. These results are in accordance with those obtained by HET-CAM test.

3.7. In vivo anti-inflammatory efficacy

Fig. 4 shows the anti-inflammatory efficacy effect of different formulations containing pranoprofen in the ocular edema induced by instillation of SA.

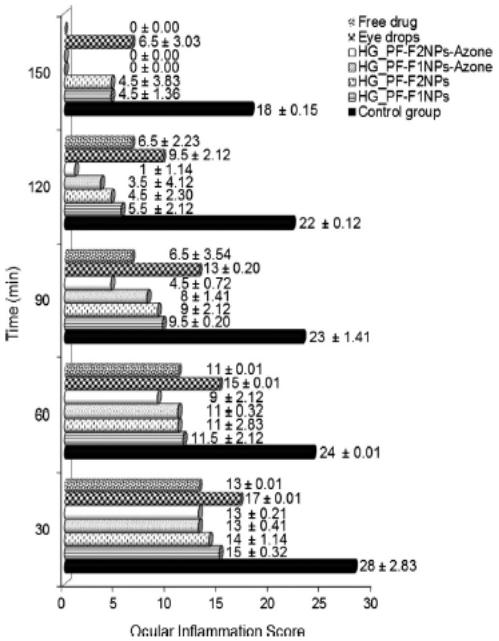

Fig. 4. Anti-inflammatory activity of PF from the HG_PF-F1NPs, HG_PF-F2NPs, HG_PF-F1NPs-Azone, HG_PF-F2NPs-Azone formulations, commercial eye drops and free drug solution. Mean ± SD. $n = 6$.

Although the commercial eye drops and free drug solution show the highest Q_R values of pranoprofen in the cornea, the anti-inflammatory efficacy values obtained for the commercial eye drops are lower compared to the other tested formulations (Fig. 4). Until 120 min, the free drug solution exhibits slower anti-inflammatory activity than the HG_PF-NP formulation with or with azone. The results obtained for the commercial eye drops and free drug solution could be explained by the fact that these formulations show T_L values greater than those obtained for the HG_PF-NPs with or without azone. Thus, the commercial eye drops and free drug solution reach slower steady state equilibrium than the HG_PF-NPs, therefore show slower anti-inflammatory activity than the other tested formulation. Fig. 4 also shows that the HG_PF-F1NPs-Azone and HG_PF-F2NPs-Azone formulations significantly reduced the ocular edema, compared to the HG_PF-F1NP and HG_PF-F2NP formulations, respectively. According to the results obtained in this study, the inclusion of azone into the HG_PF-NP formulations leads to the increase of the anti-inflammatory efficacy of pranoprofen in the cornea. The anti-inflammatory efficacy values exhibited for the HG_PF-F1NPs-Azone and HG_PF-F2NPs-Azone formulations are correlated directly with the amount of drug retained in the cornea. Therefore, the ocular application of the HG_PF-F1NPs-Azone or HG_PF-F2NPs-Azone formulations could more effective in the treatment of ocular edema that the HG_PF-F1NP or HG_PF-F2NP formulations.

4. Conclusions

The optimized PF-F1NP and PF-F2NP suspensions were successfully dispersed into blank hydrogels or hydrogels containing 1% azone. The hydrogel formulations showed a rheological behavior and physicochemical properties suitable for ocular pranoprofen delivery. The HG_PF-NPs with or without azone exhibited sustained release behavior with a slower release of pranoprofen. According to the results obtained from the corneal permeation

Please cite this article in press as: G. Abrego et al., Biopharmaceutical profile of pranoprofen-loaded PLGA nanoparticles containing hydrogels for ocular administration, Eur. J. Pharm. Biopharm. (2015), http://dx.doi.org/10.1016/j.ejpb.2015.01.026

EJPB 11820 ARTICLE IN PRESS No. of Pages 10, Model 5G
16 February 2015

and anti-inflammatory efficacy studies, the commercial eye drops and free drug solution showed the highest Q_R values of pranoprofen in the cornea. However, both formulations cannot be considered optimal in the treatment of ocular diseases due to the free drug solution is inherently irritating to the eye and additionally, pranoprofen is unstable in aqueous solution. Besides, following the instillation of commercial eye drops, the most of the drugs is removed, by ear dilution and tear turn over from the surface of the eye due to the low viscosity of these conventional dosage forms. The HG_PF-F1NPs-Azone and HG_PF-F2NPs-Azone formulations significantly reduced the ocular edema, compared with other tested formulations. These results indicate that the inclusion of azone into the HG_PF-NP formulations leads to the increase of the anti-inflammatory efficacy effect of pranoprofen in the cornea. Therefore, the ocular application of these formulations could be more effective in the treatment of ocular edema.

The HG_PF-NPs with 0% or 1% azone showed an optimal ocular tolerance by the *in vitro* e *in vivo* ocular irritation test. All these results suggest that the ocular administration of the HG_PF-F1NPs-Azone or HG_PF-F2NPs-Azone formulations could be an effective and appropriate system for ophthalmic administration of pranoprofen, improving the biopharmaceutical profile of this drug, thus enhancing the local anti-inflammatory and analgesic effect of this drug and, consequently, improving the patient's compliance. However, the formulations for ocular applications based on carbomer hydrogels must be preserved in order to avoid the growth of microorganisms, but unfortunately the action of the ophthalmic preservatives is non-specific and these can cause toxicity or damage to the ocular structure. In order to ensure the conservation of the HG_PF-NP formulation, additional studies related to sterilization by autoclave or gamma irradiation would be required.

Conflict of interest

The authors declare that they have no conflict of interest.

Acknowledgments

G. Abrego wishes to acknowledge, the Spanish Ministry of Foreign Affairs and Cooperation and the Spanish Agency for International Development Cooperation (MAEC-AECID) for a research scholarship. The authors would also like to acknowledge the financial support of the Spanish Ministry of Science and Innovation (Grant MAT2011-26994), Portuguese Science and Technology Foundation (FCT), and European funds (FEDER/COMPETE) under the reference PTDC/SAU-FAR/113100/2009.

Appendix A. Supplementary data

Supplementary data associated with this article can be found, in the online version, at http://dx.doi.org/10.1016/j.ejpb.2015.01.026.

References

[1] I. Akyol-Salman, D. Leçe-Sertöz, O. Baykal, Topical pranoprofen 0.1% is as effective anti-inflammatory and analgesic agent as diclofenac sodium 0.1% after strabismus surgery, J. Ocul. Pharmacol. Ther. 23 (2007) 280–283.
[2] M. Sawa, K. Masuda, M. Nakashima, Anti-inflammatory effect of diclofenac sodium eye drops on cataract surgery. Double masked study with pranoprofen eye drops, IOL RS 13 (1999) 193–200.
[3] A.Z. McColgin, J.S. Heier, Control of intraocular inflammation associated with cataract surgery, Curr. Opin. Ophthalmol. 11 (2000) 3–6.
[4] X. Liu, S. Wang, A.A. Kao, Q. Long, The effect of topical pranoprofen 0.1% on the clinical evaluation and conjunctival HLA-DR expression in dry eyes, Cornea 31 (2012) 1235–1239.
[5] R. Notivol, M. Martinez, M. Bergamini, Treatment of chronic nonbacterial conjunctivitis with a cyclo-oxygenase inhibitor or a corticosteroid. Pranoprofen Study Group, Am. J. Ophthalmol. 117 (1994) 651–656.
[6] M. Narashino, H. Ichikawa, S. Narita, A.S. Yotsukaido, Sustained-Release Pranoprofen Preparation, US00522506A, 1993.
[7] K. Kobe, H. Otsu, Y. kobe, Y. Kakogawa, Method for Stabilizing Pranoprofen and Stable Liquid Preparation of Pranoprofen, United States Patent. US005856345A, 1999.
[8] J. Araújo, E. Gonzalez, M.A. Egea, M.L. Garcia, E.B. Souto, Nanomedicines for ocular NSAIDs: safety on drug delivery, Nanomedicine: Nanotechnol. Biol. Med. 5 (2009) 394–401.
[9] L.S. Nair, C.T. Laurencin, Biodegradable polymers as biomaterials, Prog. Polym. Sci. 32 (2007) 762–798.
[10] A. Sabzevari, K. Adibkia, H. Hashemi, A. Hedayatfar, N. Mohsenzadeh, F. Atyabi, M.H. Ghahremani, R. Dinarvand, Polymeric triamcinolone acetonide nanoparticles as a new alternative in the treatment of uveitis: *in vitro* and *in vivo* studies, Eur. J. Pharm. Biopharm. 84 (2013) 63–67.
[11] E. Vega, M.A. Egea, M.L. Garduño-Ramírez, M.L. García, E. Sánchez, M. Espina, A.C. Calpena, Flurbiprofen PLGA-PEG nanospheres: role of hydroxy-β-cyclodextrin on *ex vivo* human skin permeation and *in vivo* topical anti-inflammatory efficacy, Colloids Surf. B. Biointerfaces 110 (2013) 339–346.
[12] S.P. Ayalasomayajula, U.B. Kompella, Subconjunctivally administered celecoxib-PLGA microparticles sustain retinal drug levels and alleviate diabetes-induced oxidative stress in a rat model, Eur. J. Pharmacol. 511 (2005) 191–198.
[13] T. Gratieri, G.M. Gelfuso, E.M. Rocha, V.H. Sarmento, O. de Freitas, R.F.V. Lopez, A poloxamer/chitosan in situ forming gel with prolonged retention time for ocular delivery, Eur. J. Pharm. Biopharm. 75 (2010) 186–193.
[14] A. Lauterbach, C.C. Müller-Goymann, Comparison of rheological properties, follicular penetration, drug release, and permeation behavior of a novel topical drug delivery system and a conventional cream, Eur. J. Pharm. Biopharm., doi: 10.1016/j.ejpb.2014.10.001.
[15] A. Zoppi, Y.G. Linck, G.a. Monti, D.B. Genovese, A.F. Jimenez Kairuz, R.H. Manzo, M.R. Longhi, Studies of pilocarpine:carbomer intermolecular interactions, Int. J. Pharm. 427 (2012) 252–259.
[16] B. Buchan, G. Kay, A. Heneghan, K.H. Matthews, D. Cairns, Gel formulations for treatment of the ophthalmic complications in cystinosis, Int. J. Pharm. 392 (2010) 192–197.
[17] P. Batheja, L. Sheihet, J. Kohn, A.J. Singer, B. Michniak-Kohn, Topical drug delivery by a polymeric nanosphere gel: Formulation optimization and *in vitro* and *in vivo* skin distribution studies, J. Control. Release. 149 (2011) 159–167.
[18] F.E. Amara, M.E. Meleis, M.A. Seif, E.Y. Moursy, Study of the metabolic effect and histopathological nasal mucosal changes after prolonged intranasal insulin administration, J. Diabetol. 1 (2011) 1–10.
[19] H. Fessi, F. Puisieux, J.P. Devissaguet, N. Ammoury, S. Benita, Nanocapsule formation by interfacial polymer deposition following solvent displacement, Int. J. Phar. 55 (1989) R1–R4.
[20] G. Abrego, H.L. Alvarado, M.A. Egea, E. Gonzalez-Mira, A.C. Calpena, M.L. Garcia, Design of nanosuspensions and freeze-dried PLGA nanoparticles as a novel approach for ophthalmic delivery of pranoprofen, J. Phar. Sci. 103 (2014) 3153–3164.
[21] J.R. Robinson, Ocular drug delivery mechanism(s) of corneal drug transport and mucoadhesive delivery systems, STP Pharma 5 (1989) 839–846.
[22] I.P. Kaur, R. Smitha, Penetration enhancers and ocular bioadhesives: two new avenues for ophthalmic drug delivery, Drug Dev. Ind. Pharm. 28 (2002) 353–369.
[23] A.C. Williams, B.W. Barry, Penetration enhancers, Adv. Drug Deliv. Rev. 64 (2012) 128–137.
[24] F. Lallemand, O. Felt-Baeyens, K. Besseghir, F. Behar-Cohen, R. Gurny, Cyclosporine A delivery to the eye: a pharmaceutical challenge, Eur. J. Pharm. Biopharm. 56 (2003) 307–318.
[25] I.M. Ismail, C.C. Chen, J.B. Richman, J.S. Andersen, D.D. Tang-Liu, Comparison of azone and hexamethylene lauramide in toxicologic effects and penetration enhancement of cimetidine in rabbit eyes, Pharm. Res. 9 (1992) 817–818.
[26] T.J. Franz, Percutaneous absorption. On the relevance of *in vitro* data, J. Investig. Dermatol. 64 (1975) 190–195.
[27] P. Costa, J.M. Sousa, Modeling and comparison of dissolution profiles, Eur. J. Pharm. 13 (2001) (2001) 123–133.
[28] K. Yamaoka, T. Nakagawa, T. Uno, Application of Akaike's information criterion (AIC) in the evaluation of linear pharmacokinetic equations, J. Pharmacokinet. Biopharm. 6 (1978) 165–175.
[29] N.P. Luepke, Heng's egg chorioallantoic membrane test for irritation potential, Food Chem. 23 (1985) 287–291.
[30] M. Warren, K. Atkinson, S. Steer, Invittox-protocol: the Ergatt/Frame data bank of *in vitro* techniques in toxicology, Heńs egg test. Nr 15 (4) (1990) 707–710..
[31] Journal Officiel de la République Française. Méthode Officiel d'evaluation du potentiel irritant par application sur la membrane chorioallantoidienne de l'oeuf de poule. Annexe IV. (1996) 1937–1938.
[32] J. Draize, G. Woodard, H. Calvery, Methods for the study of irritation and toxicity of substances applied topically to the skin and mucous membranes, J. Pharmacol. Exp. Ther. 82 (1944) 377–390.
[33] J.H. Kay, J.K Calandra, Interpretation of eye irritation test, J. Soc. Cosmet. Chem. 13 (1962) 281–289.
[34] S. Spampinato, A. Marino, C. Bucolo, M. Canossa, T. Bachetti, S. Mangiafico, Effects of sodium naproxen eye drops on rabbit ocular inflammation induced by sodium arachidonate, J. Ocul. Pharmacol. 7 (1991) 125–133.
[35] E. Gonzalez-Mira, S. Nikolić, A.C. Calpena, M.A. Egea, E.B. Souto, M.L. Garcia, Improved and safe transcorneal delivery of flurbiprofen by NLC and NLC-based hydrogels, J. Pharm. Sci. 101 (2012) 707–725.

Please cite this article in press as: G. Abrego et al., Biopharmaceutical profile of pranoprofen-loaded PLGA nanoparticles containing hydrogels for ocular administration, Eur. J. Pharm. Biopharm. (2015), http://dx.doi.org/10.1016/j.ejpb.2015.01.026

EJPB 11820
16 February 2015
ARTICLE IN PRESS
No. of Pages 10, Model 5G

[36] A. Zimmer, J. Kreuter, Microspheres and nanoparticles used in ocular delivery systems, Ocul. Drug Deliv. Rev. 168 (1995) 61–73.
[37] X. Song, Y. Zhao, S. Hou, F. Xu, R. Zhao, J. He, Z. Cai, Y. Li, Q. Chen, Dual agents loaded PLGA nanoparticles: systematic study of particle size and drug entrapment efficiency, Eur. J Pharm. Biopharm. 69 (2008) 445–453.
[38] F. Han, R. Yin, X. Che, J. Yuan, Y. Cui, H. Yin, S. Li, Nanostructured lipid carriers (NLC) based topical gel of flurbiprofen: design, characterization and *in vivo* evaluation, Int J. Pharm. 439 (2012) 349–357.
[39] Malvern Instruments. 10 Ways to Control Rheology by Changing Particles Properties. INFORM Series of White Papers, 2009.
[40] S.K. Sahoo, J. Panyam, S. Prabha, V. Labhasetwar, Residual polyvinyl alcohol associated with poly (d, l-lactide-co-glycolide) nanoparticles affects their physical properties and cellular uptake, J. Control Release 82 (2002) 105–114.
[41] M. Hamidi, A. Azadi, P. Rafiei, Hydrogel nanoparticles in drug delivery, Adv. Drug Deliv. Rev. 60 (2008) 1638–1649.
[42] M. Ahuja, A.S. Dhake, S.K. Sharma, D.K. Majumdar, Topical ocular delivery of NSAIDs, AAPS J. 10 (2008) 229–241.
[43] M.S. Rathore, D.K. Majumdar, Effect of formulation factors on *in vitro* transcorneal permeation of gatifloxacin from aqueous drops, AAPS PharmSciTech. 7 (2006) E1–E6.
[44] K. Järvinen, T. Järvinen, A. Urtti, Ocular absorption following topical delivery, Adv. Drug Deliv. Rev. 16 (1995) 3–19.
[45] P. Furrer, J.M. Mayer, R. Gurny, Ocular tolerance of preservatives and alternatives, Eur. J. Pharm. Biopharm. 53 (2002) 263–280.
[46] R.D. Schoenwald, H.S. Huang, Corneal penetration behavior of beta-blocking agents I: physiochemical factors, J. Pharm. Sci. 72 (1983) 1266–1272.
[47] J. Tavaszi, P. Budai, The use of HET-CAM test in detecting the ocular irritation, Commun. Agric. Appl. Biol. Sci. 72 (2007) 137–141.
[48] G. Durand-Cavagna, P. Duprat, S. Molon-Noblot, P. Delort, A. Rozier, Corneal endothelial changes with Azone, a penetration enhancer, Lens Eye Toxic. Res. 6 (1989) 109–117.

Supplementary Material

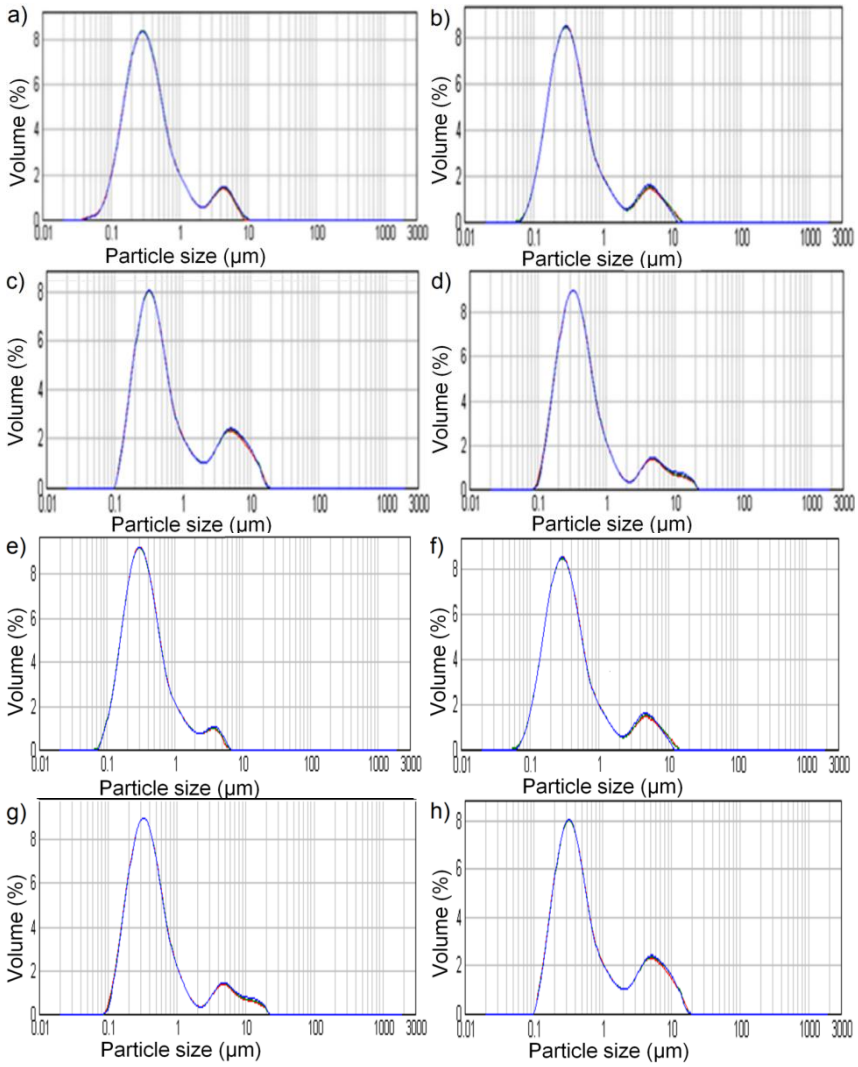

Particle size measurements by LD for a) and b) HG_PF-F1NPs, c) and d) HG_PF-F2NPs, e) and f) HG_PF-F1NPs-Azone, g) and h) HG_PF-F2NPs-Azone after 1 and 90 days of storage at 25ºC, respectively.

Please cite this article in press as: G. Abrego et al., Biopharmaceutical profile of pranoprofen-loaded PLGA nanoparticles containing hydrogels for ocular administration, Eur. J. Pharm. Biopharm. (2015), http://dx.doi.org/10.1016/j.ejpb.2015.01.026

Pranoprofen-loaded polymeric nanoparticles hydrogels for skin administration: *in vitro*, *ex vivo* and *in vivo* characterization. (Sometido a publicación)

G. Abrego, H.L. Alvarado, E. Souto, B. Guevara, L.H. Bellowa, M.L. Garduño, M.L. García, A.C. Calpena.

Nanotechnology

3.3. Artículo 3: Pranoprofen-loaded polymeric nanoparticles hydrogels for skin administration: *in vitro*, *ex vivo* and *in vivo* characterization (Artículo 3).

Resumen

Pranoprofeno fue formulado en nanopartículas poliméricas de PLGA. Los sistemas optimizados (PF-F1NPs; PF-F2NPs) fueron incorporados en un hidrogel de carbomero (HG_PF-F1NPs y HG_PF-F2NPs) o hydrogel en presencia de un 3% de azona (HG_PF-F1NPs-Azona y HG_PF-F2NPs-Azona), con el propósito de explorar y diseñar nuevas formulaciones que permitan mejorar el perfil biofarmacéutico de este fármaco, prologar el tiempo de contacto del fármaco en la superficie dérmica, incrementando la retención del fármaco en la piel y mejorando la eficacia analgésica y antiinflamatoria de pranoprofeno.

El analisis morfologico de las formulaciones semisólidas de pranoprofeno hidrogel llevado a cabo por microscopía elecronica de transmisión (TEM) reveló que el diametro de particula de las NPs antes y depués de ser incorporadas en el hidrogel son similar entre si. Al mismo tiempo, la caracterización fisicoquímica de las NPs dispersada en el hidrogel, al cabo de 90 dias de almacenamiento mostro que las formulaciones evaluadas conservan propiedades fisicoquímicas adecuadas para la aplicación dérmica. Adicionalmente, la caracterización reologica de las formulaciones de HG_PF-NPs con o sin azona exhibieron un comportamiento no-Newtoniano indicando que las formulaciones testadas se adhieren facilmente a la superficie dérmica.

Todas las formulaciones semisólidas exhibieron una liberación sostenida del fármaco comparada con la solucion de fárrmaco libre. El ajuste cinetico de las curvas de liberación de pranoprofeno a partir de las formulaciones de NPs incorporadas en el hidrogel en presencia o ausencia de azona reveló que la liberacón del PF a partir de estas formulaciones se produce por difusión pasiva, principalment a través de los poros de la matriz.

Los resultados obtenidos a partir del ensayo de permeación transdérmica *ex vivo* y la evaluación *in vivo* de la eficacia antiinflamatoria de pranoprofeno

contenido en las formulaciones semisólidas sugieren que la aplicación dérmica de la formulación HG_PF-F2NPs puede ser un sistemas más efectico para tratar el edema de la superficie de la piel, respecto al resto de formulaciones. Ningún signo de irritación dérmico fue detectado tras la aplicación de las formulaciones semisólidas de pranoprofeno en ausencia o en presencia de un 3% de azona.

Pranoprofen-loaded polymeric nanoparticles hydrogels for skin administration: *in vitro*, *ex vivo* and *in vivo* characterization

Guadalupe Abrego[a,b], Helen Alvarado[a,b], Eliana B. Souto, PhD[c], Bessy Guevara[b], Lyda Halbaut Bellowa, PhD[d], Maria Luisa Garduño, PhD[e], María Luisa Garcia, PhD[a] , Ana Calpena, PhD[b]

[a]Department of Physical Chemistry, Faculty of Pharmacy, University of Barcelona, Av. Joan XXIII s/n, 08028 Barcelona, Spain.
[b]Department of Biopharmacy and Pharmaceutical Technology, Faculty of Pharmacy, University of Barcelona, Av. Joan XXIII s/n, 08028 Barcelona, Spain.
[c]Department of Pharmaceutical Technology, Faculty of Health Sciences, Fernando Pessoa University, Porto, Portugal.
[d]Department of Pharmacy and Pharmaceutical Technology, Faculty of Pharmacy, University of Barcelona, Av. Joan XXIII s/n, 08028 Barcelona, Spain.
[e]Centro de Investigaciones Químicas de la Universidad Autónoma del Estado de Morelos. Avenida Universidad 1001, 62210, Cuernavaca, Morelos, México.

Abstract

Pranoprofen (PF)-loaded nanoparticles (PF-F1NPs and PF-F2NPs) were incorporated into blank hydrogel (HG_PF-F1NPs and HG_PF-F1NPs) or HG with a 3% azone (HG_PF-F1NPs-Azone and HG_PF-F2NPs-Azone) as a means of exploring novel formulations to improve the biopharmaceutical profile of PF for the topical application, facilitate the prolonged contact of the PF on the skin and improve its skin retention, thus enhanced anti-inflammatory and analgesic efficiency. The physicochemical characterization of the formulations showed a non-Newtonian behavior and appropiate characteristics for skin administration. All the formulations exhibited a sustained release behavior. The results obtained from *ex vivo* skin human permeation and *in vivo* anti-inflammatory efficacy studies of the semi-solid formulations suggest that the topical application of the HG_PF-F2NPs may be more effective in the treatment of edema on the skin surface respect to the others formulations. No signs of

skin irritancy were detected for all the semi-solid formulations with a 0% or 3% azone.

Key words: Pranoprofen, nanoparticles, hydrogel, biodegradable polymers, skin tolerance, physical stability.

PF (Pranoprofen) is a non-steroidal anti-inflammatory drug (NSAID) which can be used as a safe and effective alternative anti-inflammatory treatment in ocular therapy.[1,2] This drug also can be used for the treatment of the acute and long term management of osteoarthritis and rheumatoid arthritis. Although this drug has shown high anti-inflammatory and analgesic efficiency and a minimal risk of side effects on gastrointestinal tract after oral administration.[3] The pharmaceutical use of PF is limited due to its inadequate biopharmaceutical profile. PF has a short plasmatic half-life, low water solubility and is unstable in aqueous solution, particularly when exposed to light. [4,5]

The application of NSAIDs via the dermal route offers a lot of advantages such as avoid the first pass metabolism, avert the risk of gastro-intestinal disturbance and targeting only the areas of disease.[6] Nevertheless, the penetration of the drug through skin is hindered by the stratum corneum, which is the upper most layer of the epidermis. In addition, the physicochemical characteristic of the drug, its interactions with the membrane and its pharmacokinetics properties also modify the penetration of the drug.[7] Taking into account those considerations, different drug delivery systems have been most widely studied with the purpose of improving drug targeting of tissues, increase drug bioavailability across biological membranes or reducing its toxicity. Those systems can be administrated by different routes including the dermal route.[8] In this way, several authors have used these systems for topical delivery of different drug or cosmetics active. Some of the most commonly used nanostructured systems in the topical administration of drugs are liposomes, nanoemulsion and solid lipid nanoparticles.[9,10] However, there are only few studies of polymeric nanoparticles (NPs) as vehicle for skin drug delivery or semi-solid formulation containing polymeric NPs for topical application. Biodegradable polymers, such as PLGA, have been widely used in these drug delivery systems, in part due to their approval by the FDA for use in humans

and they can effectively deliver the drug to a target site with a controllable degradation.[11] Four pathways of penetration across the skin have been identified depending on physicochemical properties of the compound: intercellular, transcellular, and two transappedageal, through hair follicles and sweat glands.[12] However, the transappendageal route, via hair follicles and sweat ducts occupy for only approximately 0.1% of skin surface area. Therefore, they were not considered to represent significant transdermal penetration route. Nevertheless, when considering cutaneous transport from nanoparticles formulations, the appendageal route may play a significant role.[13]

To obtaine a topical dosage form with a desired semisolid consistency, the NPs suspension can be incorporated into commonly used dermal carriers like hydrogels (HGs) or cream.[14,15] In addition, to improve the permeability of drugs through the skin, different enhancers have been used. Azone is one of the most widely studied penetration enhancers which can be used as a safe and effective penetration enhancer for human use in the range of 1 to 10%.[16]

In previous studies, we formulated PF in PLGA nanoparticles (PF-NPs**)** using the solvent displacement technique.[17] A 2^4 central composite factorial design was used to study the main effects and interactions of four factors on average particle size (Z Ave), polydispersity index (PI), zeta potential (ZP) and entrapment efficiency **(**EE). The factors studied were PF concentration (cPF), PVA concentration (cPVA), PLGA concentration (cPLGA) and aqueous phase pH. From a total of 26 formulations obtained by factorial design, two optimum formulations (PF-F1NPs and PF-F2NPs**)** were selected for further investigation here.[18]

The main purpose of present investigation was to target the PF encapsulated within PLGA NPs in the human skin with controlled release effect. Thereby, the work was designed to exploring novel formulations to improve the biopharmaceutical profile of PF for the topical application. An attempt to facilitate the prolonged contact of the PF on the skin and improve its skin retention, thus enhanced anti-inflammatory and analgesic efficiency and improving patient compliance by reducing application frequency. The optimized PF-F1NPs and PF-F2NPs suspensions were dispersed in semisolid blank HG (HG_PF-F1NPs and HG_PF-F2NPs) or HG with a 3% azone (HG_PF-F1NPs-Azone and HG_PF-F2NPs-Azone). These formulations were characterized for

their morphometry and rheological behavior. The physical stability of the NPs incorporate into HG also was evaluated. *In vitro* release profile and *ex vivo* skin permeation of PF from the different formulations as well as their *in vivo* skin tolerance and finally, the anti-inflammatory efficacy was assessed.

Preparation and characterization of the NPs

PF was kindly supplied by Alcon Cusi (Barcelona, Spain); PLGA Resomer® 753S was obtained from Boehringer Ingelheim (Ingelheim, Germany); Polyvinyl alcohol (PVA) with 90% hydrolization was obtained from Sigma Aldrich (St. Louis, USA). The purified water used in all the experiments was obtained from a MilliQ System. All the other chemicals and reagents used in the study were of analytical grade.

The NPs were obtained by the solvent displacement technique described by Fessi et al.[17] PLGA (90 mg or 95 mg) and PF (10 mg or 15 mg) were dissolved in 5 mL of acetone. This organic phase was poured, under moderate stirring into 10 mL of an aqueous solution of PVA (5 mg/mL or 10 mg/mL) adjusted to the desired pH value (4.5 or 5.5). The acetone was then evaporated and the dispersed NPs were concentrated to 10 mL under reduce pressure (Büchi B-480 Flawil, Switzerland). Table 1 shows the composition of the optimized PF-NPs.

Table 1.
Composition of the optimized PF-NPs

PF-NPs	cPF (mg/mL)	cPVA (mg/mL)	cPLGA (mg/mL)	pH
PF-F1NPs	1.5	10.0	9.5	5.5
PF-F2NPs	1.0	5.0	9.0	4.5

Particle size and zeta potential. Z Ave and ZP of the NPs were determined by photon correlation spectroscopy (PCS) with a Zetasizer Nano ZS (Malvern Instruments, Malvern, UK) at 25°C using disposable quartz cells and disposable folded capillary zeta cells (Malvern Instruments, Malvern, UK), respectively. In all the determinations, the samples were diluted with MilliQ

water (1:20). The reported values are the mean ± SD of at least three different batches of each formulation.

Entrapment efficiency. The EE of PF in the NPs was determined indirectly by measuring the concentration of the free drug in the dispersion medium. The non-entrapped PF was separated using a filtration/centrifugation technique with Ultracel–100K (Amicon® Ultra, Milipore Corporation, Billerica, MA) centrifugal filter devices at 3000 rpm for 30 minutes at 4ºC (Heraeus, Multifuge 3 L-R, centrifuge. Osterode, Germany). Each sample was diluted with MilliQ water (1:20) prior to filtration/centrifugation. The EE was calculated using the following equation:

$$\mathrm{E}(\%) = \frac{\text{Total Amount of PF} - \text{Free drug}}{\text{Total Amount of PF}} \times 100 \quad (1)$$

The EE (%) was determined by high performance liquid chromatography (HPLC) using a method previously validated in our laboratory. The HPLC system consisted of a Waters 1525 pump (Waters, Milford, USA) with a UV-Vis 2487 detector (Waters), a flow rate of 1 mL/min and wavelength of 245 nm were used with a (Kromasil®, 100-5C18, 4.6 x 100 mm) column. The mobile phase consisted of methanol: glacial acetic acid 5% (45: 55, v: v).

Preparation and characterization of hydrogel

The gel-forming polymer (Carbomer 934) was obtained from Fagron Ibérica, S.A.U (Barcelona, Spain). The blank HG was prepared with carbomer (1% w/v), dispersed in purified water and allowed to hydrate for 24 h. Subsequently, glycerol (3% w/w) and azone (3% w/w) were incorporated into the blank HG by stirring for 5 min at 1000 rpm in a high speed stirred (Cito Unguator Konietzko, Bamberg, Germany) and then the pH was adjusted at 6.5 with 0.1 N NaOH. The HG was left to equilibrate for 24 h at room temperature before used.
The PF-NPs suspension previously optimized was incorporated into the blank HG or HG with a 3% azone using a high speed stirred by 3 min at 1000 rpm, in a concentration of 50% (w/w) of the NPs dispersion into HG.

The morphological examination of the NPs incorporated into HG was performed using a Transmission Electron Microscopy (TEM). The sample was dispersed in MilliQ water using an Elma Transsonic Digital S T490 DH ultrasonic bath (Elma, Singen, Germany). A drop of this dispersion (10 µL) was placed on copper electron microscopy grids and stained with a 2 % (w/v) uranyl acetate solution. After 1 minute the sample was washed with ultra-purified water and the excess fluid removed with a piece of filter paper. The dried sample was then examined.
The stability of the PF-NPs incorporated into HG was assessed after 1 day of the production and 90 days of storage at 25ºC. The Z Ave and ZP of the particles was determined by photon PCS as described above. The diameter of the NPs into HG also was measured by lasser diffraction (LD) data, obtained with a Mastersizer Hydro 2000MU (Malvern Instruments Ltd., Malvern, UK), using the volume distribution as diameter values of LD 10 %, LD 50 % and LD 90 %. The diameter values indicate the percentage of particles possessing a diameter equal or lower than the given value. In all the determinations, the samples were dispersed in MilliQ water using an Elma Transsonic Digital S T490 DH ultrasonic bath (Elma, Singen, Germany).

Rheological measurements. The samples were placed in glass vials with rubber top and aluminium capsule and storage at 25ºC ± 2ºC. The rheological characterization of each formulation was performed using a Haake Rheostress1 rheometer (Thermo Fisher Scientific, Karlsruhe, Germany) connected to a temperature control Thermo Haake Phoenix II + Haake C25P and equipped with parallel plate geometry (Haake PP60 Ti, 60 mm diameter, 0.5 mm gap between plates) or cone plate set-up with a fixed lower plate and a mobile upper cone (Haake C35 / 2º Ti, 35 mm diameter, 0.106 mm gap between cone-plate). The viscosity curves and flow curves were recorded under rotational runs at 25ºC for 3 min during the ramp-up period from 0 to 100 s^{-1}, 1 min at 100 s^{-1} (constant share rate period) and finally 3 min during the ramp-down period from 100 to 0 s^{-1}. Viscosity values at 100 s^{-1} were determined after 8 days of the production and 90 days of storage at 25ºC ± 2ºC, in three replicates. Oscillatory stress sweep tests were performed at a constant frequency of 1 Hz in a stress range of 0.1 and 200 Pa. Oscillation frequency tests were carried out from 0.01 and 10 Hz at a constant shear stress within the linear viscoelastic region, in

order to determine the related variation of storage modulus (*G'*) and loss modulus (*G"*) at 25ºC. The software Haake RheoWin®Job Manager V.3.3 and RheoWin®Data Manager V.3.3 (Thermo Electron Corporation, Karlsruhe, Germany) were used to carry out the test and analysis of the obtained data, respectively.

In vitro drug release

An *in vitro* release study of PF from the NPs incorporated into HG was performed in Franz diffusion cells.[19] These cells consist of a donor and a receptor chamber between which a membrane is positioned. A dialysis membrane (Dialysis Tubing Visking**,** Medicell International Ltd., London, UK) was used. The membrane was hydrated for 24 h before being mounted in the Franz diffusion cell. The experiment was performed under "sink condition". A weight of 400 mg of each sample was placed in the donor compartment and the receptor compartment was filled with phosphate buffer solution (PBS) at pH 7.4 kept at 32ºC ± 0.5ºC. A volume of 300 µL was withdrawn from the receptor compartment at fixed times and replaced by an equivalent volume of fresh PBS at the same temperature. The concentration of release PF was measured as described previously in EE. Values are reported as the mean ± SD of three replicates. The concentration of PF released was measured as described previously for EE. Values are reported as the mean ± SD of three replicates.

The amount PF release was adjusted to the following kinetic models:[20]

$$\text{Zero order}: \ \%R_t/\%R_\infty = k \times t \qquad (2)$$

$$First\ Order: \ \%R_t/\%R_\infty = \ 1 - e^{-k \times t} \qquad (3)$$

$$Higuchi: \ \%R_t/\%R_\infty = k \times t^{1/2} \qquad (4)$$

$$Korsmeyer - Peppas: \ \%R_t/\%R_\infty = \ k \times t^n \qquad (5)$$

Where $\%R_t$ is the percentage of the drug released at time t, $\%R_\infty$ is the total percentage of drug released, $\%R_t/\%R_\infty$ is the fraction of drug released at time t, k is the release rate constant and n is the diffusion release exponent that can be used to characterize the different release mechanisms; $n \leq 0.5$ (Frickian diffusion), $0.5 < n < 1.0$ (anomalous transport), and $n \geq 1$ (case II transport,i.e., zero-order release). A nonlinear least-squares regression was performed using the WinNonLin® software (WinNonLin® professional edition version 3.3 and Graphpad prism version 6 Demo) and the model parameters were calculated. Akaike´s information criterion (AIC) was determined for each model as an indicator of the model´s suitability for a given dataset.[21]

Human skin permeation studies

Ex vivo permeation experiments were carried out using human skin obtained from abdominal region of 5 healthy volunteers (40-year-old woman), provided from plastic surgery (Hospital de Barcelona, SCIAS, Barcelona, Spain). The volunteers provided a written, informed consent for skin usage in the present research. The assay was done using Franz diffusion Cells. The skin was cut starting from the stratum corneum with a thickness of 0.4 mm pieces using a dermatome (Model GA 630. Aesculap, Tuttlingen, Germany), and storage at –20ºC. The excised sample was fixed between the donor and receptor compartment of Franz cell. The skin area available for permeation was 0.64 cm^2. The receptor compartment was filled with PBS at pH 7.4, kept at 32ºC by a circulating-water jacket and stirred at 700 rpm with Teflon-coated magnetic stirring bars in order to maintaining the donor compartment at 32ºC ± 0.5ºC. A weight of 400 mg of the NPs incorporated into HG or 200 µL of the saturated solution of PF in PBS was placed in the donor compartment (covered with parafilm® in order to avoided evaporation), in direct contact with the stratum corneum. Samples (300 µL) were withdrawn from the receptor compartment at fixed times and replaced by an equivalent volume of PBS solution at the same temperature. At the end of the study, the skin was used to determine the amount of drug retained. The skin cleaned using a 0.05 % solution of sodium lauryl sulfate and washed with distilled water. The skin permeation area was then excised, weighed and treated with methanol: water (50:50, v: v) under

sonication during 30 min using an ultrasound bath. The amount of PF permeated and retained in the skin was determinate by HPLC as described previously for EE. The results are reported as the mean ± SD and mean (minimum – maximum value) of three replicates, respectively.

Experimental data were processed using Graphpad prism software (version 6 Demo) and Laplace software (Micromath. Inc., Salt Lake City, Utah, USA), according to the infinite dose method.[22] The parameters P_1 and P_2 were determined and the amount of PF permeated as a function of the time was calculated, according to Okamoto et al.[23] The steady-state flux J $(\mu g/(cm^2 s))$ across skin and the transdermal permeability coefficient $K_p(cm/s)$ were obtained from the following equations:

$$P_1 = K.L \qquad (6)$$

$$P_2 = D/L^2 \qquad (7)$$

$$Q = \frac{P_1.A.C_0}{s.(s/P_2)^{1/2}.sinh(s/P_2)^{1/2}} \qquad (8)$$

$$K_P = P_1.P_2 \qquad (9)$$

$$J = K_P.C_0 \qquad (10)$$

where K is the membrane/donor phase partition coefficient, L the effective length of diffusion through skin and D the diffusion coefficient. Q is the drug permeated. A, C_0 and s are the membrane area, concentration of PF at time zero in the donor compartment and Laplace operator, respectively. The permeation parameters were compared according to Williams et al.[24] by the application of a non-parametric statistical Kruskal-Wallis Z test followed by the Dunn´s multiple comparison test. Values were considered to be significant at $p < 0.05$.

Taking into account, the pharmacokinetics parameters of PF for young and elderly subjects, the predicted steady-state plasma concentration of the drug

that would penetrate skin after topical application was obtained using the following equation:

$$C_{SS} = \frac{JA}{CL_P} \qquad (11)$$

where C_{SS} is the plasma steady-state concentration, J is the flux determined in this study, A is the hypothetical area of application (in this case, $100\ cm^2$), and CL_P the plasmatic clearance (1146.60 cm^3/h and 609.00 cm^3/h, respectively for young and elderly subjects.[25,26]

Anti-inflammatory efficacy

The anti-inflammatory efficacy of the different PF formulations was performed following the protocol previously described by Qadeer G, et al.[27] using adult male CD-1 mice with a body weight ranging from 20 g to 25 g. Edema was induced by topical application of 2.5 µg per ear of TPA (12-o-tetradecnoylphorbol 13-acetate) dissolved in ethanol. A volume of 50 µL of the NPs suspension or the NPs incorporates into HG and free PF solution (PF dissolved in PBS) as a reference, were applied to both side of the right ear simultaneously with TPA. The ear swelling was measured before TPA application and 4 h later. The edema was expressed as the increase of thickness.

In vivo Draize test

The irritancy of the NPs incorporated into HG was evaluated in New Zealand white rabbits (2.5 -3 Kg) following the current international guidelines.[28] based on the method described by Draize et al.[29] The dorsal area of the trunk was shaved with clippers 24 h before the beginning of the assay. Two squares were drawn on each side of the back of each rabbit, and the skin of one of them was scarred with a lancet. Then 0.5 mL of each the optimized PF-NPs suspension and PF-NPs suspension incorporated into HG without or with (3% and 5%) azone was applied on each square, covering the site with gauze and a

polyethylene film (parafilm®) and fixed with hypoallergenic sticking plaster. Three animals were used for each product. After exposure for 24 h, the test substance was removed and the exposed skin was scored for the formation of edema (graded 0-4), and erythema (graded 0-4). Scoring was repeated 72 h later. The individual primary irritancy index was determined for each rabbits by adding the edema and erythema scores at 24 h and 72 h and dividing the result by 4, as suggested by the "Journal Official de la republique Française" of 24 October 1984. The mean value for the three rabbits was calculated. Taking into account the primary irritancy index value, formulations may be classified as "non-irritant" (< 0.5), "irritant" (2-5), or "highly irritant" (5 - 8).[29]

Results

Physicochemical characterization of the HG formulations

The PF-F1NPs and PF-F2NPs nanosuspensions were previously optimized using a 2^4 central composite factorial design. The effect of the independent variables, such as cPF, cPVA, cPLGA and aqueous phase pH on the physicochemical properties of the NPs was studied. From a total of 26 formulations obtained by factorial design, two optimum formulations were selected for further investigation here. The Z Ave of the optimized PF-F1NPs and PF-F2NPs formulations was around 350 nm. Both formulations had a net negative charge with ZP values of - 7.41 mV and – 8.5 mV for PF-F1NPs and PF-F2NPs, respectively. The percentage of incorporated PF in the polymeric matrix was around 80%.[18]

The size and surface morphology of the optimized PF-NPs after incorporated into HG were determinate by TEM. The mean diameters of HG_PF-NPs formulations were around 300 nm.

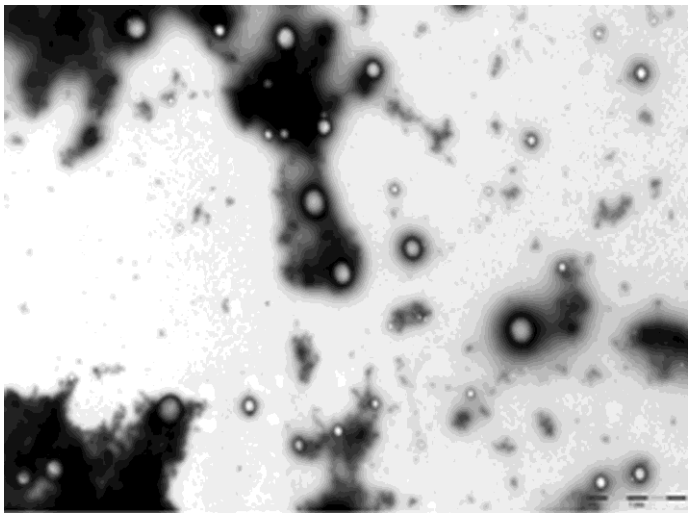

Figure 1. Transmission electron microphotograph of the optimized NPs incorporated into Hydrogel.

The stability of the PF-F1NPs and PF-F2NPs formulations incorporated into HG was assessed after 1 day of the production and 90 days of storage at 25ºC. Figure 2 and Table 2 exhibit the results of the measurements obtained by LD and PCS, respectively.

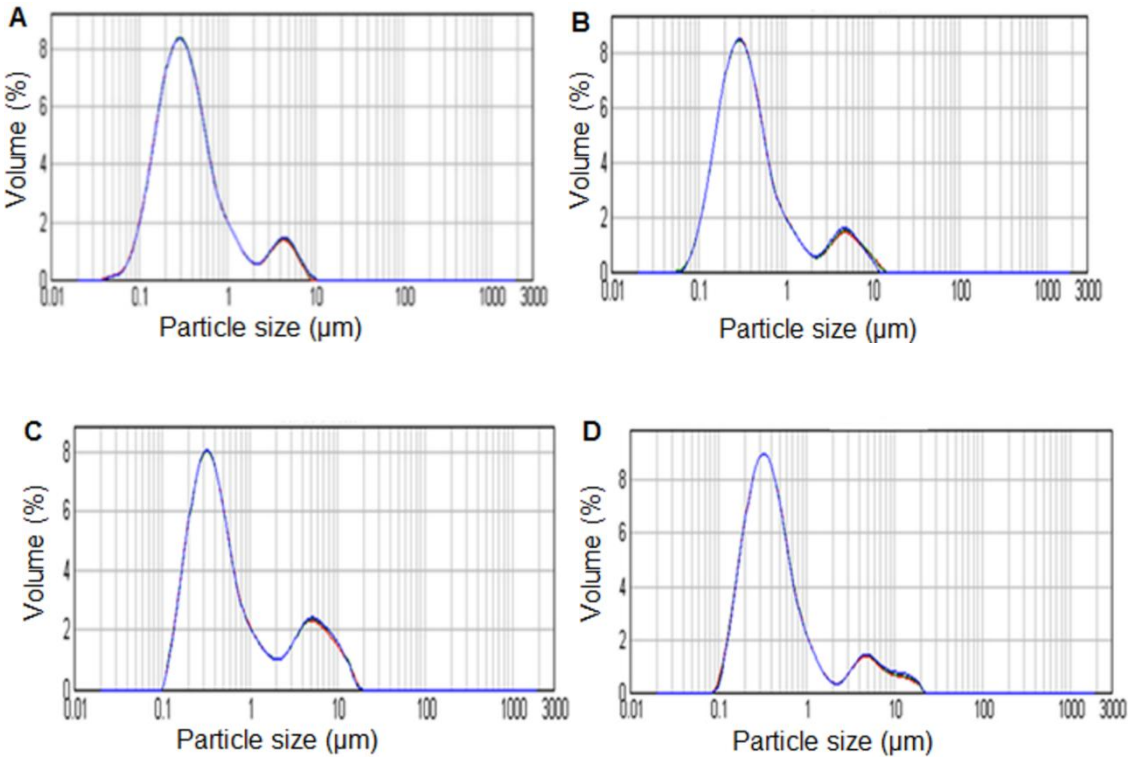

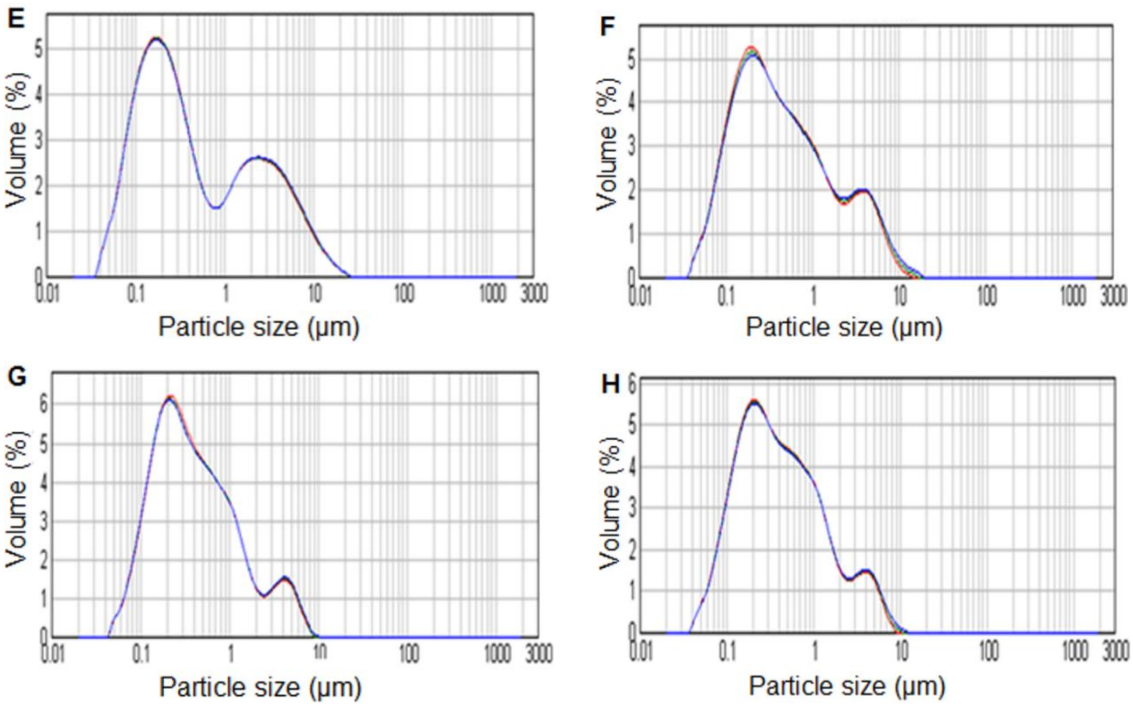

Figure 2. Particle size measurements by LD for A) and B) HG_PF-F1NPs, C) and D) HG_PF-F2NPs, E) and F) HG_PF-F1NPs-Azone, G) and H) HG_PF-F2NPs-Azone after 1 and 90 days of storage at 25ºC, respectively

Table 2

Particle size and the electrical charge at the surface of the HG_PF-F1NPs, HG_PF-F2NPs, HG_PF-F1NPs-Azone and HG_PF-F2NPs-Azone after 1 day of the production and 90 days of storage at 25ºC.

Time	HG_PF-F1NPs		HG_PF-F2NPs		HG_PF-F1NPs-Azone		HG_PF-F2NPs-Azone	
day	Size (nm)	ZP(mV)	Size (nm)	ZP(mV)	Size (nm)	ZP(mV)	Size (nm)	ZP(mV)
1	385.20 ± 0.21	-27.50 ± 0.10	391.30 ± 0.22	-37.80 ± 0.13	393.00 ± 0.27	-33.20 ± 0.12	396.90 ± 0.41	-43.90 ± 0.11
90	495.70 ± 0.33	-28.80 ± 0.11	471.50 ± 0.41	-39.4 ± 0.12	512.30 ± 0.16	-51.30 ± 0.11	467.80 ± 0.23	-51.50 ± 0.10

The results obtained by DL after 1 day of the production in Figure 2, A, C, E and G reveal that the HG_PF-F1NPs, HG_PF-F2NPs, HG_PF-F1NPs-Azone and HG_PF-F2NPs-Azone formulations exhibit a major peak around 367 nm, 380 nm, 374 nm and 380 nm, respectively. Figure 2, A, C E and G also show another small peak around 3.5 µm indicating an increase of the Z Ave and PI of the NPs after incorporated into HG. After 90 days of storage at 25ºC, all the assayed formulations showed an increase in the Z Ave values compared with

the values obtained after 1 day of the production (Figure 2, B, D, F and H). The stability studies by PCS in Table 2 show that the Z Ave values were similar to those obtained by DL measurements. The results in Table 2 also reveal an increase of ZP values for the PF-F1NPs and PF-F2NPs suspension after incorporated into HG.

Table 3 exhibits the results obtained from the rheological characterization of the semisolid formulations.

Table 3.

Rheological properties of the HG_PF-F1NPs, HG_PF-F2NPs, HG_PF-F1NPs-Azone and HG_PF-F2NPs-Azone formulations after 8 days of the production and 90 days of storage at 25ºC

Time	HG_PF-F1NPs		HG_PF-F2NPs		HG_PF-F1NPs-Azone		HG_PF-F2NPs-Azone	
days	Viscosity $(Pa.s)$	Thixotropy (Pa/s)	Viscosity $(Pa.s)$	Thixotropy (Pa/s)	Viscosity $(Pa.s)$	Thixotropy (Pa/s)	Viscosity $(Pa.s)$	Thixotropy (Pa/s)
8	1.64 ± 0.002	586.30	2.38 ± 0.001	1935	1.99 ± 0.004	1141.60	2.90 ± 0.006	4203
90	1.10 ± 0.001	542.45	0.93 ± 0.002	555.1	1.63 ± 0.001	1076.00	1.13 ± 0.001	565.15

Regarding the viscosity results show in Table 3 the viscosity values obtained after 8 day of the production for the HG_PF-F1NPs, HG_PF-F2NPs, HG_PF-F1NPs-Azone and HG_PF-F2NPs-Azone formulations exhibited a decreased respect to the values observed at 90 days of storage. Table 3 reveals also a slight decreased of the thixotropy values for the HG_PF-F1NPs and HG_PF-F1NPs-Azone formulations compared with the initial values. For the HG_PF-F2NPs and HG_PF-F2NPs-Azone formulations in Table 3, it was found that the thixotropy of the corresponding flow curves were notably major respect to the HG_PF-F1NPs and HG_PF-F1NPs-Azone formulations. However, a significant decreased in the thixotropy values were obtained at 90 days of the storage for the HG_PF-F2NPs and HG_PF-F2NPs-Azone formulations. The oscillation frequency test was carried out from 0.01 and 10 Hz at a constant shear stress within the linear viscoelastic region, in order to determine the related variation of storage modulus (G') and loss modulus (G") at 25ºC.

Figure 3 displays the results of the oscillatory measurements obtained for the HG_PF-F1NPs, HG_PF-F2NPs, HG_PF-F1NPs-Azone and HG_PF-F2NPs-Azone formulations.

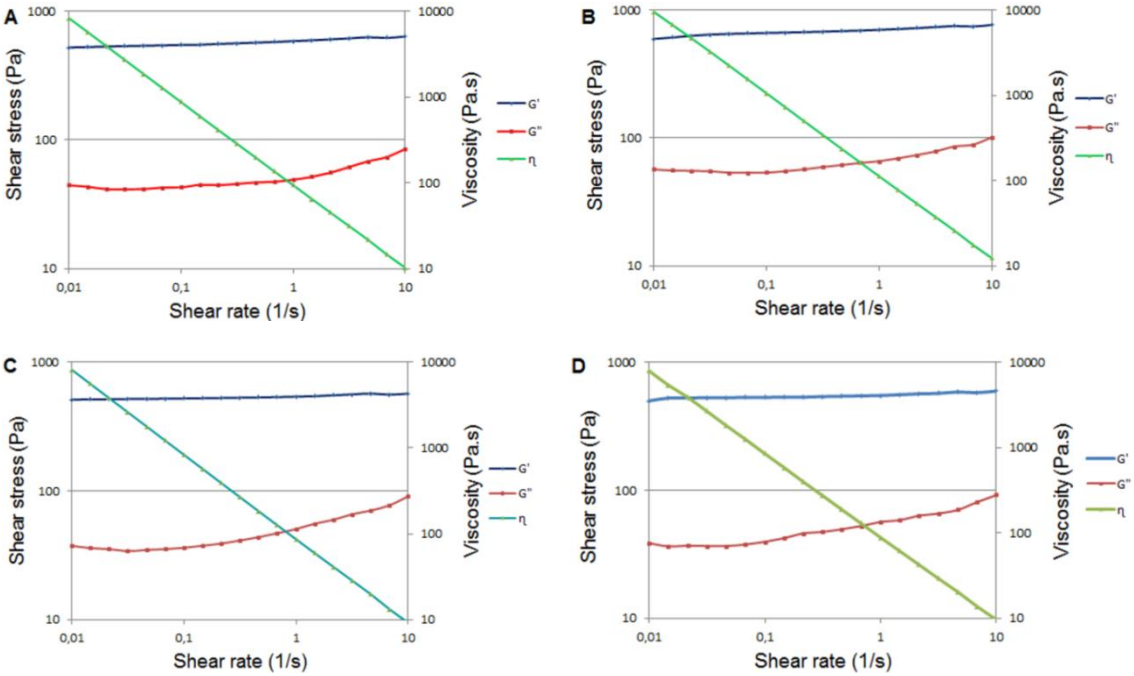

Figure 3. Rheograms of the oscillation frequency test obtained for A) HG_PF-F1NPs, B) HG_PF-F2NPs, C) HG_PF-F1NPs-Azone and D) HG_PF-F2NPs-Azone formulations.

In vitro drug release

In previous studies, we assessed the release profile of PF from the optimized NPs (PF-F1NPs and PF-F2NPs). The results obtained from this study revealed that both formulations showed a sustained release behavior, with an initial burst attributed to the PF adsorbed to the NP surface, followed by a slower release phase while the trapped PF slowly diffuses out of the polymeric matrix into the release medium. The accumulative amount of PF released from PF-F1NPs and PF-F2NPs after 7 h was 78.18% and 82.17%, respectively. The release curves of PF from these NPs fitted to the first order kinetic model with a value of $n < 0.5$ indicanting that the release of PF from the NPs occurs by passive diffusion, mainly through the pores of the matrix.[18]

An *in vitro* release study of PF from the HG_PF-F1NPs, HG_PF-F2NPs, HG_PF-F1NPs-Azone, HG_PF-F2NPs-Azone formulations and the free drug (dissolved in PBS) was performed in Franz diffusion cell.

As can be observed in Figure 4, the release profile of PF from the free drug solution shows faster release than from the PF-NPs incorporated into HG with or without azone. After 3 h, 100% of the drug was released from the free drug solution. As shown in Figure 4, the accumulative amount of PF released from HG_PF-F1NPs, HG_PF-F2NPs, HG_PF-F1NPs-Azone and HG_PF-F2NPs-Azone after 24 h were 41.99%, 64.35%, 67.62% and 76.26%, respectively.

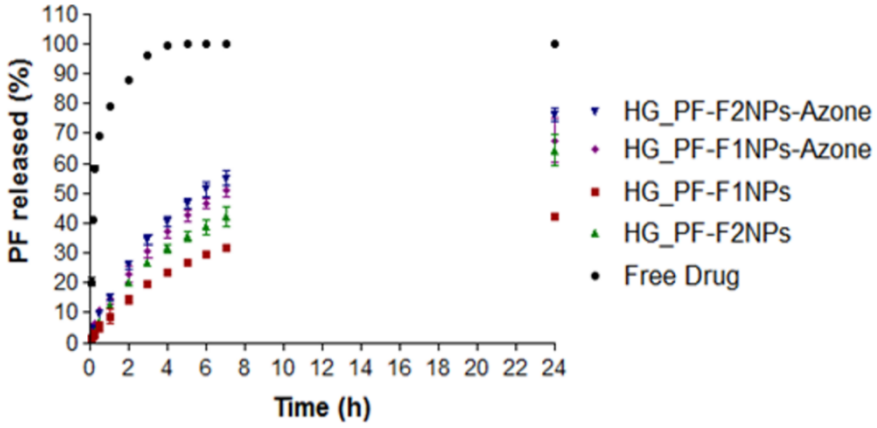

Figure 4. *In vitro* release profiles of PF from HG_PF-F1NPs, HG_PF-F2NPs, HG_PF-F1NPs-Azone, HG_PF-F2NPs-Azone and free drug solution. Mean ± SD, $n = 3$

The amount of PF released from the HG_PF-F1NPs, HG_PF-F2NPs, HG_PF-F1NPs-Azone and HG_PF-F2NPs-Azone formulations was adjusted to various kinetic models, such as zero-order, first-order, Higuchi and Korsmeyer-Peppas (Table 4). The AIC was determined for each model. This parameter is an indicator of the model´s suitability for a given dataset. The smaller the value of AIC, the better the model adjusts the data.

Table 4

Mean parameter obtained after fitting the release data of PF from the HG_PF-F1NPs, HG_PF-F2NPs, HG_PF-F1NPs-Azone and HG_PF-F2NPs-Azone formulations to different kinetic models.

Models	Parameters	HG_PF-F1NPs	HG_PF-F2NPs	HG_PF-F1NPs-Azone	HG_PF-F2NPs-Azone
Zero Order	AIC	118.67	127.18	137.32	135.84
First Order	AIC	118.67	127.18	130.84	133.32
Higuchi	AIC	71.10	68.58	81.10	83.10
Korsmeyer-	n	0.43	0.47	0.43	0.44
Peppas	AIC	68.55	68.27	77.81	81.18

n, diffusional release exponent; AIC, Akaike information criterion

Human skin permeation studies

In the present work, an *in vitro human* skin permeation study of PF from the PF-F1NPs, PF-F2NPs, HG_PF-F1NPs, HG_PF-F2NPs, HG_PF-F1NPs-Azone, HG_PF-F2NPs-Azone formulations and saturated solution of PF (dissolved in PBS) was performed in order to determine the permeation profile of drug from these formulations and its skin permeation parameters. The results of this study are show in Figure 5 and Table 5.

Figure 5 shows the accumulative amounts of PF permeated from the PF-F1NPs, PF-F2NPs, HG_PF-F1NPs, HG_PF-F2NPs, HG_PF-F1NPs-Azone, HG_PF-F2NPs-Azone formulations and saturated solution of PF after 24 h.

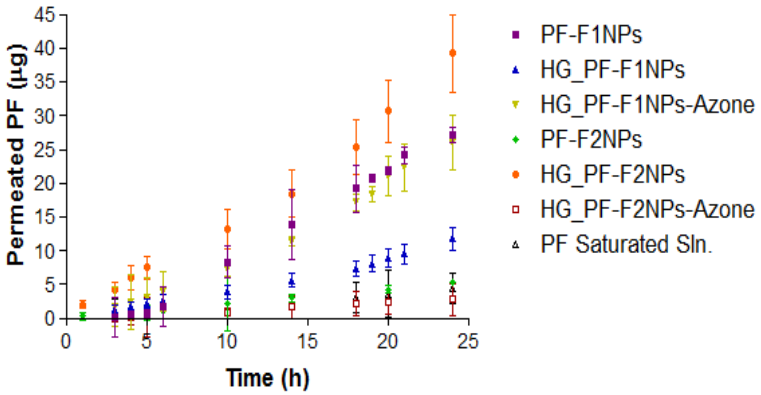

Figure 5. Permeation of PF through human skin from: PF-F1NPs, PF-F2NPs, HG_PF-F1NPs, HG_PF-F2NPs, HG_PF-F1NPs-Azone, HG_PF-F2NPs-Azone formulations and saturated solution of PF. Mean ± SD, $n = 3$

Table 5 shows the permeation parameter of PF calculated from the amounts permeated across the skin and the retained amount of PF from the PF-F1NPs, PF-F2NPs, HG_PF-F1NPs, HG_PF-F2NPs, HG_PF-F1NPs-Azone, HG_PF-F2NPs-Azone formulations and saturated solution of PF.

Table 5

Permeability coefficient(K_P), P_1 and P_2 parameters, flux (J), lag time (TL) and the retained amount (Q_R) of PF at 24 h from the assayed formulations.

Samples	$K_P \times 10^4$ (cm/h)	$P_1 \times 10^3$ (cm)	$P_2 \times 10^2$ (h^{-1})	$J \times 10^1$ $(\mu g/(cm^2 h))$	TL (h)	Q_R $(\mu g/cm^2 g)$
PF-F1NPs	3.42 (3.36-3.99)	7.78 (7.52-9.95)	4.40 (4.01-4.47)	5.13 (5.04-5.98)	3.80 (3.73-4.20)	393.69 (279.79-467.05)
PF-F2NPs	1.05 (0.54-1.06)[d]	0.30 (0.26- 0.53)	21.20 (19.84-34.72)	1.05 (0.54-1.06)	0.50 (0.79-0.80)	267.61 (153.93-289.43)
HG_PF-F1NPs	4.48 (1.63-5.41)	13.40 (4.72-36.56)	3.35 (1.48-3.45)	3.36 (1.22-4.06)	5.00 (4.83-11.30)	69.80 (38.69-80.82)
HG_PF-F2NPs	17.70 (16.27-19.84)[b,f]	77.60 (22.86-125.23)[f]	2.28 (1.30-8.68)	8.86 (8.13-9.92)	3.60 (1.92-12.83)	174.05 (148.39-199.84)
HG_PF-F1NPs-Azone	5.20 (4.50-13.83)	2.90 (2.29-85.04)	17.92 (1.63-19.61)	3.90 (3.37-10.37)	0.90 (0.85-10.30)	68.58 (24.53-96.51)
HG_PF-F2NPs-Azone	0.84 (0.73-1.07)[d]	0.29 (0.12-1.23)[d]	6.80 (25.64-89.10)	0.42 (0.37-0.54)	1.60 (2.80-3.21)	77.15 (73.34-82.09)
Saturated sln.	3.83 (3.60-7.87)	16.09 (6.21-18.94)	4.16 (2.38-5.78)	5.38 (2.87-5.91)	2.08 (1.06-7.07)	166.89 (44.24-574.87)

Differences with [a]PF-F1NPs, [b]PF-F2NPs, [c]HG_PF-F1NPs, [d]HG_PF-F2NPs, [e]HG_PF-F1NPs-Azone, [f]HG_PF-F2NPs-Azone and [g]PF saturated solution. Results are reported as median value and minimum - maximum range values ($n = 3$)

The permeation parameters K_P, P_1 and P_2 were compared by the application of a non-parametric statistical Kruskal-Wallis Z test.

In order to determinate the ability of PF to penetrate through the human skin, a permeation study under conditions of maximum thermodynamic activity was carried out with a PF saturated solution. As shown Table 5 the permeation parameter values obtained were $16.09\times 10^{-3}\ cm$, $4.16\times 10^{-2}\ h^{-1}$ and $3.83 \times 10^{-4}\ cm/h$ for P_1, P_2 and K_P, respectively. At 2.08 h, the skin was saturated of drug until it begins steady state equilibrium, reaching thereafter permeation constant flux of 5.28 $\mu g/cm^2 h$. The amount of PF retained for this formulation was 166.89 $\mu g/cm^2 g$.

The permeation parameter showed in Table 5 for the PF-F1NPs and PF-F2NPs suspension after incorporate into HG, were firstly compared for PF-F1NPs, HG_PF-F1NPs and HG_PF-F1NPs-Azone formulations and then, we studied the same parameter for the PF-F2NPs, HG_PF-F2NPs and HG_PF-F2NPs-Azone formulations.

The P_1 mean values obtained in Table 5 for the PF-F1NPs, HG_PF-F1NPs and HG_PF-F1NPs-Azone formulations were $7.78\times 10^{-3}\,cm$, $13.40\times 10^{-3}\,cm$ and $2.90\times 10^{-3}\,cm$, respectively. The P_2 mean values obtained for these formulations were $4.40\times 10^{-2}h^{-1}$, $3.35\times 10^{-2}h^{-1}$ and $17.92\times 10^{-2}\,h^{-1}$, respectively. The K_P mean values obtained were $3.42\times 10^{-4}\,cm/h$, $4.48\times 10^{-4}\,cm/h$ and $5.20\times 10^{-4}\,cm/h$, respectively. The statistical analysis of the K_P, $P_1$and P_2 permeation parameters obtained from these formulations not showed statistically significant different ($p > 0.05$). The retained amount of PF at 24 h, the PF-F1NPs suspension shows the highest Q_R value of PF in the skin (393 $\mu g/cm^2 g$) compared to the Q_R value obtained for HG_PF-F1NPs and HG_PF-F1NPs-Azone formulations.

The permeation parameter in Table 5 for the PF-F2NPs, HG_PF-F2NPs and HG_PF-F2NPs-Azone formulations also were compared. The P_1 mean values obtained were $0.30\times 10^{-3}\,cm$, $77.60\times 10^{-3}\,cm$ and $0.29\times 10^{-3}\,cm$, respectively. From the statistical analysis of this permeation parameter, statistically significant differences ($p < 0.05$) were found between HG_PF-F2NPs and HG_PF-F2NPs-Azone formulations. The P_2 mean values obtained for these formulations were $21.20\times 10^{-2}h^{-1}$, $2.28\times 10^{-2}h^{-1}$ and $6.80\times 10^{-2}\,h^{-1}$, respectively. Statistically significant different ($p < 0.05$) were found between these formulations for this parameter. The K_P mean values obtained were $1.05\times 10^{-4}\,cm/h$, $17.70\times 10^{-4}\,cm/h$ and $0.84\times 10^{-4}\,cm/h$, respectively. Statistically significant different ($p < 0.05$) were found between PF-F2NPs and HG_PF-F2NPs formulations and between HG_PF-F2NPs and HG_PF-F2NPs-Azone formulations for the K_P parameter. The Q_R values for these formulations in Table 5 show that the PF-F1NPs formulations showed the highest Q_R values of PF in the skin (267 $\mu g/cm^2 g$) respect to the Q_R value observed for the HG_PF-F2NPs and HG_PF-F2NPs-Azone formulations. Table 6 shows the prediction steady-state plasma concentration (C_{SS}) of the PF following the

topical application of each formulation on 100 cm^2 of skin calculated from the pharmacokinetics parameters of PF for young and elderly subjects.

Table 6

Predicted steady-state plasma concentration (C_{SS}) of the PF after the application of each formulation on 100 cm^2 of skin

Formulation	Young subject C_{ss} (μ/cm^3) × 10^2	Elderly subject C_{ss} (μ/cm^3) × 10^2
PF-F1NPs	4.47	8.42
PF-F2NPs	0.92	1.72
HG_PF-F1NPs	2.93	5.52
HG_PF-F2NPs	7.73	14.55
HG_PF-F1NPs-Azone	3.40	6.40
HG_PF-F2NPs-Azone	0.37	0.69

Therapeutic plasma concentration : 4.89 ± 1.29 $\mu g/cm^3$ and 10.19 ± 2.43 $\mu g/cm^3$ for young and elderly subjects, respectively.[26]

Anti-inflammatory efficacy

The polymeric NPs with small size have relatively more specific surface area. Additionally, due to their accumulation on the skin can lead to favors the local anti-inflammatory effect of the drug. Figure 6 shows the results obtained of the anti-inflammatory efficacy effect of different formulations containing PF in the TPA induced edema.

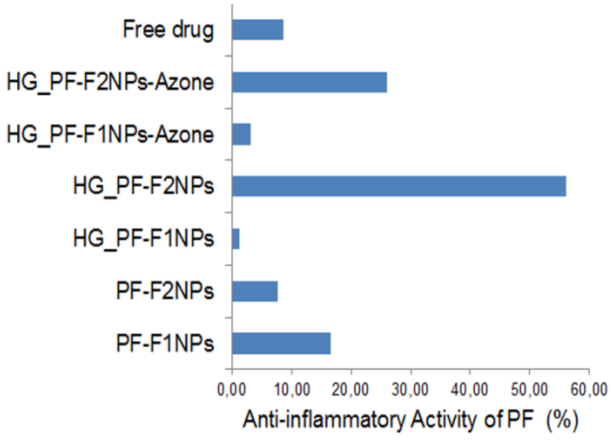

Figure 6. Anti-inflammatory activity of PF from the PF-F1NPs, PF-F2NPs, HG_PF-F1NPs and HG_PF-F2NPs, HG_PF-F1NPs-Azone, HG_PF-F2NPs-Azone formulations and free drug solution of PF (dissolved in PBS). $n = 6$

In vivo Draize skin test

The irritancy of PF-F1NPs, PF-F2NPs, HG_ PF-F1NPs, HG_ PF-F2NPs and HG_PF-NPs with a 3% or 5% azone (HG_PF-F1NPs-Azone and HG_PF-F2NPs-Azone) was evaluated in New Zealand white rabbits. The individual primary irritancy index determined in three male albino rabbits was less than 0.5 for the optimized PF-NPs, PF-NPs incorporated into HG without or with a 3% azone. However, when a percentage of 5% of azone was added to the HG_PF-NPs formulations**,** the irritancy index obtained was 3. For this reason, the formulations containing a 5 % azone no were considered to carry out additional studies.

Discussion

In this study, with the purpose of obtaine a topical dosage form with a desired semi-solid consistency, the optimized PF-F1NPs and PF-F2NPs suspensions was incorporated into HG.

The morphological examination of the semi-solid formulations was performed using a TEM. This technique gives information about NPs structure, highlighting the polymer envelope and the inner cavity.[30] TEM image depicts in Figure 1 reveals that the optimized NPs after incorporated into HG were spherical shape and nonaggregated. The results obtained show that the Z Ave of the NPs incorporated into HG was similar to those of the NPs suspension.

The physicochemical stability of the semi-solid formulations was assessed by PCS and LD after 1 day of the production and 90 days of storage at 25ºC. The results of stability study obtained by DL for the semi-solid formulations are show in Figure 2 reveals the presence of two peaks of particle size distribution indicating an increase of the Z Ave and PI. However, Elisabet Gonzalez- Mira et al,[31] consider that an increase in the apparent mean particle size could be due to that the particles are strongly entrapped within the tridimensional gel structure, rather than real particle agglomerates. The Z Ave values obtained from the stability studies by PCS are in accordance with those obtained by DL. Additionally, the results obtained by PCS also reveal a significant increase of the ZP values of the PF-F1NPs and PF-F2NPs suspensions after incorporated

into HG (Table 2). These results could be attributed to the adsorption of negatively charge of the jellifying agent molecules onto the surface of the NPs. An increased ZP provides increased stability by electrostatic repulsion.[32] Since that the PF-NPs incorporated into HG remained appropriates physicochemical properties after 90 days of storage at 25ºC, it can be concluded that the NPs were not aggregated and they are stables. These results are in accordance with those obtained by TEM, which indicate that the gel network of carbomer could not notably influence the morphology and size of the NPs.

The topical application of the NPs entails the use of semi-solid formulations due to the low viscosity of the NPs suspension; therefore the influence of the rheological properties of the formulations is a very important physical parameter.[33] The results obtained from the rheological characterization of the PF-F1NPs and PF-F2NPs after incorporated into HG with or without azone show a non-Newtonian behavior and the pseudo-plastic character. These properties are desirable for the local application on the skin of the NPs base HG semisolid formulations due to the spreading properties on the skin and the ability of controlling their viscosity, which can provide appropriate characteristics for topical application.

The results obtained from the rheological characterization at 90 days of the storage of the PF-NPs incorporated into HG formulations revealed a decrease in the viscosity values for all the semisolid formulations (Table 3). Additionally, the results in Table 3 confirmed that the inclusion of azone in the HG_NPs formulations produced a significant viscosity increase in the HG_PF-F1NPs-Azone and HG_PF-F2NPs-Azone formulations. These results are in accordance with the increase of the Z Ave and PI obtained after 90 days of storage at 25ºC obtained by LD (Figure 2, B, D, F and H) and PCS (Table 2). These results could be explained by the fact that the NPs characterized by a wide polydispersity could pack better than those with a narrow polydispersity. The particles with a large polydispersity has more free space to move around, which means that it was easier for the sample to flow and a lower viscosity would be measured.[34] Concerning the stress sweep test of the oscillatory study, the critical stress was found about 10 Pa for all the formulations under study. These results indicate that no formulations presented a weak structure. According to the results of oscillatory stress sweeps, a constant shear stress of

2 Pa (20% of the critical value) was selected to perform the frequency sweep tests. Figure 3, A, B, C and D display the oscillatory measurements applied to the formulations revealed prevalence of the elastic over the viscous behavior (G'>G'') for all the formulations.

The *in vitro* release study of PF from HG_PF-F1NPs, HG_PF-F2NPs, HG_PF-F1NPs-Azone, HG_PF-F2NPs-Azone and free drug solution in Figure 4 shows that the release profile of PF from the free drug solution shows faster release than the HG_NPs formulations. The optimized PF-F1NPs and PF-F2NPs suspensions incorporated into HG with or without azone exhibit a sustained release behavior. Figure 4 also reveals that the amount released of PF from HG_PF-F1NPs and HG_PF-F1NPs-Azone was slightly smaller than HG_PF-F2NPs and HG_PF-F2NPs-Azone, respectively. These results might be attributed to the fact that during the preparation of the NPs the viscosity increases when there is an increase in the cPVA from 5 mg/mL (PF-F2NPs) to 10 mg/mL (PF-F1NPs). This viscosity increase could result in a more compact polymer matrix leading to slower degradation of the polymer or slower diffusion of the encapsulated PF from the NPs.[35] However, the PF release rate was faster from the PF-NPs suspension than from the HG_PF-NPs with or without azone. These results suggest that the diffusion velocity of PF from NPs can be attributed to higher viscosity of the NPs incorporated into HG compared to the NPs suspensions. The results of this release study confirm that the PF-NPs suspension or HG_PF-NPs with or without azone could offer sustained release of the PF compared to the free drug solution. The amount of PF released from the HG_PF-F1NPs, HG_PF-F2NPs, HG_PF-F1NPs-Azone and HG_PF-F2NPs-Azone formulations were adjusted to different kinetic models. The AIC was determined for each model. The smaller the value of AIC, the better the model fits the data. From the AIC values presented in Table 4 , it can be concluded that the release curves of PF from the HG_PF-F1NPs, HG_PF-F2NPs, HG_PF-F1NPs-Azone and HG_PF-F2NPs-Azone formulations fitted to the Korsmeyer-Peppas model very well. These models had the smaller AIC value and, therefore, statistically, described best the drug release mechanism. Taking into account the diffusional exponent value (n) that is used to characterize different release mechanisms, n values less than 0.5 was obtained in all the investigated formulations suggesting that the release of PF from the semi-solid formulations

occurs by passive diffusion.[36] From the results of the release study, it could be conclude that the main factors that govern the release of the drug from the different semi-solid formulations are the amount of PVA present in the formulation. Furthermore, the release rate is influenced by presence of PF in crystalline form, since the drug in crystalline form should dissolve first before being transported out to the matrix by diffusion. As previously reported, in our study that the intensity of some of the peaks of crystalline PF present in these NPs slightly increased when cPF increased from 1.0 mg/mL (PF-F2NPs) to 1.5 mg/mL (PF-F1NPs) by X-ray diffraction technique.[18] Additionally, the drug diffusion out of a hydrogel matrix dependent on mechanical strength degradability, diffusivity, and other physical properties of hydrogel network.[37]

An *in vitro human* skin permeation study of PF from PF-F1NPs, PF-F2NPs HG_PF-F1NPs, HG_PF-F2NPs, HG_PF-F1NPs-Azone, HG_PF-F2NPs-Azone and saturated solution of PF was performed with the purpose of determine the permeation profile of drug from these formulations and its skin permeation parameters. The permeation parameters K_P, P_1 and P_2 were compared by the application of the non-parametric statistical Kruskal-Wallis Z test. The statistical analysis of K_P, P_1 and P_2 parameters obtained in Table 5 for the PF-F1NPs, HG_PF-F1NPs and HG_PF-F1NPs-Azone formulations not showed statistically significant different ($p > 0.05$) between these formulations. These results suggest that these formulations no improve the permeation of PF through the skin. In this case, the only advantage respect to PF-F1NPs suspension is that the HG_PF-F1NPs and HG_PF-F1NPs-Azone formulations can be easily applied on the skin due to the presence of the bioadhesive agent.

The statistical analysis of the P_1 parameter exhibited in Table 5 for the PF-F2NPs, HG_PF-F2NPs and HG_PF-F2NPs-Azone formulations revealed statistically significant differences ($p < 0.05$) between HG_PF-F2NPs and HG_PF-F2NPs-Azone formulations. The partition coefficient between the vehicle and the skin is one of the factors which control the drug permeability. An increase in the partition coefficient value leads to a large transfer of permeant from the vehicle into stratum corneum. Thus, higher values of P_1 indicate a higher distribution in the skin than in the vehicle and vice versa.[38] In this case, HG_PF-F2NPs showed the highest P_1 value. For the P_2 parameter statistically significant different ($p < 0.05$) were found between PF-F2NPs, HG_PF-F2NPs

and HG_PF-F2NPs-Azone formulations using the Kruskal-Wallis Z test, but the Dunn´s multiple comparison test was not able of identifying from which formulations are these differences. However, the statistically significant different found for K_P parameter has allowed to highlight the statistically significant differences in the diffusion that were not noted for the P_2 parameter between PF-F2NPs and HG_PF-F2NPs formulations, since K_P depends directly of P_1 and P_2. The penetration of the NPs through the skin is affected by some factors such as the chemical composition of the ingredients, the particle size and the viscosity of the formulation.[33] Therefore, the efficacy of a drug for cutaneous application depends on the correlation between the permeability coefficient in the stratum corneum and drug chemical properties. The vehicle in which a drug is applied to the skin must be not only support, but a delivery system that drives the drug to an appropriated area o biophase with optimal rate release. Therefore, it must exist an equilibrium between drug-vehicle and drug-skin affinity in order to ensure the maximal thermodynamic activity, and this is possible when the drug contained in the vehicle chamber is saturated. Additionally, the diffusion coefficient of drug in the vehicle must be optimal, for it drug must be solubilized, without possessing a selective affinity toward the vehicle.[39,40]

Table 6 exhibits the results obtained from the predicted steady-state plasma concentration of the drug after the application of each formulation on 100 cm^2 of skin. All the C_{SS} values obtained for the assayed formulations were below the therapeutic plasma concentration. These results might ensure that the topical application of these formulations would not have any systemic effect and ensure a local anti-inflammatory and analgesic effect of this drug.

PLGA NPs have been described as systems for topical drug delivery. This nanocarries show affinity preferentially for the hair follicles which providing a reservoir where the NPs can be accumulated and create local amount of drugs. The hair follicle delivery has some advantages such as a decrease of the transepidermal absorption, reduction of the drug systemic toxicity when the follicle act as long term delivery reservoir and increasing additionally the therapeutic index of some drug as well as reducing the applied dose or frequency of administration.[41,42]

Although many studies performed by some researchers, the ability of polymeric NPs to penetrate the skin is not completely clear. Many researchers had attempted to use NPs for topical drug delivery, and they found that the drug permeation was enhanced by gradual drug release from the NPs on the skin surface, but did not find the particles carriers inside the skin.[43,44,45] Lademann J. et al, reported that the nanoparticles are able to permeated efficiently into the hair follicles. The nanocarriers were stored in the hair follicles up to 10 days. However, this systems were unable to unable to penetrate the skin.[46] Wei Zhang et al., reported that the PLGA nanoparticles with microneedles were found into the epidermis and the dermis of the human skin. Nevertheless, the concentration of nanoparticles deposited in the skin were located in the epidermis was greater than in the dermis.[47] De Jalon et al, investigated the distribution of the PLGA-microparticles loaded with rhodamine in skin porcine. From the results of this study, they reported that PLGA-microparticles loaded with rhodamine could penetrate throught the stratum corneum and reach the epidermis.[48]

The Q_R values presented in Table 5 show that the PF-F1NPs and PF-F2NPs suspensions showed the highest Q_R values of PF in the skin. These results suggest that the permeated and retained amount of PF do not depend on the nanoparticle size, since the Z Ave of the optimized PF-F1NPs and PF-F2NPs is very similar to each other (around 350 nm). These results are in accordance with those obtained by Estefania Vega et al.[49]

Respect to Q_R values obtained for the semi-solid formulations in Table 5 the HG_PF-F2NPs formulation showed the highest Q_R respect to the other gel formulations. The results obtained in Table 5 and Figure 5 show that the inclusion of azone in the NPs incorporated into HG formulation did not show any increase in the amount of drug permeated and retained amount of PF in the skin.

Although the PF-F1NPs and PF-F2 NPs formulations showed the highest Q_R values of PF in the skin, the anti-inflammatory efficacy values obtained for these formulations are intermediate respect to all assayed formulations. This could be due to the low viscosity of the NPs suspensions, thus not easily adhere to the skin and the drug is removed from the surface of the skin, following the topical application. As shown the Figure 6, the Q_R values of PF in the skin obtained for

the HG_PF-F1NPs and HG_PF-F1NPs-Azone formulations were lower than PF-F1NPs, and the percentages of anti-inflammatory activity showed were almost nulls.

The HG_PF-F2NPs formulation with desired semisolid consistency significantly reduced the edema, compared to the PF-F2NPs suspension as shown in Figure 6. The HG_PF-F2NPs formulation also show anti-inflammatory efficacy values correlate directly with the amount of drug retained in the skin (Table 5). Therefore, the topical application of the HG_PF-F2NPs formulation could more effective in the treatment of edema on the skin surface that the PF-F2NPs suspension.

Shin et al, also formulated PF in ethylene-vinyl acetate matrix containing diethyl phthalate as plasticizer which showed the best enhancing effects in drug release.[50] Shin et al, also developed a PF sustained and controlled delivery formulation using hydroxypropyl methylcellulose-poloxamer gel with octanoic acid as enhancer. The anti-inflammatory effect of this formulation was assessed using a rat paw-edema model. A reduction of edema by approximately 73% compared with that of the control group was reported.[51] However, the optimal results of efficacy anti-inflammatory obtained by Shin et al cannot be compared with those obtained in our study because animal species and the area of application on the skin that have been used are different. Nevertheless, the results obtained in these studies confirmed that this drug is suitable for topical administration.

Respect to *in vivo* Draize skin test of the optimized NPs incorporated into HG with a 0% or 3% azone. No signs of skin irritancy were detected, since the individual primary irritancy index determined for these formulations were less than 0.5. These results were in accordance to the reported in vitro outcomes, allowing classifying both formulations as ‘‘nonirritant’’ according to the ‘‘Journal Official de la Republique Franc¸aise’’ of October 24, 1984.

Conclusion

The topical application of the NPs implies the use of semi-solid formulations due to the low viscosity of the NPs suspension. In this way, the optimized PF-F1NPs and PF-F2NPs suspensions were succsessfully incorporated into blank HG or

HG with a 3% azone. The semi-solid formulations containing PF exhibited a non-Newtonian behavior, pseudo-plastic character and appropiate characteristics for topical PF delivery. According to the results of the physicochemical characterization and stability studies can concluded that the NPs incorporated into HG were not aggregated and they are remain adequate properties at 90 day of storage. The semi-solid formulations containing PF exhibit a sustained release behavior with a slower release of drug respect the NPs suspensions. On basis of *ex vivo* skin human permeation and anti-inflammatory efficacy of the HG_PF-F1NPs and HG_PF-F1NPs-Azone formulations the retained amount of PF were lower than PF-F1NPs, and the percentages of anti-inflammatory activity showed were almost nulls. However, the HG_PF-F2NPs formulation not only provide an adequate drug release, but also show anti-inflammatory efficacy values correlate directly with the amount of drug retained in the skin and the permeation flux value. These results suggest that the topical application of the HG_PF-F2NPs could be more effective in the treatment of edema on the skin surface that the other semi-solid formulations. The inclusion of azone in the semi-solid formulations did not show any increase in the amount of drug permeated and retained amount of PF in the skin. The optimized PF-NPs suspensions and semi-solid formulations with 0% or 3% azone showed an optimal skin tolerance.

All these results suggest that the HG_PF-F2NPs formulations could be an effective system for the delivery and controlled release of PF on the skin, improving the biopharmaceutical profile of this drug. This formulation could facilitate the prolonged contact of the PF on the skin and improve its skin retention, thus enhanced the local anti-inflammatory and analgesic effect of this drug and, consequently, favors patient compliance by reducing application frequency.

Acknowledgments

G. Abrego, wishes to acknowledge, the Spanish Ministry of Foreign Affairs and Cooperation and the Spanish Agency for International Development Cooperation (MAEC-AECID) for a research scholarship. Also, the authors would

like to acknowledge the financial support of the Spanish Ministry of Science and Innovation (grant MAT2011-26994).

References

1. Akyol-Salman I, Lece-Sertoz D, Baykal O. Topical pranoprofen 0.1% is as effective anti-inflammatory and analgesic agent as diclofenac sodium 0.1% after strabismus surgery. J Ocul pharmacol Ther. 2007; 23:280–283.

2. Sawa M, Masuda K, Nakashima M. Anti-inflamatory effect of diclofenac sodium eye drops on cataract surgery. Double masked study with pranoprofen eye drops. IOL RS. 1999;13:193–200.

3. Ghosal K, Chakrabarty S, Nanda A. Hydroxypropyl methylcellulose in drug delivery. Pelagia Res Library. 2011; 2:152-168

4. Narashino M, Ichikawa H, Narita S, Yotsukaido AS. Sustained-Release Pranoprofen Preparation. 1993. United States patent. US00522506A.

5. Kobe K, Otsu H, Kobe Y, Kakogawa Y. Method for stabilizing pranoprofen and stable liquid preparation of pranoprofen. 1999. United States patent. US005856345A.

6. Ting W, Vest C, Sontheimer R. Review of traditional and novel modalities that enhance the permeability of local therapeutics across the stratum corneum. Int. J. Dermatol. 2004; 43: 538-547

7. Kalia YN, Guy RH. Modeling transdermal drug release. Adv. Drug Deliv. Rev. 2001; 48:159–172.

8. Barratt GM. Therapeutic applications of colloidal drug carriers. Pharm. Sci. Technolo. Today. 2000; 3:163–171.

9. Pardeike J, Hommoss A, Müller RH. Lipid nanoparticles (SLN, NLC) in cosmetic and pharmaceutical dermal products. Int. J. Pharm. 2009; 366:170–184.

10. Bawarski WE, Chidlowsky E, Bharali DJ, Mousa SA. Emerging nanopharmaceuticals. Nanomedicine. 2008; 4:273–282.

11. Nair LS, Laurencin CT. Biodegradable polymers as biomaterials. Prog Poly Sci. 2007; 32:762–798.

12. Mechanism of percutaneous absorption II. Transient diffusion and the relative importance of various routes of skin penetration. J. Invest. Dermatol. 1966; 48:79–89.

13. Du Plessis J, Ramachandran C, Weiner N, Muller DG. The influence of particle size of liposomes on the deposition of drug into skin. Int. J. Pharm. 1994; 103:277–282.

14. Bhalekar MR, Pokharkar V, Madgulkar A, Patil N, Patil N. Preparation and evaluation of miconazole nitrate-loaded solid lipid nanoparticles for topical delivery. AAPS pharmSciTech. 2009; 10:289–296.

15. Montenegro L, Sinico C, Castangia I, Carbone C, Puglisi G. Idebenone-loaded solid lipid nanoparticles for drug delivery to the skin: in vitro evaluation. Int. J. Pharm. 2012; 434:169–174.

16. Amara FE, Meleis ME, Seif MA, Moursy EY. Study of the metabolic effect and histopathological nasal mucosal changes after prolonged intranasal insulin administration. Journal of Diabetology. 2011;1:1–10.

17. Fessi H, Puisieux F, Devissaguet JP, Ammoury N, Benita S. Nanocapsule formation by interfacial polymer deposition following solvent displacement. Int. J Pharm. 1989 ; 55:R1–R4.

18. Abrego G, Alvarado HL, Egea MA, Gonzalez-Mira E, Calpena AC, Garcia ML. Design of Nanosuspensions and Freeze-Dried PLGA Nanoparticles as a Novel Approach for Ophthalmic Delivery of Pranoprofen. J. Pharm Sci. 2014. DOI:10.1002/jps.24101

19. Franz TJ. Percutaneous absorption. On the relevance of in vitro data. J. Investig Dermatol. 1975;64:190–195.

20. Costa P, Sousa JM. Modeling and comparison of dissolution profiles. European J. Pharm. Sci. 2001;13:123–133.

21. Yamaoka K, Nakagawa T, Uno T. Application of Akaike's information criterion (AIC) in the evaluation of linear pharmacokinetic equations. J. Pharmacokinet Biopharm.1978;6:165-175.

22. OECD Environmental health and safety publications. Draft guidance document for the conduct of skin absorption studies. N. 28. Paris, 2000;10, 13, 25.

23. Okamoto H, Komatsu H, Hashida M, Sezaki H. Effects of β-cyclodextrin and di-O-methyl-β-cyclodextrin on the percutaneous absorption of butylparaben, indomethacin and sulfanilic acid. Int. J. Pharm. 1986;30:35–45.

24. Williams A, Cornwell P, Barry B. On the non-Gaussian distribution of human skin permeabilities. Int.J. Pharm.1992;86:69–77.

25. Yoshio I, Iwata A, Isobe M, Takamatsu R, Higashi M. The pharmacokinetics of pranoprofen in humans. Yakugaku Zasshi.1990;110:509–515.

26. Kajiyama H, Fujimura A, Ebihara A, Hino Y. Pharmacokinetics of pranoprofen in the elderly. Clin. Pharmacol. Res. 1991;11:123–127.

27. Qadeer G, Rama NH, Garduño-Ramírez ML. Synthesis and anti-inflammatory activity of fluorinated isocoumarins and 3,4-dihydroisocoumarins. J. Fluorine Chem. 2007;128:641–646.

28. OECD. Guideline for the testing of chemicals. No 404: Acute Dermal Irritation/Corrosion 2002.

29. Draize J, Woodard G, Calvery H. Methods for the study of irritation and toxcicity of substances applied topically to the skin and mucous membranes. J. Pharmacol. Exp. Ther. 1944;82:377–390.

30. Vega E, Gamisans F, Garcia ML, Chauvet A, Lacoulonche F, Egea MA. PLGA nanospheres for the ocular delivery of flurbiprofen: drug release and interactions. J. Pharm. Sci. 2008;97:5306–5317.

31. Gonzalez-Mira E, Nikolić S, Calpena AC, Egea MA, Souto EB, AC, Garcia ML. Improved and safe transcorneal delivery of flurbiprofen by NLC and NLC-based hydrogels. J. Pharm. Sci. 2012;101:707–725.

32. Han F, Yin R, Che X, Yuan J, Cui Y, Yin H, Li S. Nanostructured lipid carriers (NLC) based topical gel of flurbiprofen: Design, characterization and in vivo evaluation. Int. J. Pharm. 2012;439:349–357.

33. Guterres S, Alves M, Pohlmann A. Polymeric nanoparticles, nanospheres and nanocapsules, for cutaneous applications. Drug Target Insights. 2007 ;2:147–157.

34. Malvern Instruments. 10 ways to control rheology by changing particles properties. 2009. INFORM series of white papers.

35. Sahoo SK, Panyam J, Prabha S, Labhasetwar V. Residual polyvinyl alcohol associated with poly (D,L-lactide-co-glycolide) nanoparticles affects their physical properties and cellular uptake. J Control. Release. 2002;82:105–114.

36. Ford J, Rubinstein M, McCaul F, Hogan J, Edgar P. Importance of drug type, tablet shape and added diluents on drug release kinetics from hydroxypropylmethylcellulose matrix tablets. Int. J. Pharm. 1987;40:223–234.

37. Hamidi M, Azadi A, Rafiei P. Hydrogel nanoparticles in drug delivery. Adv. Drug Deliv. Rev. 2008;60:1638–1649.

38. Jiménez M, Pelletier J, Bobin MF, Martini MC. Influence of encapsulation on the in vitro percutaneous absorption of octyl methoxycinnamate. Int. J. Parm. 2004;272:45–55.

39. Calpena AC, Clares B. Fernandez F. Technological, biopharmaceutical and pharmacokinetic advances: New formulations of application on the skin and oral mucosa. Diego Muñoz-Torreo. Recent advance in pharmaceutical science. 2011;661:175-198.

40. Morganti P, Ruocco E, Wolf R, Ruocco V. Percutaneous absorption and delivery systems. Clin. Dermatol. 2001;19:489–501.

41. Ehdaie B. Enhanced delivery of transdermal drugs through human skin with novel carriers. J. Pharm. Biomed. Sci. 2011;1:161–166.

42. Lademann J, Richter H, Schaefer UF, Blume-Peytavi U, Teichmann A, Otberg N, Sterry W. Hair follicles-a long-term reservoir for drug delivery. Skin Pharmacol. Physiol. 2006;19:232–236.

43. Alvarez-Román R, Naik A, Kalia YN, Guy RH, Fessi H. Enhancement of topical delivery from biodegradable nanoparticles. Pharm. Res. 2004;21:1818–1825.

44. Luengo J, Weiss B, Schneider M, Ehlers A, Stracke F, König K, Kostka KH, Lehr CM, Schaefer UF. Influence of nanoencapsulation on human skin transport of flufenamic acid. Skin Pharmacol. Physiol. 2006;19:190–197.

45. Alvarez-Román R, Naik A, Kalia YN, Guy RH, Fessi H. Skin penetration and distribution of polymeric nanoparticles. J. Control. Release. 2004;99:53–62.

46. Lademann J, Richter H, Teichmann A, Otberg N, Blume-Peytavi U, Luengo J, Weiß B, Schaefer UF, Lehr CM, Wepf R, Sterry W. Nanoparticles--an efficient carrier for drug delivery into the hair follicles. Eur. J. Pharm. Biopharm. 2007;66:159–164.

47. Zhang W, Jin G, Zhu Q, Min Z, Ding X, Wang X, Hou X, Fan W, Ding B, Wu X, Wang X, Gao S. Penetration and distribution of PLGA

nanoparticles in the human skin treated with microneedles. Int. J. Pharm. 2010;402:205–212.

48. De Jalón E, Blanco-Príeto M, Ygartua P, Santoyo S. PLGA microparticles: possible vehicles for topical drug delivery. Int. J. Pharm. 2001;226:181–184.

49. Vega E, Egea MA, Garduño-Ramírez ML, García ML, Sánchez E, Espina M, Calpena AC. Flurbiprofen PLGA-PEG nanospheres: role of hydroxy-β-cyclodextrin on ex vivo human skin permeation and in vivo topical anti-inflammatory efficacy. Colloids Surf. B. Biointerfaces. 2013;110:339–346.

50. Cho C, Choi J, Shin S. Controlled release of pranoprofen from the ethylene-vinyl acetate matrix using plasticizer. Drug Dev. Ind. Pharm. 2007;33:747–753.

51. Choi J, Choi J, Shin S. Preparation and evaluation of pranoprofen gel for percutaneous administration. Drug Dev. Ind. Pharm. 2007;33(1):19–26.

4. DISCUSIÓN

El presente trabajo de investigación versa sobre el diseño, optimización y evaluación de la eficacia terapéutica in *vitro*, *ex vivo* e *in vivo* de pranoprofeno (PF) asociado a nanopartículas (NPs) poliméricas destinadas a la aplicación tópica. Las formulaciones de PF-NPs fueron desarrolladas con el objetivo de favorecer la biodisponibilidad de este fármaco a través de las membranas biológicas para prevenir y/o tratar el dolor y la inflamación.

4.1. Preparación, optimización y caracterización de las formulaciones de pranoprofeno asociado a nanopartículas poliméricas.

Las sistemas nanoestructurados conteniendo PF se prepararon mediante la técnica de desplazamiento del solvente descrita por Fessi et al [48], usando un polímero biodegradable y no tóxico (PLGA 75:25; Resomer®753S), el cual ha sido ampliamente utilizado en el diseño de sistemas de liberación controlada de diversos fármacos debido a que permite suministrar eficazmente el fármaco en el sitio deseado y, por lo tanto, aumentar el beneficio terapéutico, y reducir al mínimo efectos adversos [37]. El Polivinil alcohol (PVA) fue elegido como tensoactivo para estabilizar las nanopartículas desarrolladas, ya que debido a sus características hidrofilicas y biocompatibilidad, es uno de los agentes estabilizantes más usados en la formulación de NPs estables [84].

Se utilizó un diseño central compuesto 2^4 + principal para optimizar las PF-NPs. Este tipo de diseño, se utiliza frecuentemente en la planificación de una investigación, debido a que con un mínimo de experimentos, proporciona un máximo de información [85]. A través del diseño factorial se estudió el efecto individual de diferentes factores y las interacciones entre ellos, en el tamaño promedio de partícula (TMP), el índice de polidispersión (IP), el potencial zeta (ZP) y la eficiencia de encapsulación (EE). Los factores o variables independientes investigadas fueron la concentración de PF (cPF), la concentración de PVA (cPVA), la concentración de PLGA (cPLGA) y el pH de la fase acuosa (Tabla 1 artículo 1). Se preparon un total de 26 formulaciones, incluyendo 16 puntos factoriales, 8 puntos axiales y 2 puntos centrales (Tabla 2 artículo 1).

Se llevo a cabo, un análisis de varianza (ANOVA) para identificar la significancia ($P < 0.05$) de los efectos individuales de los factores y las interacciones entre ellos, en las propiedades de las partículas.

El diámetro promedio de las partículas y el índice de polidispersión de las 26 formulaciones obtenidas a partir del diseño factorial, varían en el rango de 265.4 ± 5.75 a 784.3 ± 5.63 nm y desde 0.013 ± 0.02 a 0.391 ± 0.02, respectivamente (Tabla 2 artículo 1). Los resultados del análisis estadístico (Tabla 3 artículo 1, Figuras 1 y 2 artículo 1) revelaron que el único factor que tiene un efecto significativo (p-valor <0.05) en el TMP y el IP es el pH de la fase acuosa (Tabla 3 artículo 1). Los resultados del diseño factorial revelan una tendencia a la formación de partículas con tamaño pequeño y polidispersidad baja a valores de pH entre 4.5 y 6.5, mientras que a valores de pH inferiores al pKa (4.35), se produjo un aumento en los valores de estas dos propiedades de las NPs (Figuras 1a y 1b artículo 1).

La penetración de los fármacos asociados a NPs administrados por vía tópica depende de factores, tales como la composición química de los componentes de la formulación, el tamaño de partícula y la viscosidad de la formulación [86]. El tamaño de partícula de las formulaciones diseñadas para la administración ocular es de crucial importancia, ya que no debe exceder a 10 micras para evitar una sensación de malestar en el ojo [54,55]. Otra consideración importante en el tamaño de las partículas es: que las partículas muy pequeñas poseen un área superficial grande, lo que puede conducir a una liberación más rápida del fármaco y desempeña un papel muy importante en la captación celular [56, 57].

Por otra parte, las NPs poliméricas se han descrito como sistemas adecuados para la liberación de los fármacos a través de la piel. Estos nanosistemas muestran afinidad preferente por los folículos pilosos, los cuales proveen un reservorio en el que las NPs se acumulan y crean un depósito local del fármaco [87].

Algunos investigadores han reportado que la penetracion y retencion de los fármaco asociados a NPs poliméricas a través de la piel depende del tamaño de particula [88, 89,90].

Otra propiedad fisicoquímica de las NPs es su carga superficial; evaluada en base al potencial zeta, que puede influir en su estabilidad y mucoadhesión. Las

repulsiones electrostáticas entre las partículas con la misma carga eléctrica evitan la agregación entre ellas [91].

Todas las formulaciones obtenidas a partir del diseño factorial presentan una carga negativa, en el rango de - 2.15 ± 0.13 a - 12.92 ± 0.29 mV (Tabla 2 artículo 1). La ANOVA muestra que la cPVA y el pH de la fase acuosa, ejercen un efecto significativo ($p < 0.05$) en el ZP, pero no la interacción entre ambos (Tabla 3 artículo 1). Un incremento en los valores del ZP fueron observados al incrementar la cPVA a valores de pH bajos (Figura 2a artículo 1). Estos resultados podrían atribuirse a la adsorción de PVA en la superfície de partículas, así como también, a los grupos carboxilo de PLGA, resultando una carga ligeramente negativa en la superfície de las partículas [92].

La EE de PF en las NPs desarrolladas oscila entre 40 y 91% (Tabla 2 artículo 1). El análisis de la ANOVA reveló que el pH de la fase acuosa y la cPF, tienen un efecto significativo ($p < 0.05$) en la EE. Sin embargo, la interacción entre ambos factores, no puede considerarse estadísticamente significativa (Tabla 3 artículo 1). Al aumentar la cPF a valores de pH más bajo que el pKa, se observa una tendencia a incrementar la EE de PF en las NPs (Figura 2b artículo 1). Estos resultados pueden atribuirse al hecho de que, a valores de pH inferiores al pKa, el fármaco atrapado en las NPs está en su forma no disociada y en este estado, el fármaco es más afín a la matriz polimérica, produciéndose una mayor retención de fármaco en la matriz polimérica [93]. Por el contrario, a valores de pH de la fase acuosa superiores al pKa, probablemente más moléculas del fármaco están ionizadas, y por esta razón, menos fármaco podría ser reteniendo, lo que conduce a una ligera disminución de EE de PF [55]. Por lo tanto, la determinación de un valor óptimo de pH de la fase acuosa es crucial, ya que puede afectar a la ionización del principio activo y, en consecuencia, su afinidad al polímero y/o modificar el tamaño y polidispersidad de las NPs [94, 95].

A partir de los resultados obtenidos en el diseño factorial y de acuerdo con los objetivos de este estudio, las condiciones experimentales en las que se obtuvieron las formulaciones de PF-NPs con los mejores valores de TMP, IP y un porcentaje alto de PF encapsulado en la matriz polimérica (80 %), son las descritas en la Tabla 1.

Tabla 1. Composición de las formulaciones optimizadas de PF-NPs.

PF-NPs	cPF (mg/mL)	cPVA (mg/mL)	cPLGA (mg/mL)	pH
PF-F1NPs	1.5	10.0	9.5	5.5
PF-F2NPs	1.0	5.0	9.0	4.5
PF-F3NPs	1.0	25.0	9.0	4.5

La estabilidad física de las PF-NPs optimizadas, después de 1, 8, 15 y 30 días de almacenamiento a 4ºC se analizó usando el analizador óptico TurbiScanLab®. Un discreto aumento de la señal retrodispersada en el lado izquierdo de la gráfica indicó una migración de partículas a la parte inferior del vial, por lo tanto, un proceso de sedimentación (Figura 3 artículo 1). Esta ligera desestabilización observada en los perfiles de las formulaciones PF-F1NPs (Figura 3a artículo 1) y PF-F2NPs (Figura 3c artículo) fue reversible. Las partículas se re-suspendieron fácilmente después de una agitación suave. En contraste, la formulación PF-F3NPs (Figura 3b artículo 1), exhibió en el perfil de retrodispersión variaciones superiores a ± 10%, a los 30 días de la producción, lo que denota una baja estabilidad de dicha formulación.

Por otra parte, la cantidad de PVA adherida en la superfície de las NPs, se determinó usando un método colorimétrico, a través de la formación de un complejo estable entre dos grupos hidroxilos adyacentes del PVA y una molécula de yodo en presencia de ácido bórico (artículo 1) [96]. Los resultados obtenidos sugieren que la cantidad de PVA adsorbida en la superfície de las NPs aumenta con un incremento de la cPVA en la fase acuosa de la formulación y la fracción de PVA asociada a la superfície de las NPs, parece conservarse a pesar de repetidos lavados con agua. Estos resultados podrían atribuirse a la interacción hidrófoba entre el grupo acetato del PVA y la matriz hidrófoba del PLGA. Los segmentos de PVA penetran en la fase orgánica y permanece atrapado en la matriz polimérica de las NPs. La unión de PVA en la superfície de la partícula, ocurre probablemente cuando se elimina el disolvente orgánico de la interface, permitiendo la interpenetración de las moléculas de PVA y PLGA [92].

Liofilización de las PF-NPs optimizadas. La inestabilidad de las NPs, después de un largo período de almacenamiento, es uno de los principales problemas

que limitan el uso de los sistemas coloidales [70]. En este sentido, para preservar las propiedades de las NPs, estas fueron liofilizadas y se determinaron sus características fisicoquímicas; comparándolas con las de las NPs antes de liofilizar. Los resultados obtenidos muestran que tanto el TMP como el IP de las NPs liofilizadas rehidratadas, son similares a los obtenidos para las NPs antes de liofilizar (Tabla 4 artículo 1). Los resultados sugieren que el PVA utilizado en la preparación de las NPs, como estabilizador estérico, actúa también como crioprotector, debido a su elevado peso molecular. La capa de este estabilizador estérico es lo suficientemente grande para evitar la aglomeración de las mismas durante el proceso de congelación, siendo este el paso más crítico en el proceso de liofilización. Además, la presencia de PVA en la superficie partículas favorece una apropiada rehidratación de las mismas, lo cual puede atribuirse a la hidrofilicidad de las moléculas de PVA [67, 97].

Las **interacciones fisicoquímicas** fármaco – polímero en las PF-NPs antes y después de liofilizar, se evaluaron por difracción de rayos X, espectroscopia de IR con transformada de Fourier (FTIR) y análisis de calorimetría diferencial de barrido (DSC). El análisis de los difractogramas obtenidos por rayos X para las PF-NPs (Figura 4 artículo 1), reveló una combinación de dos estructuras (PF y PLGA). La intensidad de algunos de los picos cristalinos de PF presentes en las NPs antes de liofilizar, aumenta ligeramente al incrementar la cPF. Algunos investigadores, han reportado que cuando la cantidad de fármaco sobrepasa la solubilidad en el polímero, una parte precipita en forma de nanocristales [98, 99, 100].

Los difractogramas de rayos X para las PF-NPs liofilizadas (Figura 4 artículo 1) muestran una forma amorfa, lo que podría atribuirse, a que a baja temperatura durante la liofilización, las capas de PVA en las superfície de las NPs presenta un estado vítreo – amorfo. Adicionalmente, los enlaces de hidrógeno formados entre el PVA y las moléculas de agua, previenen la agregación de las partículas durante la liofilización [70]. Al mismo tiempo, esta capa formada en la superfície de las NPs, favorece la redispersión de la formulación liofilizada después de la rehidratación [96]. El análisis de FTIR reveló que las PF-NPs antes de liofilizar muestran un espectro FTIR similar al del PLGA, mientras que una vez liofilizadas exhiben un espectro que combina la estructura de PLGA y PVA

(Figura 5 artículo 1). Estos resultados indican que no existe evidencia de ninguna interacción química o formación de enlaces fuertes entre PF y PLGA.
Las posibles interacciones fisicoquímicas entre PF y PLGA, también fueron evaluadas por DSC. Los termogramas obtenidos para las PF-NPs antes de liofilizar muestran que las NPs son muy similares entre sí y similares al PLGA puro, exhibiendo eventos térmicos alrededor de la temperatura de transición vítrea del PLGA (Figura 6 artículo 1). Por otra parte, los termogramas de las mismas formulaciones después de liofilizar revelan picos característicos correspondientes al PLGA y PVA. Sin embargo, todos estos eventos térmicos en las NPs liofilizadas se registran a una temperatura inferior en comparación con los termogramas del PLGA y PVA puros (Figura 6 artículo 1), lo que podría ser debido al hecho de que las NPs pueden retener cantidades significativas de agua después de un proceso típico de fabricación, que podrian tener un efecto plastificante en las NPs y al mismo tiempo, podría ser debido a las condiciones de secado utilizadas durante el proceso de liofilización [101]. La intensidad de los eventos térmicos observados en las PF-NPs antes y después de liofilizar está directamente relacionada con la cPVA utilizada en la preparación de la formulación. Adicionalmente, la ausencia de un pico correspondiente a la fusión del PF en las NPs antes o después de liofilizar (Figura 6 articulo 1) indica que el fármaco presente dentro de las NPs esta molecularmente disperso [102].

4.2. Preparación y caracterización de las formulaciones de semisólidas de pranoprofeno asociado a sistemas nanopartículares.

Debido a la baja viscosidad de las suspensiones de las NPs, estas formulaciones frecuentemente se incorporan en hidrogeles (HGs) o cremas para obtener formas de dosificacion tópicas con una consistencia adecuada [103, 104].
El Cabomero 934 fue elegido para vehiculizar las PF-NPs optimizadas, debido a sus propiedades bioadhesivas, baja toxicidad, caracteristicas reológicas y biocompatibilidad. En la literatura, los HGs de acido poliacrilico tales como, carbomero 934 y carboximetilcelulosa han sido descritos como polimeros con las mejores caracteriscas bioadhesivas [105]. La viscosidad de los hidrogeles de Carbomero asegura una retención prolongada de la formulación en el área

de aplicación, mejorando la biodisponibilidad de los fármacos [4]. Además, promotores de la permeación de fármacos pueden ser adicionados a dichas formulaciones sin modificar sus características fisicoquímicas.

En el presente estudio, la azona fue selecionada como promotor de la permeación debido a que su baja irritabilidad y toxicidad. Este promotor se ha usado ampliamente para favorecer la permeación topica de fármaco lipófilos e hidrófilos, siendo segura y efectiva en humanos en el rango de 1 al 10% [80]. Sin embargo, este promotor de la permeación de fármacos, ha mostrado ser mas efectivo en una concentracion del 1% al 3% [106].

El estudio de predicción de la estabilidad de las NPs optimizadas en suspensión, puso de manifiesto una discreta sedimentación de las mismas (que desaparece por agitación manual) sin evidenciar cambios significativos de tamaño para las formulaciones PF-F1NPs y PF-F2NPs. En contraste, los perfiles de retrodispersión de PF-F3NPs revelaron variaciones de retrodispersión superiores a ± 10%, a los 30 días de la producción, lo que denota una baja estabilidad de esta formulación. Por esta razón, la formulación PF-F3NPs, no fue considerada en los estudios adicionales llevados a cabo en este trabajo.

Las suspensiones de NPs optimizadas (PF-F1NPs y PF-F2NPs) fueron incorporadas en HGs (HG_PF-F1NPs y HG_PF-F2NPs), con el propósito de obtener un efecto de liberación controlada del fármaco, mejorar el perfil biofarmacéutico de PF, prologar el tiempo de contacto y la retención del fármaco, favoreciendo su eficacia antiinflamatoria y analgésica y reduciendo la frecuencia de aplicación. Al mismo tiempo, la azona fue adicionada a las formulaciones semisólidas de PF (HG_PF-F1NPs-Azona y HG_PF-F2NPs-Azona) destinadas a la administración oftálmica (1% de azona, p/p) y a la aplicación dérmica (3% de azona, p/p), con el objetivo de facilitar e incrementar la permeabilidad de PF a través de estas vías.

Las características fisicoquímicas de las NPs después de su incorporación en el HG fueron analizadas por microscopia electronica de transmision (TEM), difracción laser (LD) y espectroscopia de correlación de fotones (PCS).

El tamaño y morfología de las PF-NPs incorporadas en HG se determinaron por TEM. Los resultados obtenidos revelaron que las PF-NPs tienen una forma

esferica, sin agregados y un diametro medio alrededor de 300 nm (Figura 1 artículo 2 y Figura 1 articulo 3). Los resultados obtenidos por TEM muestran que las NPs incorporadas en el HG exhiben un tamaño de partícula similar al obtenido para las NPs en suspensión (Tabla 2 artículo 1, Figura 1 artículo 2 y Figura 1 artículo 3).

La estabilidad fisicoquímica de las PF-NPs incorporadas en el HG se evaluó por LD y por PCS transcurridas 24 h de la producción de las formulaciones y 90 días de almacenamiento a 25ºC. Los resultados obtenidos por LD a los 90 días del estudio revelan un incremento aparente del tamaño de partícula respecto a los valores observados después de un día de la producción de las formulaciones de HG_PF-NPs en presencia de azona (1% ó 3%) o en ausencia de este promotor (Material suplementario artículo 2 y Figura 2 artículo 3). Los estudios de estabilidad de las formulaciones HG_PF-NPs en ausencia o en presencia de azona (1% ó 3%), llevados a cabo por PCS, muestran que los valores del TMP son similares a los obtenidos en las mediciones por LD. Sin embargo, Gonzalez- Mira et al, [75] reportaron que un incremento aparente del tamaño medio de particula podria ser debido a que las particulas se encuentren fuertemente atrapadas dentro de la estructura tridimensional del gel, más que a una aglomeracion real de las particulas.

Los resultados observados en el estudio de estabilidad de las formulaciones semisólidas de PF, están en concordancia con los obtenidos por TEM (Figura 1 artículo 2 y Figura 1 articulo 3), ya que las PF-NPs incorporadas en HG mantienen tamaños de partícula similares a los observados para las PF-NPs en suspensión. El análisis por PCS, también reveló un incremento en los valores del ZP de las PF-NPs incorporadas en el HG respecto al observado para las PF-NPs en suspensión (Tabla 2 artículo 1y artículo 3, respectivamente). Estos resultados podrían ser atribuidos a la absorción de las cargas negativas de las moléculas del agente gelifícante sobre la superficie de las NPs. Un incremento de los valores del ZP favorece la estabilidad por la repulsión electroestática que se establece entre las NPs [77]. Al final del estudio de estabilidad, las formulaciones de HG_PF-NPs ensayadas muestran que las PF-NPs incorporadas en el HG no forman agregados y conservan las propiedades fisicoquímicas apropiadas para la administración ocular y/o dérmica, indicando

que el agente gelifícante no modificó significativamente la morfología y el tamaño de las NPs.

Las **propiedades reológicas** de las formulaciones de HG_PF-NPs en ausencia o en presencia de azona (1% ó 3%), se evaluó después de 8 y 90 días de almacenamiento a 25ºC. La caracterización reológica de todas las formulaciones de HG_PF-NPs ensayadas exhiben un comportamiento no Newtoniano y pseudo-plástico, indicando que las formulaciones se adhieren fácilmente al aplicarse sobre la superficie ocular y/o dérmica. Los resultados obtenidos revelan que la inclusión de un 1% ó 3% de azona en las formulaciones produce un incremento significativo de los valores de viscosidad (HG_PF-F1NPs-Azona y HG_PF-F2NPs-Azona) respecto a los obtenidos para las formulaciones HG_PF-F1NPs y HG_PF-F2NPs. Adicionalmente, se observó que los resultados de las mediciones reológicas a los 90 días del almacenamiento de las formulaciones muestran una disminución de los valores de viscosidad y tixotropía para todas las formulaciones semisólidas ensayadas respecto a los valores obtenidos a los 8 días de la producción (Tabla 3 artículo 2 y artículo 3, respectivamente). Estos resultados están en concordancia con el incremento en el TMP e IP obtenidos a los 90 días del almacenamiento a 25ºC determinado por LD (Material suplementario artículo 2 y Figura 2 artículo 3) y por PCS (Tabla 2 artículo 2 y Tabla 2 artículo 3), lo que puede explicarse por el hecho de que las NPs caracterizadas por un índice de polidispersión alto pueden ser más fácilmente empaquetadas que las que tienen una polidispersidad baja. Las partículas con una distribución de tamaño elevado tienen más espacio libre para moverse, lo que significa que la muestra puede fluir fácilmente, disminuyendo su viscosidad y viceversa [107]. El ensayo de frecuencia oscilatoria fue llevado a cabo desde 0.01 a 10 Hz, a un esfuerzo de cizallamiento constante dentro de la región viscoelástica, con el objetivo de determinar la variación relacionada con el módulo de almacenamiento (G') y el módulo de perdida (G") a 25ºC. Las mediciones oscilatorias aplicadas a las formulaciones HG_PF-NPs en ausencia o en presencia de azona (1% ó 3%), muestran una prevalencia del comportamiento elástico sobre el viscoso (G'>G'') para todas las formulaciones testadas (Figura 3 artículo 3).

4.3. Ensayos *in vitro* de las formulaciones de pranoprofeno desarrolladas.

Un estudio de **liberación *In vitro*** de PF desde las formulaciones destinadas a la aplicación ocular y dérmica fue llevado a cabo en células de Franz. Las formulaciones destinadas a la administración ocular: nanopartículas optimizadas (antes y después de liofilizar) en suspensión (PF-NPs) y en geles (HG_PF-NPs) en ausencia o en presencia de azona (1% p/p), se compararon con el colirio comercial (Oftalar®, 1.0 mg/mL) y/o con la solución del fármaco libre (1.0 mg/mL en PBS pH 7.4).

Por otra parte, las formulaciones semisólidas de PF sin o con azona (3% p/p), se compararon con una solución de fármaco libre (1.0 mg/mL en PBS pH 7.4). Los resultados obtenidos revelan que el perfil de liberación de PF desde la solución de fármaco libre y del colirio comercial, fue más rápido comparado con las PF-NPs o con HG_PF-NPs en ausencia o en presencia de un 1% de azona (Figura 7 artículo 1 y Figura 2 artículo 2). Las formulaciones HG_PF-NPs destinadas a la aplicación dérmica, también exhiben un perfil de liberación más lento respecto al observado para la solución de fármaco libre (Figura 4 artículo 3). A las 3 h del análisis, el 100 % del fármaco se había liberado desde la solución del fármaco libre o el colirio comercial (Figura 7 artículo 1, Figura 2 artículo 2 y Figura 4 artículo 3). En términos generales, la liberación del fármaco a partir de partículas de PLGA puede ocurrir a través de la difusión, erosión del polímero o una combinación de estos [61]. Si la difusión del fármaco es más rápido que la degradación de la matriz, el mecanismo de liberación del fármaco se produce principalmente por difusión. Una liberación rápida del fármaco puede ser atribuida, a la fracción del mismo adsorbida o débilmente unida a la superfície de la NPs [62]. Los perfiles de liberación de PF desde las NPs antes y después de liofilizar, son similares entre sí, exhibiendo un comportamiento de liberación sostenido, con una liberación rápida al inicio, debido a la cantidad PF presente en la superfície de las NPs, seguido por una fase de liberación lenta, correspondiente a la difusión del fármaco atrapado en el interior de las mismas (Figura 7 artículo 1). Sin embargo, la velocidad de liberación y las cantidades de PF liberadas a partir de las PF-NPs son mayores respecto a los valores exhibidos por las formulaciones de las NPs incorporadas

en el HG en ausencia o en presencia de un 1% o un 3% de azona (Figura 7 artículo 1, Figura 2 artículo 2 y Figura 4 artículo 3). Estos resultados sugieren que la velocidad de difusión del fármaco puede ser afectada por un incremento de la viscosidad de las formulaciones semisólidas comparado con la suspensión de las NPs. No obstante, tanto las PF-NPs como las formulaciones de HG_PF-NPs en ausencia o en presencia de azona garantizan una liberación sostenida del fármaco respecto al colirio comercial y a la solución de fármaco libre. Adicionalmente, el ensayo de liberación in vitro de PF reveló que a medida se incrementa la cPVA en la formulación de las NPs, el fármaco se libera más lentamente y viceversa (Figura 7 artículo 1). Estos resultados pueden ser atribuidos a que un aumento en la cPVA en las NPs produce un aumento en la viscosidad, originando una matriz polimérica más compacta, en la que la velocidad de degradación del polímero y /o la difusión PF es más lenta [92]. Los resultados obtenidos a partir del ensayo de liberación de PF desde las NPs testadas son consistentes con los obtenidos en el análisis de FTIR (Figura 5 artículo 1), ya que no se detectó ninguna formación de enlaces fuertes entre PF y PLGA.

Por otra parte, la cantidad PF liberado dese las formulaciones ensayadas, se ajustó a diferentes modelos cinéticos; calculándose el valor de AIC para cada uno de ellos. Este parámetro es un indicador de la idoneidad del modelo para un determinado conjunto de datos. Cuanto menor sea el valor de AIC, el modelo ajusta mejor al conjunto de los datos. Los valores de AIC obtenidos a partir de las cantidades de PF liberadas y acumuladas a las 7 h del ensayo para las formulaciones ensayadas muestran que las curvas de liberación de PF de la solución de fármaco libre, colirio comercial, PF-F1NPs y PF-F2NPs (antes y después de la liofilización), se ajustan adecuadamente al modelo cinético de orden uno (Tabla 5 artículo 1). Sin embargo, el perfil de liberación de PF desde PF-F3NPs, antes y después de liofilizar, se ajusta adecuadamente al modelo de Korsmeyer – Peppas y a primer orden, respectivamente (Tabla 5 artículo 1). Por otra parte, los valores de AIC obtenidos a las 24 h del estudio de liberación *in vitro* de PF desde las formulaciones semisólidas en ausencia o en presencia de un 1% azona comparado con la solución de fármaco libre y el colirio comercial revelan que las curvas de liberación de PF desde HG_PF-F1NPs, HG_PF-F2NPs, HG_PF-F2NPs-Azona, colirio comercial y la solución de

fármaco libre ajustan a una hipérbola, mientras que la formulación HG_PF-F1NPs-Azona ajusta a un modelo de primer orden (Tabla 4 artículo 2). Las curvas de liberación de PF de todas las formulaciones semisólidas destinadas a la aplicación dérmica se ajustan adecuadamente al modelo de Korsmeyer – Peppas (Tabla 4 artículo 3). El valor de AIC obtenido para este modelo es inferior al encontrado para los otros modelos cinéticos calculados (Tabla 5 artículo 1, Tabla 4 artículo 2 y Tabla 4 artículo 3), por lo tanto, estadísticamente, describe mejor el mecanismo de liberación del fármaco. Según la primera ley de Fick, el valor de n, se utiliza para caracterizar los diferentes mecanismos de liberación [108]. Valores de $n \leq 0.5$ fueron obtenidos para las PF-NPs o HG_PF-NPs con o sin azona (Tabla 5 artículo 1, Tabla 4 artículo 2 y Tabla 4 artículo 3), indicando que la liberación de PF desde estas formulaciones, se produce por difusión pasiva, principalmente a través de los poros de la matriz [109]. En su conjunto, los resultados obtenidos en el ensayo de liberacion de PF a partir de las formulaciones analizadas indica que este proceso esta governado por factores tales como, la cantidad de PVA presente en la formulación, la presencia de PF en estado cristalino, ya que el fármaco en su forma cristalina debe disolverse antes de liberarse y difundir a traves de la matriz polimerica (Figura 4 artículo 1). Adicionalmente, la difusion del fármaco fuera de la matriz del hidrogel depende de la fuerza mecanica de degradabilidad, la difusividad, y otras propiedades fisicas de la estructura del agente gelificante [110].

La **tolerancia ocular *in vitro*** de las formulaciones PF-NPs y HG_PF-NPs en ausencia o en presencia de un 1% de azona fue evaluada por HET-CAM. El ensayo de HET-CAM basado en la observación de reacciones, tales como hemorragia, coagulación intravascular o lisis de los vasos sanguíneos; proporciona una alternativa adecuada al método Draize para evaluar la irritación ocular [111]. Los resultados obtenidos, a través del HET-CAM, revelan una tolerancia ocular óptima para las formulaciones PF-NPs y HG_PF-NPs en ausencia o en presencia de un 1% de azona, ya que no se detectó ninguna reacción de irritación a los 5 minutos de la prueba.

4.4. Ensayos *ex vivo e in vivo* de las formulaciones de pranoprofeno para administración ocular.

El estudio de **permeación transcorneal** de PF llevado a cabo en conejos blancos New Zealand, permitió de determinar el perfill de permeación de PF a partir de las formulaciones de las PF-NPs incorporadas en HG en ausencia de azona (HG_PF-NPs) o en presencia de un 1% de promotor (HG_PF-NPs-Azona) comparadas con el colirio comercial (Oftalar®, PF 1 mg/mL) y con la solución de fármaco libre (PF en PBS, 1 mg/mL). Los resultados del ensayo pusieron de relieve que los perfiles de permeación de PF a partir del colirio comercial y de la solución de fármaco libre son muy similares entre sí (Figura 3 artículo 2). Respecto a las formulaciones semisólidas de PF, se observó que las curvas de permeación del fármaco desde las formulaciones HG_PF-F1NPs-Azona y HG_PF-F2NPs-azona exhiben un incremento en la cantidad de PF permeado a través de la córnea comparado con HG_PF-F1NPs y HG_PF-F2NPs, respectivamente (Figura 3 artículo 2).

Las NPs poliméricas se aglomeran en el saco conjuntival, formando un reservorio del fármaco, desde el cual el principio activo encapsulado difunde lentamente desde la matriz polimérica al área pre-corneal internalizándose en las células del epitelio corneal a través de un mecanismo de endocitosis [112].

El análisis estadístico de los parámetros de permeación de PF calculados a partir de las cantidades del fármaco permeadas a través de la córnea desde las formulaciones HG_PF-NPs con o sin azona, colirio comercial y la solución de fármaco libre reveló para el parámetro C_P diferencias estadísticamente significativas $(p < 0.05)$ entre HG_PF-F1NPs y HG_PF-F2NPs, HG_PF-F1NPs y colirio comercial, HG_PF-F1NPs-Azona y HG_PF-F2NPs, HG_PF-F1NPs-Azona y colirio comercial (Tabla 5 artículo 2). Así mismo, diferencias estadísticamente significativas $(p < 0.05)$ fueron encontradas para el parámetro P_1 entre HG_PF-F1NPs y HG_PF-F2NPs, entre HG_PF-F1NPs y colirio comercial, entre HG_PF-F1NPs y la solución del fármaco libre, entre HG_PF-F2NPs-Azona y la solución del fármaco libre, entre HG_PF-F1NPs-Azona y el colirio comercial y entre HG_PF-F1NPs-Azona y la solución del fármaco libre (Tabla 5 artículo 2). El análisis estadístico de los parámetros P_2 y T_L mostró diferencias significativas $(p < 0.05)$ entre HG_PF-F1NPs y el colirio

comercial, entre HG_PF-F1NPs y la solución de fármaco libre, entre HG_PF-F2NPs-Azona y la solución del fármaco libre, entre HG_PF-F1NPs-Azona y el colirio comercial, entre HG_PF-F1NPs-Azona y la solución del fármaco libre (Tabla 5 artículo 2). Los valores de C_P obtenidos para HG_PF-F2NPs, colirio comercial y la solución de fármaco libre están directamente relacionados al parámetro P_1. Por otra parte, los valores exhibidos por las formulaciones HG_PF-F1NPs-Azona and HG_PF-F2NPs-Azona para el parámetro P_2 sugieren que el coeficiente de difusión del fármaco está influenciado por la presencia de azona en la formulación. Por lo tanto, estas formulaciones alcanzan el equilibrio estacionario con mayor rapidez respecto al colirio comercial o la solución del fármaco libre.

Las cantidades de PF retenidos en la córnea y el nivel de hidratación de la córnea fueron determinados al final del estudio de permeación. Las formulaciones HG_PF-F1NPs y HG_PF-F1NPs-Azona exhibe una cantidad de PF retenido en la córnea superior a la observada para las formulaciones HG_PF-F2NPs y HG_PF-F2NPs-Azona (Tabla 6 artículo 2). Estos resultados pueden atribuirse a que la cPVA en PF-F1NPs es superior a la presente en PF-F2NPs, favoreciendo la retención de las NPs sobre la superfície ocular [113]. Por otra parte, el análisis de permeación de PF a través de la córnea, reveló así mismo, que las cantidades de PF permeadas o retenidas en la córnea a partir del colirio comercial o de la solución del fármaco libre son superiores a las observadas para las formulaciones de HG_PF-NPs en ausencia o en presencia de un 1% de azona (Tabla 6 artículo 2). Sin embargo, la solución de PF libre es inherentemente irritante para el ojo e inestable en solución acuosa [114]. Por otra parte, el incremento en los valores de las cantidades de PF permeados a tavés de la córnea a partir del colirio comercial pueden ser explicados por la combinacion de cloruro de benzalconio y edetato sodico presensentes en la formulación comercial de PF. El cloruro de benzalconio incrementa la permeación de los fármacos a través de la córnea por la disrupción del epitelio corneal. Adicionalmente, este compuesto puede emulsificar el epitelio corneal conduciendo a un incremento del coeficiente de partición del fármaco [115]. Por otra parte, el edetato sodico aumenta la permeabilidad de diversos fármacos a través de la córnea removiendo los iones calcio extracelulares y en

consecuencia, incrementando la permeabilidad de las uniones estrechas [116, 117].

Los resultados obtenidos en el ensayo de permeación transcorneal de PF a partir de las formulaciones semisólidas de PF revelan que las cantidades de PF permeadas o retenidas desde las formulaciones HG_PF-F1NPs-Azona y HG_PF-F2NPs-Azona son mayores a las obtenidas para las formulaciones HG_PF-F1NPs y HG_PF-F2NPs, respectivamente. Estos resultados sugieren que la inclusión de azona en la formulación produce un incremento en las cantidades permeadas o retenidas de PF en la córnea.

A pesar de que la azona ha sido usada para favorecer la permeación de los fármacos durante más de 25 años, muchos investigadores continúan estudiando su mecanismo de acción. Algunos trabajos sugieren que el mecanismo de la azona puede estar relacionado con las modificaciones en la unión de las células epiteliales, aumentando el flujo del agua y la permeación transcorneal de los fármacos hidrófilos y retardando aparentemente la permeación de los fármacos lipófilos a través de la córnea [106].

Respecto la determinación del nivel de hidratación corneal en el ensayo de permeación transcorneal de PF a partir de las nanopartículas incorporadas en HG en ausencia o en presencia de un 1% de azona, el colirio comercial y la solución del fármaco libre, los resultados obtenidos revelan valores en el rango 76 - 80%, correspondiente a los niveles de hidratación de la córnea sana. Los resultados obtenidos sugieren que la córnea no sufrió daños durante la realización del ensayo (Tabla 6 artículo 2) [118].

La **eficacia antiinflamatoria** de PF contenido en las formulaciones HG-PF-NPs sin o con un 1% de azona fueron comparadas con el colirio comercial y la solución de fármaco libre. Los resultados del ensayo de permeación transcorneal revelaron que para el colirio comercial y la solución de fármaco libre las cantidades de PF permeadas y/o retenidas en la córnea fueron superiores a las observadas para las formulaciones HG_PF-NPs o HG_PF-NPs-Azona (Tabla 6 artículo 2). Sin embargo, el efecto antinflamatorio de PF a partir el colirio comercial o la solución de fármaco libre es más lento comparado con el observado en las formulaciones HG_PF-NPs o HG_PF-NPs-Azona (Figura 4 artículo 2). A los 120 min del ensayo de eficacia antiinflamatoria, la

solución de PF libre exhibe un efecto antiinflamatorio más lento respecto a las formulaciones de HG_PF-NPs con o sin azona (Figura 4 artículo 2). Los resultados observados en este ensayo para la solución de fármaco libre y el colirio comercial podrían explicarse por el hecho de que estas dos formulaciones exhiben valores de tiempos de latencia superiores a los obtenidos para las formulaciones HG_PF-NPs (con o sin azona). Ello indica que, ambas formulaciones alcanzan el equilibrio estacionario de manera más lenta que las formulaciones semisólidas, consecuentemente, estas dos formulaciones revelaron un efecto antiinflamatorio más lento comparado con las formulaciones semisólidas. Por otra parte, los resultados de este análisis, ponen de relieve, así mismo, que las formulaciones HG_PF-F1NPs-Azona y HG_PF-F2NPs-Azona reducen significativamente el edema ocular comparadas con las correspondientes formulaciones sin azona. Estos resultados sugieren que la inclusión de azona en la formulación conduce a un incremento del efecto antiinflamatorio de PF en el ojo (Figura 4 artículo 2). Los valores de eficacia antiinflamatoria exhibidos por las formulaciones HG_PF-NPs con un 1% de azona se correlacionan directamente con la cantidad de PF retenido en la córnea. Por lo tanto, la aplicación de las formulaciones HG_PF-F1NPs-Azona o HG_PF-F2NPs-Azona podrían ser más efectivas para tratar el dolor y la inflamación ocular.

La **tolerancia ocular *in vivo*** de las formulaciones HG_PF-NPs en ausencia o en presencia de un 1% de azona fue evaluada siguiendo el método descrito por Draize et al. [119,120]. Ningún signo de irritación ocular fue detectado durante el ensayo para las formulaciones evaluadas. Estos resultados están en concordancia con los obtenidos por el método HET-CAM.

4.5. Ensayos *ex vivo e in vivo* de las formulaciones de pranoprofeno para administración dérmica.

Un estudio de **permeación transdérmica** *ex vivo* de PF a partir de diferentes formulaciones fue llevado a cabo, con el fin de determinar el perfil de permeación y los parámetros de permeación de PF. Las cantidades permeadas

y acumuladas de PF fueron determinadas al cabo de 24 h del estudio de permeación (Figura 5 artículo 3).

Para evaluar la capacidad del fármaco libre de penetrar la piel humana, un ensayo de permeación intrínseca de PF a través de la vía dérmica fue realizado usando una solución saturada de este fármaco. Los parámetros de permeación calculados a partir de la permeación intrínseca de PF revelan un tiempo de latencia de 2 h. A este tiempo, el fármaco se encuentra en equilibrio estacionario y la piel está saturada de PF, alcanzando un flujo de permeación constante. (Tabla 5 artículo 3). Los parámetros de permeación P_1, P_2 y la constante de permeación C_P, se compararon estadísticamente a través de un test no paramétrico (Kruskal-Wallis Z test) y un test de comparación múltiple (Dunn´s test). El análisis estadístico de los parámetros de permeación C_P, P_1 y P_2 obtenidos para las formulaciones PF-F1NPs, HG_PF-F1NPs y HG_PF-F1NPs-Azona no reveló diferencias estadísticamente significativas ($p > 0.05$) entre ellas (Tabla 5 artículo 3). Estos resultados sugieren que estas formulaciones no mejoran significativamente el perfil de permeación de PF a través de la piel. En este caso, la única ventaja que ofrecen las formulaciones HG_PF-F1NPs y HG_PF-F1NPs-Azona respecto a las PF-F1NPs en suspensión, es que las formulaciones semisólidas se adhieren fácilmente sobre la piel debido a la presencia del agente gelifícante.

Diferencias estadísticamente significativas ($p < 0.05$) fueron encontradas para parámetro P_1 entre las formulaciones HG_PF-F2NPs y HG_PF-F2NPs-Azona. El coeficiente de partición entre el vehículo y la piel es un factor, a través del cual se puede regular la permeabilidad de los fármacos a través de la piel. Un aumento en valor del coeficiente de partición produce un incremento en la transferencia del fármaco desde el vehículo al estrato córneo. Así, valores de P_1 altos indican una mayor distribución en la piel que en el vehículo y viceversa [121]. En este caso, la formulación HG_PF-F2NPs exhibió el valor más alto de P_1 respecto a los valores observados para las formulaciones PF-F2NPs y HG_PF-F2NPs-azona (Tabla 5 artículo 3). El análisis estadístico de los datos obtenidos para el parámetro P_2 reveló diferencias estadísticamente significativas ($p < 0.05$) entre las formulaciones PF-F2NPs, HG_PF-F2NPs y HG_PF-F2NPs-Azona aplicando el test Kruskal-Wallis Z. Sin embargo, el test

de comparación Dunn´s múltiple no fue capaz de identificar entre que formulaciones se encontraban estas diferencias estadísticas.

El análisis estadístico del parámetro C_P reveló diferencias estadísticamente significativas $p < 0.05)$ entre las formulaciones PF-F2NPs y HG_PF-F2NPs y entre las formulaciones HG_PF-F2NPs y HG_PF-F2NPs-Azona (Tabla 5 artículo 3). Las diferencias estadísticamente significativas encontradas para el parámetro C_P, permiten poner de manifiesto las diferencias estadísticas encontradas para las formulaciones PF-F2NPs, HG_PF-F2NPs y HG_PF-F2NPs-Azona respecto al parámetro P_2, ya que el parámetro C_P depende directamente de los parámetros P_1 y P_2.

La eficacia de un fármaco destinado a la aplicacion cutanea depende de la correlación entre el coeficiente de permeabilidad en el estrato córneo y las propiedades fisicoquimicas del fármaco. El vehículo en cual un fármaco es administrado sobre la piel, además de ser un soporte que debe permitir la liberacion del fármaco en el area apropiada con una velocidad de liberacion óptima. Por consiguiente, debe existir un equilibrio entre fármaco - vehículo y una adecuada afinidad entre fármaco - piel, con el objetivo de asegurar una maxima actividad termodinamica. Adicionalmente, el coeficiente de difusion del fármaco en el vehiculo debe ser óptimo, de tal manera que el fármaco pueda solubilizarse sin poseer una afinidad selectiva por el vehículo que lo contiene [16, 122].

Al final del ensayo de permeación, se determinaron las cantidades de PF retenido en la piel para todas las formulaciones. Los resultados obtenidos muestran que las formulaciones de nanopartículas (PF-F1NPs y PF-F2NPs) presentan los valores más altos de PF retenido en la piel comparadas con el resto de las formulaciones analizadas. Respecto las formulaciones semisólidas, los resultados revelan que la formualcion HG_PF-F2NPs exhibe una cantidad de PF retenido en la piel mayor que las demás formulaciones semisólidas evaluadas (Tabla 5 artículo 3). Los resultados obtenidos en el ensayo de permeación, también revelan que la inclusión de azona en las formulaciones semisólidas de PF no exhibe ningún incremento en la cantidad permeada o retenida del fármaco a través de la piel (Tabla 5 artículo 3).

Por otra parte, la concentración plasmática de PF en estado estacionario después de la administración tópica de las formulaciones ensayadas sobre 100

cm^2 de piel, se determinó a partir del valor de flujo calculado para cada formulación testada, teniendo en cuenta los parámetros farmacocinéticos de PF. En la literatura se ha descrito una concentración plasmática terapéutica de PF para sujetos jóvenes y geriátricos de 4.89 ± 1.29 $\mu g \ cm^3$ y 10.19 ± 2.43 $\mu g \ cm^3$, respectivamente [24]. Los resultados obtenidos muestran que todos los valores de las concentración plasmática de PF en estado estacionario después de la administración tópica de las formulaciones de PF desarrolladas son inferiores a los valores de las concentraciones plasmáticas terapéuticas reportados en la bibliografía para este fármaco (Tabla 6 artículo 3). Estos resultados permiten garantizar que la aplicación tópica de las formulaciones de PF ensayadas, no tendría ningún efecto sistémico del fármaco y al mismo tiempo, aseguran un efecto local analgésico y anti-inflamatorio de PF.

La **eficacia antiinflamatoria de PF** a partir de diferentes formulaciones fue evaluada siguiendo el método descrito por Qadeer et al [123].

A pesar de que las formulaciones PF-F1NPs y PF-F2 NPs exhiben los valores más altos de PF retenido en la piel (Tabla 5 artículo 3), los valores de eficacia antiinflamatoria de PF asociado a estas formulaciones son intermedios respecto a las otras formulaciones ensayadas. Estos resultados podrían ser explicados a partir de la viscosidad de estas formulaciones. Las suspensiones de las NPs se caracterizan por poseer una viscosidad baja, y en consecuencia, no se adhieren fácilmente a la piel y el fármaco es removido de la superficie dérmica después de la aplicación tópica. Las cantidades de PF retenidas en la piel y los porcentajes del efecto anti-inflamatorio de PF a partir de las formulaciones HG_PF-F1NPs y HG_PF-F1NPs-Azona fueron inferiores respecto a los obtenidos para la formulación PF-F1NPs (Tabla 5 artículo 3 y Figura 6 artículo 3). Por otra parte, la formulación HG_PF-F2NPs reduce significativamente la inflamación comparada con PF-F2NPs y HG_PF-F2NPs-Azona. Los valores de eficacia antiinflamatoria presentados por la formulación HG_PF-F2NPs se correlacionan directamente con la cantidad de fármaco retenida en la piel (Tabla 5 artículo 3 y Figura 6 artículo 3). Los resultados obtenidos indican que la aplicación tópica de la formulación HG_PF-F2NPs podría ser más efectiva en el tratamiento del edema de la piel respecto al resto de las formulaciones analizadas. Shin et al [124], formularon PF en una matriz

de co-polímeros de etileno y acetato de vinilo conteniendo dietilftalato como plastificante, el cual mostró un incremento en la liberación del fármaco. Estos autores, también desarrollaron una formulación de liberación sostenida y controlada de PF utilizando hidroxipropilmetilcelulosa - gel de poloxamer con ácido octanoico como promotor de la permeación. El efecto anti-inflamatorio de esta formulación fue evaluado induciendo el edema en la región plantar de la rata, obteniéndose una reducción del 73 % del edema respecto al grupo control [125]. Sin embargo, los resultados de eficacia anti-inflamatoria obtenidos por estos investigadores, no pueden compararse con los obtenidos en la presente investigación debido a que las especies animales y el área de aplicación usados en estos estudios son diferentes. No obstante, los resultados obtenidos en estos estudios confirman que el PF es adecuando para la administración tópica.

La **tolerancia dérmica** de formulaciones HG_PF-NPs y HG_PF-NPs-Azona, evaluada usando el metodo Draize [119] y siguiendo las directrices de las normativas internaciones [126], puso de relieve un índice de irritación primario individual inferior a 0.5 (artículo 3) para todas formulaciones ensayadas en ausencia de azona o presencia de un 3% de promotor. Sin embargo, las formulaciones semisólidas con un 5% de azona en su composición exhibieron un índice de irritación de 3 (artículo 3). Por esta razón, las formulaciones semisólidas de PF conteniendo un 5 % de azona no fueron consideradas para llevar a cabo estudios adicionales en el presente trabajo.

5. CONCLUSIONES

In this work, pranoprofen was formulated in PLGA nanoparticles for topical administration. Taking into account all the results obtained from the different assays carried out with the optimized colloidal systems, and the formulations of the nanoparticles incorporated into hydrogel containing pranoprofen, it can be concluded that:

1. The optimization of polymeric pranoprofen-loaded NPs by a factorial design revealed that the experimental conditions to prepare nanoparticles with physicochemical properties suitable for topical application are: aqueous phase pH values of 4.5 and 5.5; a pranoprofen concentrations of 1.0 mg/mL and 1.5 mg/mL; PLGA concentrations of 9.0 mg/mL and 9.5 mg/mL and different PVA concentrations. The formulations prepared by the solvent displacement technique under these experimental conditions showed an average size appropriate (around 350 nm) and high entrapment efficiency (80%).

2. The evaluation of the physical stability of the optimized nanostructured systems over a short time period showed a discrete sedimentation. This slight destabilization observed in the profiles of the PF-F1NPs and PF-F2NPs formulations was reversible and quickly disappeared after shaking. The results obtained suggest there is no evidence of significant change in the particle size for these formulations.

3. The results observed from the characterization of the optimized PF-loaded NPs after freeze-drying showed that the physicochemical properties of these formulations were similar to those of the nanoparticles before freeze-drying.

4. The evaluation of the physical state of the PF in the polymeric matrix and the possible interactions between drug and polymer of the nanospheres before and after freeze-drying, using X-ray diffraction, infrared spectroscopy and thermal methods suggest there is no evidence of any chemical interaction or strong bond formation between PF and PLGA.

5. The optimized PF-F1NPs and PF-F2NPs suspensions were successfully dispersed into blank hydrogels or hydrogels containing azone as permeation enhancer. The hydrogel formulations showed physicochemical, morphological and rheological properties suitable for topical pranoprofen delivery.

6. The pranoprofen polymeric nanosuspension and the formulations of the nanoparticles incorporated into hydrogel containing pranoprofen modify the release profile of this drug, exhibiting a sustained release behavior. The release of PF from these formulations occurs by passive diffusion, mainly through the pores of the matrix. Therefore, these formulations could be an effective and appropriate system for ocular treatment.

7. According to the results obtained from the corneal permeation, anti-inflammatory efficacy and ocular tolerance studies of the pranoprofen formulations revealed that both the optimized nanospheres and the semisolid formulations containing PF-loaded NPs in presence of azone significantly reduced the ocular oedema, compared with other tested formulations. These results indicate that the inclusion of azone into the HG_PF-NPs formulations leads to the increase of the anti-inflammatory efficacy effect of pranoprofen in the cornea. The semisolid formulation of pranoprofen with or without azone exhibited an optimal ocular tolerance by the *in vitro* e *in vivo* ocular irritation test. Therefore, the ocular application of these formulations could be more effective in the treatment ocular oedema.

8. On the basis of *ex vivo* skin human permeation and anti-inflammatory efficacy of the formulations of PF-loaded nanoparticles incorporate into hydrogel, it can be concluded that the inclusion of azone in the semi-solid formulations did not show any increase in the amount of drug permeated and retained amount of PF in the skin. The results obtained from these studies, also revealed that HG_PF-F2NPs formulation not only provide an adequate drug release, but also show anti-inflammatory efficacy values which correlate directly with the amount of drug retained in the skin. These

results suggest than the topical application of the HG_PF-F2NPs could be more effective in the treatment of edema on the skin surface that the other semi-solid formulations. This formulation could facilitate the prolonged contact of the PF on the skin and improve its skin retention, thus enhancing the local anti-inflammatory and analgesic effect of this drug and, consequently, improves patient compliance by reducing application frequency. In addition, all these semisolid formulation of pranoprofen with (3%) or without azone showed an optimal skin tolerance.

9. All the results obtained suggest that PF formulated in polymeric NP and the incorporation of these systems into Carbomer hydrogel guarantee a sustained release of PF, improving the biopharmaceutical profile of this drug, preventing the inherent irritating of the PF and avoiding the physical degradation of this drug.

6. REFERENCIAS

[1] Sasaki H., Yamamura K., Nishida K., Nakamura J., Ichikawa M., Delivery of drugs to the eye by topical application, *Prog. Retin. Eye Res.*, 1996; 15: 583–620.

[2] Chrai S. S., Makoid M. C., Eriksen S. P., Robinson J. R., Drop size and initial dosing frequency problems of topically applied ophthalmic drugs, *J. Pharm. Sci.*, 1974; 63: 333–338.

[3] Watsky M. A., Jablonski M. M., Edelhauser H. F., Comparison of conjunctival and corneal surface areas in rabbit and human, *Curr. Eye Res.*, 1988; 7: 483–486.

[4] Pal Kaur I., Kanwar M., Ocular Preparations: The Formulation Approach, *Drug Dev. Ind. Pharm.*, 2002; 28: 473–493.

[5] Mannermaa E., Vellonen K. S., Urtti A., Drug transport in corneal epithelium and blood-retina barrier: emerging role of transporters in ocular pharmacokinetics., *Adv. Drug Deliv. Rev.*, 2006; 58:1136–1163.

[6] Grass G. M., Robinson J. R., Mechanisms of corneal drug penetration II: Ultrastructural analysis of potential pathways for drug movement, *J. Pharm. Sci.*, 1988; 77:15–23.

[7] Komai Y., Ushikif T., The three-dimensional organization of collagen fibrils in the human cornea and sclera, 1991; 32: 2244-2258.

[8] Järvinen K., Järvinen T., Urtti A., Ocular absorption following topical delivery, *Adv. Drug Deliv., Rev.*, 1995; 16:3–19.

[9] Lai-Cheong J. E., McGrath J. A., Structure and function of skin, hair and nails, *Medicine*, 2009; 37: 223–226.

[10] Venus M., Waterman J., McNab I., Basic physiology of the skin, *Surgery.*, 2011; 29: 471–474.

[11] Wilkes, G.L., Brown, I.A., Widnauer, R.H., The Biomecanical Properties of Skin. Crit. Rev. Bioeng., 1973, 452.

[12] Venus M., Waterman J., McNab I., Basic physiology of the skin, *Surgery.*, 2011; 29: 471–474.

[13] Roberts M. S., Walters K. A., Human Skin Morphology and Dermal Absorption, Dermal Absorpt. Toxic. Assess., Informa Healthcare, New York, 2008;1-15

[14] Schoenwald R. D., Ward R. L., Relationship between steroid permeability across excised rabbit cornea and octanol-water partition coefficients, *J. Pharm. Sci.*, 1978; 67: 786–788.

[15] Grass G. M., Robinson J. R., Mechanisms of corneal drug penetration I: In vivo and in vitro kinetics, *J. Pharm. Sci.*, 1988; 77: 3–14.

[16] Calpena A. C., Clares B., Fernandez F., Technological, biopharmaceutical and pharmacokinetic advances: New formulations of application on the skin and oral mucosa. Diego Muñoz-Torreo. Recent advance in pharmaceutical science. 2011; 661:175-198.

[17] Rojanasakul Y., Wang L.Y., Bhat M., Glover D., Malanga C., Ma. J. H., The Transport Barrier of Epithelia: A Comparative Study on Membrane Permeability and Charge Selectivity in the Rabbit. *Pharm. Res.*, 1992; 9: 1029–1034.

[18] Sieg J. W., Robinson J. R., Vehicle effects on ocular drug bioavailability II: Evaluation of pilocarpine, *J. Pharm. Sci.*, 1977; 66: 1222–1228.

[19] Friedrich S. W., Cheng Y.L., Saville B. A., Theoretical Corneal Permeation Model for Ionizable Drugs, *J. Ocul. Pharmacol. Ther.*, 1993; 9: 229–249.

[20] Rojanasakul Y., Robinson J. R., Transport mechanisms of the cornea: characterization of barrier permselectivity, *Int. J. Pharm.*, 1989; 55: 237–246.

[21] Lorenzo-Velázquez B., Lorenzo-Fernández P., Cabelloro-Collado R., Manual de farmacología básica y clínica, Editorial medica panamericana, Madrid, España, 2012; 319-328.

[22] Rang H.P., Dale M.M., Ritter J.M., Flowe R.J., Herderson G., Farmacología,Séptima edición, Elsevier, España, S.L., 2012.

[23] Japanese pharmacopoeia. Fifteeth edition. The Society of Japanese Pharmacopoeia, Tokyo, 2010; 1018

[24] Kajiyama H., Fujimura A., Ebihara A., Hino Y., Pharmacokinetics of pranoprofen in the elderly. Clin. Pharmacol. Res. 1991;11:123–127.

[25] Akyol-Salman I., Leçe-Sertöz D., Baykal O., Topical pranoprofen 0.1% is as effective anti-inflammatory and analgesic agent as diclofenac sodium 0.1% after strabismus surgery. J Ocul Pharmacol Ther. 2007; 23: 280–283.

[26] Sawa M., Masuda K., Nakashima M., Anti-inflamatory effect of diclofenac sodium eye drops on cataract surgery. Double masked study with pranoprofen eye drops. IOL RS. 1999; 13: 193–200.

[27] McColgin A.Z., Heier J.S., Control of intraocular inflammation associated with cataract surgery. Curr. opin. ophthalmol. 2000; 11: 3–6.

[28] Liu X., Wang S., Kao A.A., Long Q., The effect of topical pranoprofen 0.1% on the clinical evaluation and conjunctival HLA-DR expression in dry eyes. Cornea. 2012; 31: 1235–1239.

[29] Notivol R., Martinez M., Bergamini M., Treatment of chronic nonbacterial conjunctivitis with a cyclo-oxygenase inhibitor or a corticosteroid. Pranoprofen Study Group. Am J ophthalmol. 1994; 117: 651–656.

[30] Ghosal K, Chakrabarty S, Nanda A. Hydroxypropyl methylcellulose in drug delivery. Pelagia Res Library. 2011; 2:152-168.

[31] Narashino M., Ichikawa H., Narita S., Yotsukaido A.S., Sustained-Release Pranoprofen Preparation. 1993. United States patent. US00522506A.

[32] Kobe K., Otsu H., Kobe Y., Kakogawa Y., Method for stabilizing pranoprofen and stable liquid preparation of pranoprofen. 1999. United States patent. US005856345A.

[33] Kalia Y.N., Guy R.H., Modeling transdermal drug release. Adv. Drug Deliv. Rev. 2001; 48:159–172.

[34] Pardeike J., Hommoss A., Müller R.H., Lipid nanoparticles (SLN, NLC) in cosmetic and pharmaceutical dermal products. Int. J. Pharm. 2009; 366:170–184.

[35] Bawarski W.E., Chidlowsky E., Bharali D.J., Mousa SA. Emerging nanopharmaceuticals. Nanomedicine. 2008; 4:273–282.

[36] Kreuter J., Particulates (nanoparticles and microparticles). In: Mitra AK, editor. Ophthalmic drug delivery systems. New York: Marcel Dekker, 1993; 275–285

[37] Soppimath K. S., Aminabhavi T. M., Kulkarni A. R., Rudzinski W. E., Biodegradable polymeric nanoparticles as drug delivery devices. *J. Control Release.* 2001; 70:1–20.

[38] Nair L.S., Laurencin C.T., Biodegradable polymers as biomaterials. Prog Poly Sci. 2007; 32:762–798.

[39] Park T. G., Degradation of poly(lactic-co-glycolic acid) microspheres: effect of copolymer composition, *Biomaterials. 1995;* 16: 1123–1130.

[40] Anderson J. M., Shive M. S., Biodegradation and biocompatibility of PLA and PLGA microspheres, *Adv. Drug Deliv. Rev.*, 2012; 64: 72–82.

[41] Witt C., Morphological characterization of microspheres, films and implants prepared from poly(lactide-co-glycolide) and ABA triblock copolymers: is the erosion controlled by degradation, swelling or diffusion?, *Eur. J. Pharm. Biopharm.* 2001; 51:171–181.

[42] Raghuvanshi R. S., Singh M., Talwar V., Biodegradable delivery system for single step immunization with tetanus toxoid, *Int. J. Pharm.*, 1993; 93: R1–R5.

[43] Crotts G., Park T. G., Protein delivery from poly(lactic-co-glycolic acid) biodegradable microspheres: Release kinetics and stability issues, *J. Microencapsul.*, 1998; 15: 699–713.

[44] Kranz H., Ubrich N., Maincent P., Bodmeier R., Physicomechanical properties of biodegradable poly(D,L-lactide) and poly(D,L-lactide-co-glycolide) films in the dry and wet states. *J. Pharm. Sci.*, 2000; 89: 1558–1566.

[45] Reeve M. S., McCarthy S. P., Downey M. J., Gross R. A., Polylactide stereochemistry: effect on enzymic degradability, *Macromolecules*. 1994; 27: 825–831.

[46] Williams D. F., Mort E., Enzyme-accelerated hydrolysis of polyglycolic acid, *J. Bioeng.*, 1977; 1:231—238.

[47] Cai Q., Enzymatic degradation behavior and mechanism of Poly(lactide-co-glycolide) foams by trypsin, *Biomaterials*, 2003; 24: 629–638.

[48] Fessi H., Puisieux F., Devissaguet J.P., Ammoury N., Benita S., Nanocapsule formation by interfacial polymer deposition following solvent displacement. Int. J Pharm., 1989 ; 55:R1–R4.

[49] Quintanar-Guerrero D., Allémann E., Fessi H., Doelker E., Preparation techniques and mechanism of formation of biodegradable nanoparticles from preformed polymers, *Drug Dev. Ind. Pharm.*, 1998; 24: 1113–1128

[50] Nagavarma B.V., Yadav H., Ayaz A., Vasudha L. S., Shivakumar H. G., Different techniques for preparation of polymeric nanoparticles-A review., Asian J Pharm Clin Res., 2012; 5:16-23.

[51] Pinto Reis C., Neufeld R. J., Ribeiro A. J., Veiga F., Nanoencapsulation I. Methods for preparation of drug-loaded polymeric nanoparticles, *Nanomedicine Nanotechnology, Biol. Med.*, 2006; 2: 8–21.

[52] Couvreur P., Dubernet C., Puisieux F., Controlled drug delivery with nanoparticles : current possibilities and future trends, *Eur. J. Pharm. Biopharm.*, 1995; 41: 2–13.

[53] Mora-Huertas C. E., Fessi H., Elaissari A., Polymer-based nanocapsules for drug delivery., *Int. J. Pharm.*, 2010; 385: 113–142.

[54] Zimmer A., Kreuter J., Microspheres and nanoparticles used in ocular delivery systems. Ocul Drug Deliv Rev. 1995; 16:61-73.

[55] Song X., Zhao Y., Hou S., Xu F., Zhao R., He J., Cai Z., Li Y., Chen Q., Dual agents loaded PLGA nanoparticles: Systematic study of particle size and drug entrapment efficiency. Eur. J Pharm. Biopharm. , 2008; 69: 445-453.

[56] Yoncheva K., Vandervoort J., Ludwig A., Influence of process parameters of high-pressure emulsification method on the properties of pilocarpine-loaded nanoparticles, *J. Microencapsul.*, 2003; 20: 449–458.

[57] Calvo P., Alonso M. J., Vila-Jato J. L., Robinson J. R., Improved ocular bioavailability of indomethacin by novel ocular drug carriers, *J. Pharm. Pharmacol.*, 1996; 48: 1147–1152.

[58] Deshiikan S. R., Papadopoulos K. D., Modified Booth equation for the calculation of zeta potential, *Colloid Polym. Sci.*, 1998; 276: 117–124.

[59] Teeranachaideekul V., Junyaprasert V. B., Souto E. B., Müller R. H., Development of ascorbyl palmitate nanocrystals applying the nanosuspension technology., *Int. J. Pharm.*, 2008; 354: 227–234.

[60] Makadia H. K., Siegel S. J., Poly Lactic-co-Glycolic Acid (PLGA) as Biodegradable Controlled Drug Delivery Carrier., *Polymers.*,2011; 3: 1377–1397.

[61] Faisant N., Siepmann J., Benoit J.P., PLGA-based microparticles: elucidation of mechanisms and a new, simple mathematical model quantifying drug release. European J Pharm Sci., 2002; 15:355-366.

[62] Niwa T., Takeuchi H., Hino T., Kunou N., Kawashima Y., Preparations of biodegradable nanospheres of water-soluble and insoluble drugs with D,L-lactide/glycolide copolymer by a novel spontaneous emulsification solvent diffusion method, and the drug release behavior. J Controlled Release., 1993; 25:89-98.

[63] Kamaly N., Xiao Z., Valencia P. M., Radovic-Moreno A. F., Farokhzad O. C., Targeted polymeric therapeutic nanoparticles: design, development and clinical translation., *Chem. Soc. Rev.*, 2012; 41: 2971–3010.

[64] Peer D., Karp J. M., Hong S., Farokhzad O. C., Margalit R., Langer R., Nanocarriers as an emerging platform for cancer therapy, *Nat Nano.*, 2007; 2: 751–760.

[65] Dillen K., Vandervoort J., Van den Mooter G., Verheyden L., Ludwig A., Factorial design, physicochemical characterisation and activity of ciprofloxacin-PLGA nanoparticles, *Int. J. Pharm.*, 2004; 275: 171–187.

[66] Clas S.D., Dalton C. R., Hancock B. C., Differential scanning calorimetry: applications in drug development, *Pharm. Sci. Technolo. Today*, 1999; 2: 311–320.

[67] Abdelwahed W., Degobert G., Stainmesse S., Fessi H., Freeze-drying of nanoparticles: Formulation, process and storage considerations. Adv Drug Deliv Rev, 2006; 58:1688-1713.

[68] Vandervoort J., Ludwig A., Biocompatible stabilizers in the preparation of PLGA nanoparticles: a factorial design study, *Int. J. Pharm.*, 2002; 238: 77–92.

[69] Layre A., Couvreur P., Richard J., Requier D., Eddine Ghermani N., Gref R., Freeze -drying of composite core-shell nanoparticles, Drug Dev Ind Pharm., 2006; 32:839-846.

[70] Takeuchi H., Yamamoto H., Toyoda T., Toyobuku H., Hino T., Kawashima Y., Physical stability of size controlled small unilameller liposomes coated with a modified polyvinyl alcohol, *Int. J. Pharm.*, 1998; 164:103–111.

[71] Flory P. J., Rehner J., Statistical Mechanics of cross-linked polymer networks II. Swelling, *J. Chem. Phys.*,1943;11:521-526

[72] Baek G., Kim C., Rheological properties of Carbopol containing nanoparticles, *J. Rheol.* , 2011; 55:313-330.

[73] Islam M., Rodríguez-Hornedo N., Ciotti S., Ackermann C., Rheological characterization of topical carbomer gels neutralized to different pH, *Pharm. Res.*, 2004; 21:1192–1199.

[74] Hamidi M., Azadi A., Rafiei P., Hydrogel nanoparticles in drug delivery. Adv. Drug Deliv. Rev., 2008; 60:1638–1649.

[75] Gonzalez-Mira E., Nikolić S., Calpena A.C., Egea M.A., Souto E.B., Garcia M.L., Improved and safe transcorneal delivery of flurbiprofen by NLC and NLC-based hydrogels. J. Pharm. Sci., 2012;101: 707–725.

[76] Chen X., Peng L.H., Shan Y.H., Li N., Wei W., Yu L., Li Q.M., Liang W.Q., Gao J.Q., Astragaloside IV-loaded nanoparticle-enriched hydrogel

induces wound healing and anti-scar activity through topical delivery, *Int. J. Pharm.*, 2013; 447:171–181.

[77] Han F., Yin R., Che X., Yuan J., Cui Y., Yin H., Li S., Nanostructured lipid carriers (NLC) based topical gel of flurbiprofen: Design, characterization and in vivo evaluation. Int. J. Pharm., 2012; 439:349–357.

[78] Barry B. W., *Dermatological formulations: percutaneous absorption*, Informa Health Care; 1983.

[79] Williams A. C., Barry B. W., Penetration enhancers. Adv. Drug Deliv. Rev., 2012; 64:128–137.

[80] Amara F.E., Meleis M.E., Seif M.A., Moursy E.Y., Study of the metabolic effect and histopathological nasal mucosal changes after prolonged intranasal insulin administration. Journal of Diabetology. 2011;1:1–10.

[81] Nicolazzo J. A., Reed B. L., Finnin B. C., Enhanced buccal mucosal retention and reduced buccal permeability of estradiol in the presence of padimate O and Azone®: A mechanistic study, *J. Pharm. Sci.*, 2005; 94: 873–882.

[82] Lallemand F., Felt-Baeyens O., Besseghir K., Behar-Cohen F., Gurny R., Cyclosporine A delivery to the eye: A pharmaceutical challenge., Eur. J. Pharm. Biopharm., 2003; 56: 307-318.

[83] Batheja P., Sheihet L., Kohn J., Singer A. J., Michniak-Kohn B., Topical drug delivery by a polymeric nanosphere gel: Formulation optimization and in vitro and in vivo skin distribution studies. J. Control. Release. 2011; 149:159–167.

[84] Laurent S., Forge D., Port M., Roch A., Robic C., Vander Elst L., Muller R.N., Magnetic iron oxide nanoparticles: synthesis, stabilization, vectorization, physicochemical characterizations, and biological applications. Chem Rev., 2008; 108: 2064–2110.

[85] Erden V., Celebi N., Factors influencing release of salbutamol sulphate from poly(lactide-co-glycolide) microspheres prepared by water-in-oil-in-water emulsion technique, *Int. J. Pharm.*, 1996; 137: 57–66.

[86] Guterres S., Alves M., Pohlmann A., Polymeric nanoparticles, nanospheres and nanocapsules, for cutaneous applications, Drug Target Insights., 2007; 2 :147–157.

[87] Lademann J., Richter H., Schaefer U.F., Blume-Peytavi U., Teichmann A., Otberg N., Sterry W., Hair follicles-a long-term reservoir for drug delivery. Skin Pharmacol. Physiol. 2006;19: 232–236.

[88] Alvarez-Román R., Naik A., Kalia Y.N., Guy R.H., Fessi H., Enhancement of topical delivery from biodegradable nanoparticles., Pharm. Res., 2004; 21: 1818–1825

[89] Luengo J., Weiss B., Schneider M., Ehlers A., Stracke F., König K., Kostka K.H., Lehr C.M., Schaefer U.F., Influence of nanoencapsulation on human skin transport of flufenamic acid., Skin Pharmacol. Physiol., 2006;19: 190–197.

[90] Alvarez-Román R., Naik A., Kalia Y.N., Guy R.H., Fessi H., Skin penetration and distribution of polymeric nanoparticles., J. Control. Release., 2004; 99: 53–62.

[91] Feng S., Huang G., Effects of emulsifiers on the controlled release of paclitaxel (Taxol®) from nanospheres of biodegradable polymers. J Controlled Release., 2001; 71:53-69

[92] Sahoo S.K., Panyam J., Prabha S., Labhasetwar V., Residual polyvinyl alcohol associated with poly (d,l-lactide-co-glycolide) nanoparticles affects their physical properties and cellular uptake. J Controlled Release, 2002; 82:105-114.

[93] Araujo J., Vega E., Lopes C., Egea M.A., Garcia M.L., Souto E.B., Effect of polymer viscosity on physicochemical properties and ocular tolerance

of FB-loaded PLGA nanospheres, Colloids Surface B Biointerfaces, 2009; 72:48-56.

[94] Vega E., Egea M.A., Valls O., Espina M, García M.L., Flurbiprofen loaded biodegradable nanoparticles for ophtalmic administration. J Pharm Sci., 2006; 95:2393-2405.

[95] Jiang B., Hu L., Gao C., Shen J., Ibuprofen-loaded nanoparticles prepared by a co-precipitation method and their release properties. Int J Pharm., 2005; 304:220-230.

[96] Allémann E., Leroux J.C., Gurny R., Doelker E., In vitro extended-release properties of drug-loaded poly(DL-lactic acid) nanoparticles produced by a salting-out procedure, *Pharm. Res.*, 1993; 10:1732–1737.

[97] Murakami H., Kawashima Y., Niwa T., Hino T., Takeuchi H., Kobayashi M., Influence of the degrees of hydrolyzation and polymerization of poly(vinylalcohol) on the preparation and properties of poly(dl-lactide-co-glycolide) nanoparticle, *Int. J. Pharm.*, 1997;149: 43–49.

[98] Vega E., Gamisans F., Garcia M.L., Chauvet A., Lacoulonche F., Egea M.A., PLGA nanospheres for the ocular delivery of flurbiprofen: drug release and interactions. J Pharm Sci., 2008; 97:5306-5317.

[99] Gamisans F., Lacoulonche F., Chauvet A., Espina M., García M.L., Egea M.A., Flurbiprofen-loaded nanospheres: analysis of the matrix structure by thermal methods, *Int. J. Pharm.*, 1999; 179: 37–48.

[100] Ertl B., Platzer P., Wirth M., Gabor F., Poly(d,l-lactic-co-glycolic acid) microspheres for sustained delivery and stabilization of camptothecin, *J. Control. Release*, 1999; 61:305–317.

[101] Passerini N., Craig D.Q. An investigation into the effects of residual water on the glass transition temperature of polylactide microspheres using modulated temperature DSC, J. Controlled Release, 2001; 73:111-115.

[102] Dubernet C., Rouland J. C., Benoit J. P., Ibuprofen-loaded ethylcellulose microspheres: Analysis of the matrix structure by thermal analysis," *J. Pharm. Sci.*, 1991; 80:1029–1033.

[103] Bhalekar M. R., Pokharkar V., Madgulkar A., Patil N., Patil N., Preparation and evaluation of miconazole nitrate-loaded solid lipid nanoparticles for topical delivery., *AAPS PharmSciTech*, 2009; 10: 289–296.

[104] Montenegro L., Sinico C., Castangia I., Carbone C., Puglisi G., Idebenone-loaded solid lipid nanoparticles for drug delivery to the skin: in vitro evaluation, Int. J. Pharm., 2012; 434:169–174.

[105] Robinson J. R., Ocular drug delivery mechanism (s) of corneal drug transport and mucoadhesive delivery systems, *STP Pharma*, 1989; 5: 839–846.

[106] Kaur I. P., Smitha R., Penetration enhancers and ocular bioadhesives: two new avenues for ophthalmic drug delivery, Drug Dev Ind Pharm., 2002; 28:353 – 369.

[107] Malvern Instruments, 10 ways to control rheology by changing particles properties, 2009, INFORM series of white papers.

[108] Costa P, Sousa J.M., Modeling and comparison of dissolution profiles, European J. Pharm. Sci., 2001;13:123–133.

[109] Ford J., Rubinstein M., McCaul F., Hogan J., Edgar P., Importance of drug type, tablet shape and added diluents on drug release kinetics from hydroxypropylmethylcellulose matrix tablets, Int. J. Pharm., 1987; 40:223–234.

[110] Hamidi M., Azadi A., Rafiei P., Hydrogel nanoparticles in drug delivery. Adv. Drug Deliv. Rev., 2008; 60:1638–1649.

[111] Tavaszi J., Budai P., The use of HET-CAM test in detecting the ocular irritation. Commun Agric Appl Biol Sci., 2007; 72:137-141.

[112] Qaddoumi M. G., Gukasyan H. J., Davda J., Labhasetwar V., Kim K., Lee V. H., Clathrin and caveolin-1 expression in primary pigmented rabbit conjunctival epithelial cells : Role in PLGA nanoparticle endocytosis, 2003; 9:569-568.

[113] Gupta H., Aqil M., Khar R. K., Ali A., Bhatnagar A., Mittal G., Sparfloxacin-loaded PLGA nanoparticles for sustained ocular drug delivery, *Nanomedicine Nanotechnology, Biol. Med.*, 2010; 6:324–333.

[114] Ahuja M., Dhake A. S., Sharma S. K., Majumdar D. K., Topical ocular delivery of NSAIDs, 2008; 10:229-241.

[115] Rathore M. S., Majumdar D. K., Effect of formulation factors on in vitro transcorneal permeation of gatifloxacin from aqueous drops, AAPS PharmSciTech., 2006; 7: E1- E6

[116] Järvinen K., Järvinen T., Urtti A., Ocular absorption following topical delivery, Adv. Drug Deliv. Rev., 1995; 16: 3–19.

[117] Furrer P., Mayer J. M., Gurny R., Ocular tolerance of preservatives and alternatives, Eur. J. Pharm. Biopharm., 2002; 53: 263–280.

[118] Schoenwald R.D., Huang H.S., Corneal penetration behavior of beta-blocking agents I: physiochemical factors, J Pharm Sci., 1983; 72: 1266 – 1272.

[119] Draize J., Woodard G., Calvery H., Methods for the study of irritation and toxcicity of substances applied topically to the skin and mucous membranes. J. Pharmacol. Exp. Ther., 1944; 82:377–390.

[120] Kay J.H., Calandra J.K., Interpretation of eye irritation test, J. Soc. Cosmet Chem., 1962; 13: 281 – 289.

[121] Jiménez M., Pelletier J., Bobin M.F., Martini M.C., Influence of encapsulation on the in vitro percutaneous absorption of octyl methoxycinnamate, Int. J. Parm., 2004; 272:45–55.

[122] Morganti P., Ruocco E., Wolf R., Ruocco V., Percutaneous absorption and delivery systems, Clin. Dermatol., 2001;19:489–501.

[123] Qadeer G., Rama N.H., Garduño-Ramírez M.L., Synthesis and anti-inflammatory activity of fluorinated isocoumarins and 3,4-dihydroisocoumarins, J. Fluorine Chem., 2007; 128:641–646.

[124] Cho C., Choi J., Shin S., Controlled release of pranoprofen from the ethylene-vinyl acetate matrix using plasticizer, Drug Dev. Ind. Pharm., 2007; 33:747–753.

[125] Choi J., Choi J., Shin S., Preparation and evaluation of pranoprofen gel for percutaneous administration, Drug Dev. Ind. Pharm., 2007; 33:19–26.

[126] OECD, Guideline for the testing of chemicals, No 404: Acute Dermal Irritation/Corrosion, 2002.